最終講義　2013.3.7（工学部一号館201講義室）

「分光の夢を追いつつ四拾年虹の七色未だ見えず」

エコトピア科学研究所エネルギー科学研究部門
応用化学分野エネルギー変換化学講座
北川邦行

- ***分光分析研究時代***
- ＜学生時代＞
- 〇原子分光分析法研究（主に解析）
- ＊竹内次夫先生の指導の下、卒業研究において、容量結合性マイクロウェーブプラズマ発光分光分析；共存元素による干渉（おもに、アルカリ・アルカリ土類元素による増感効果）について研究した。励起温度、イオン率の測定方法を確立、後にトイレの中で思い付いた、補正のための4線法は修士研究の1つとなった。
- ＊原子化器（火炎＆電気加熱）の分光解析；励起温度、原子化率の測定を発　光、吸光方で行い化学干渉の基本パラメータの測定に成功した。競合者にSturgeon先生がいた。三重大学の太田先生や我妻先生らも原子吸光による励起温度の計測の研究をされた。

Analytical Chemistry

- History & Essence –

分析化学ー歴史と真髄

Japan Society for

Analytical Chemistry ➡ Analytical Sciences

分析化学 分析科学

応用計測化学

Solitons with chaos

Hand Analyses　Gravimetric

手分析 { 重量分析 / 容量分析　⇒ 機器分析

Volmetric

図 6・3　沪過の方法

$$Ba^{2+} + SO_4^{2-} \rightarrow BaSO_4\downarrow$$

図 6・12　灰化の際のるつぼのおき方

図 3・3　分銅

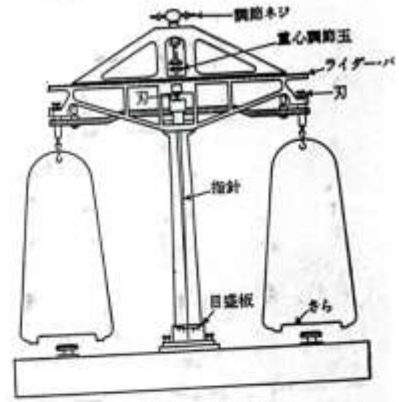

図 3・1　化学ハカリ

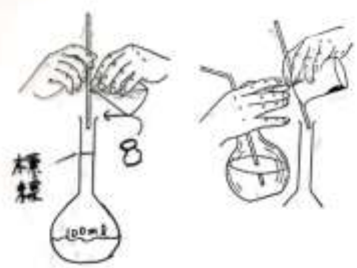

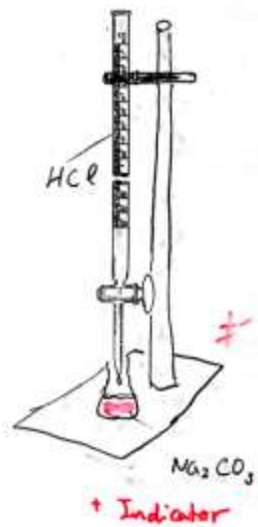

HCl / $NaOH$ − Na_2CO_3

$KMnO_4$ / COONa–COONa　Ca

$AgNO_3$ / Cl^-

NaOOCH₂C, HOOCH₂C >NCH₂CH₂N< COONa, COOH / Ca^{2+}

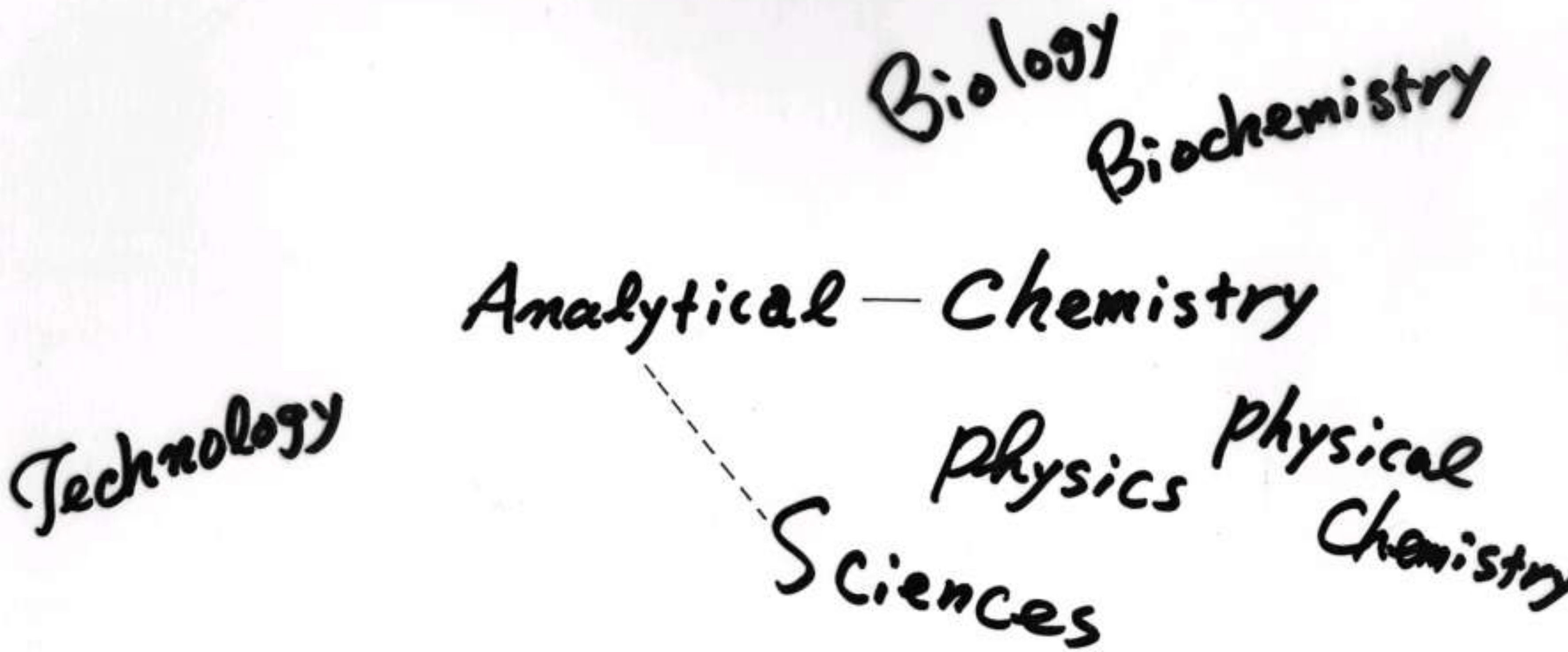

International Congress on Analytical Sciences (ICAS)

International Conference on Atomic Spectroscopy (ICAS)

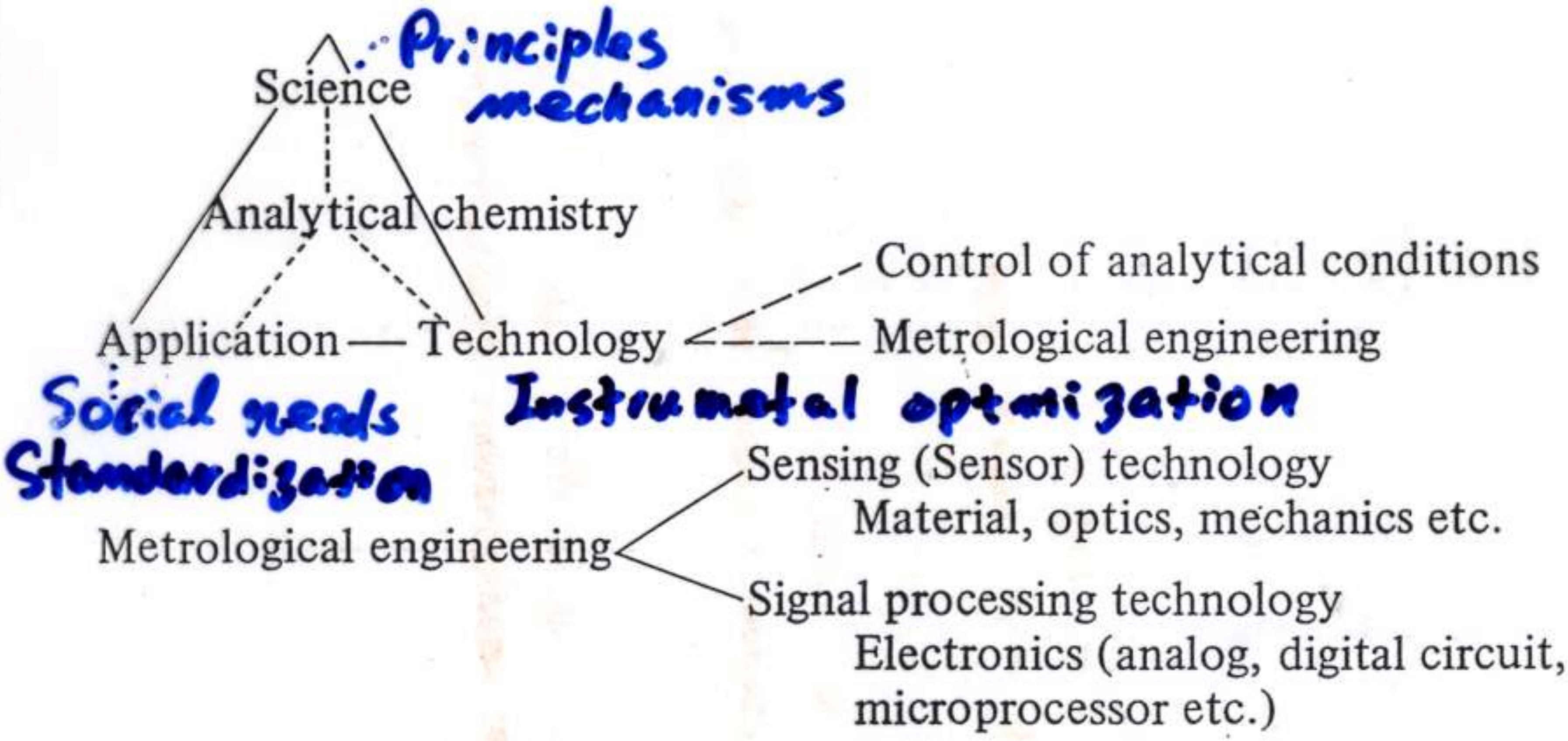

Fig. 1 Triangle of analytical chemistry

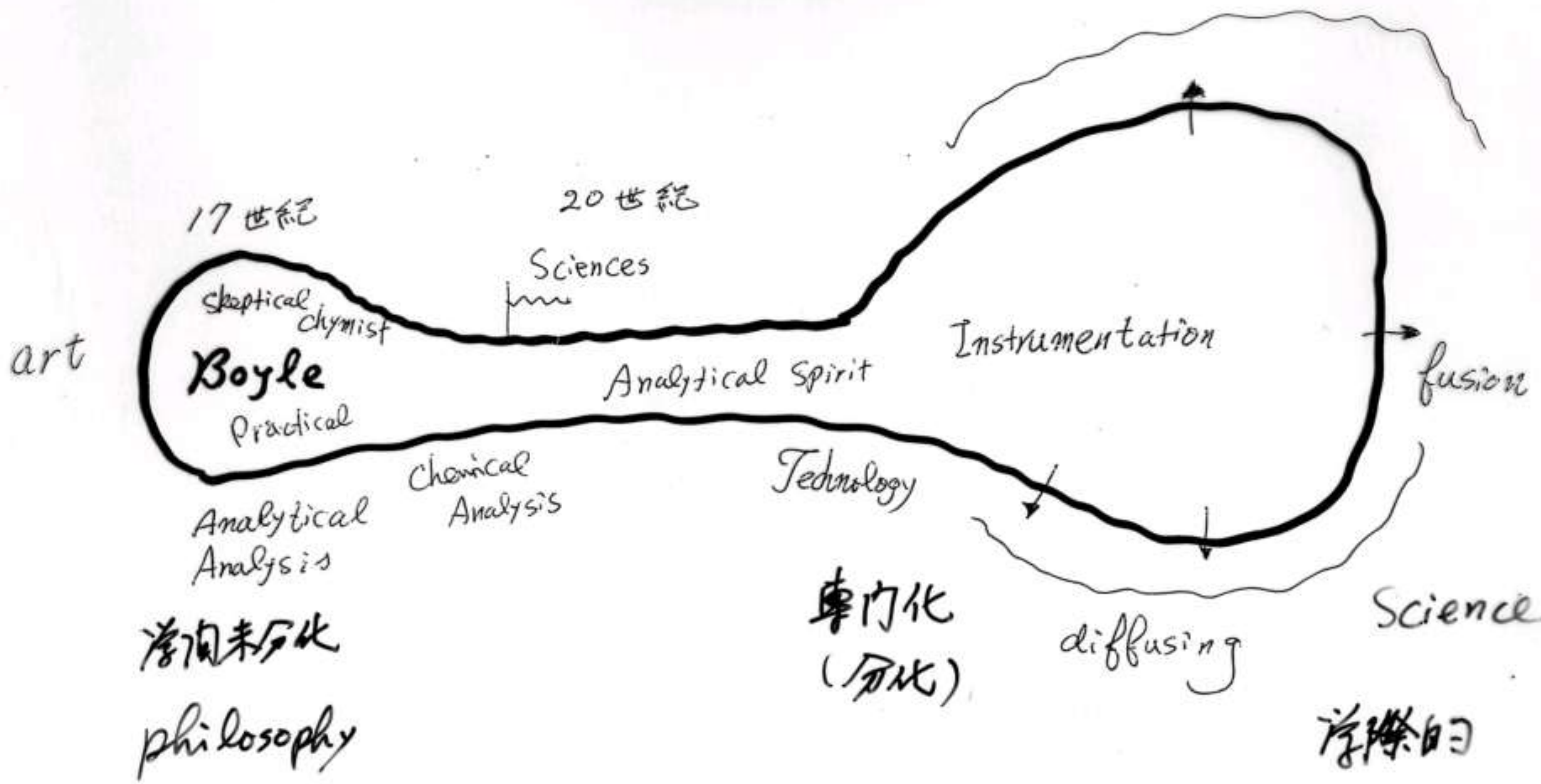
17世紀
20世紀
Sciences
Skeptical chymist
art
Boyle
Practical
Analytical Spirit
Instrumentation
fusion
Chemical Analysis
Technology
Analytical Analysis
学問未分化
philosophy
専門化
(分化)
diffusing
Science
学際的

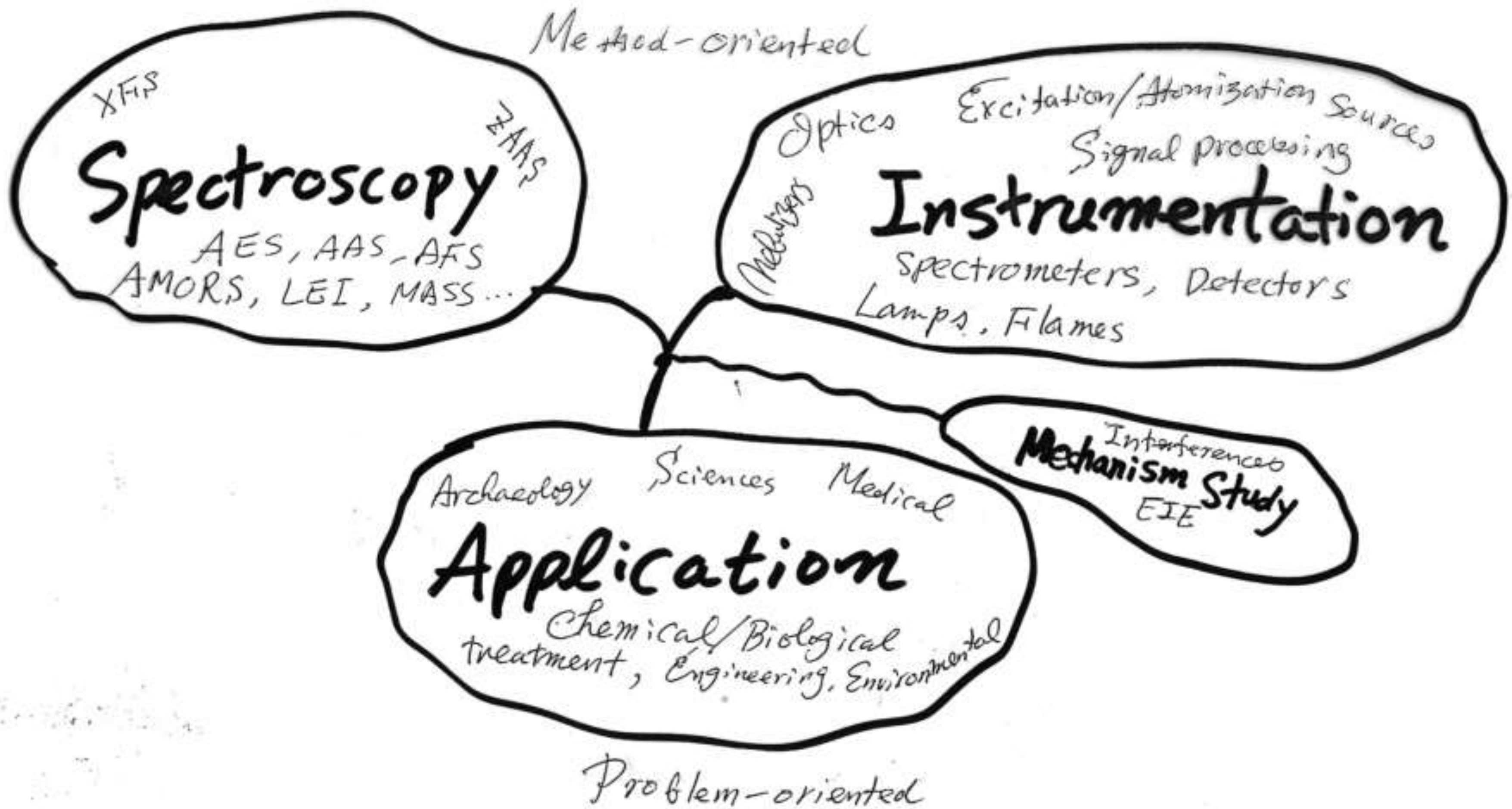

Analytical Atomic Spectroscopy

Mechanism study (Feedback concept)

Table 1-2 Time flow chart of the progress of an instrumental analytical method

1. Concept, theoretical basis or principle
2. Experimental verification of the concept applicability
3. Instrumental design and hardware (technological) optimization
4. Standardization and software (procedure) optimization in practical applications

hyphened methods

Feed forward, Quantum Leap non-linear

Fig. 1.

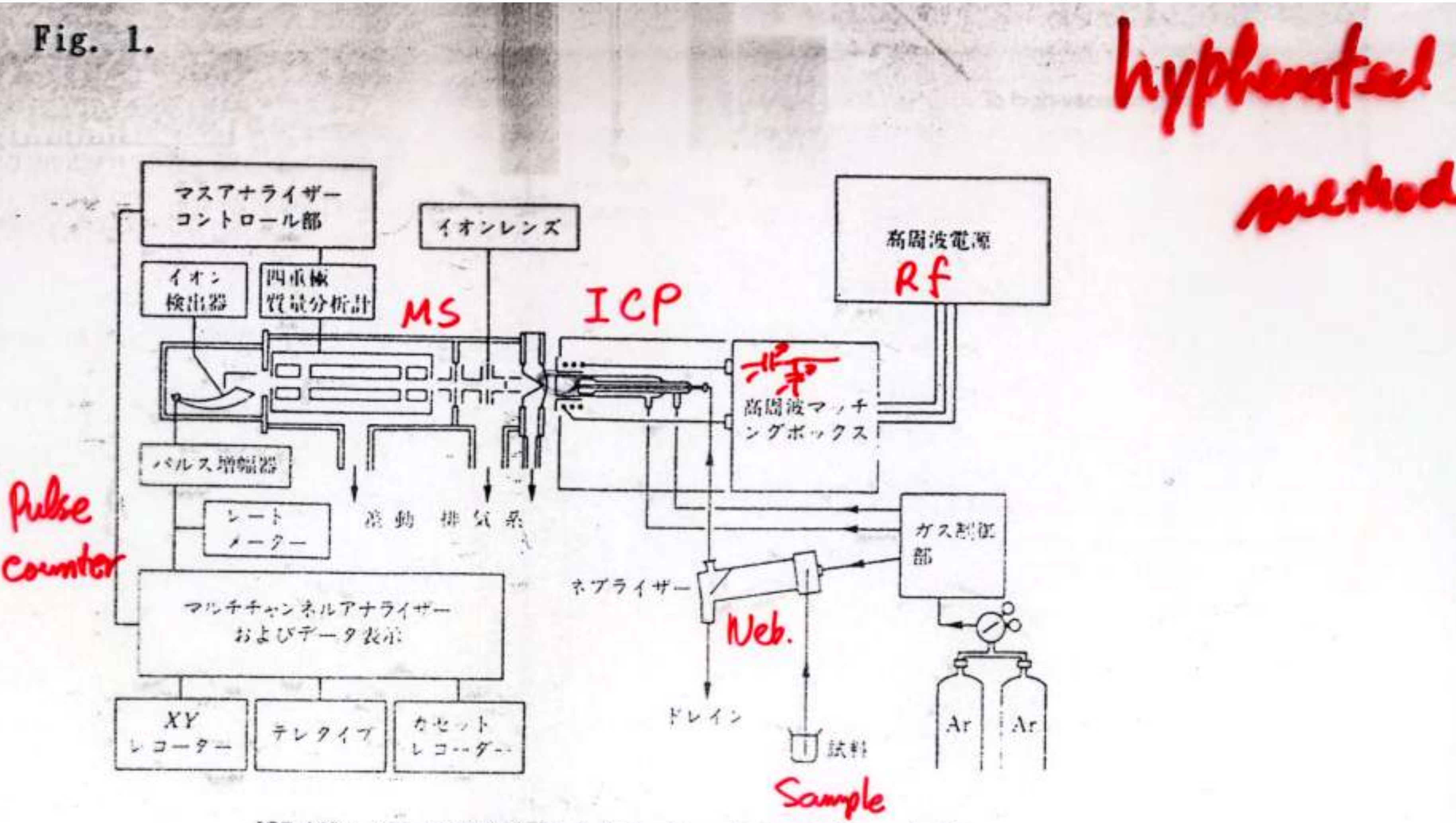

ICP-MS システムの概略図 [A. R. Date, *Trends Anal. Chem.*, 2, 225 (1983)]

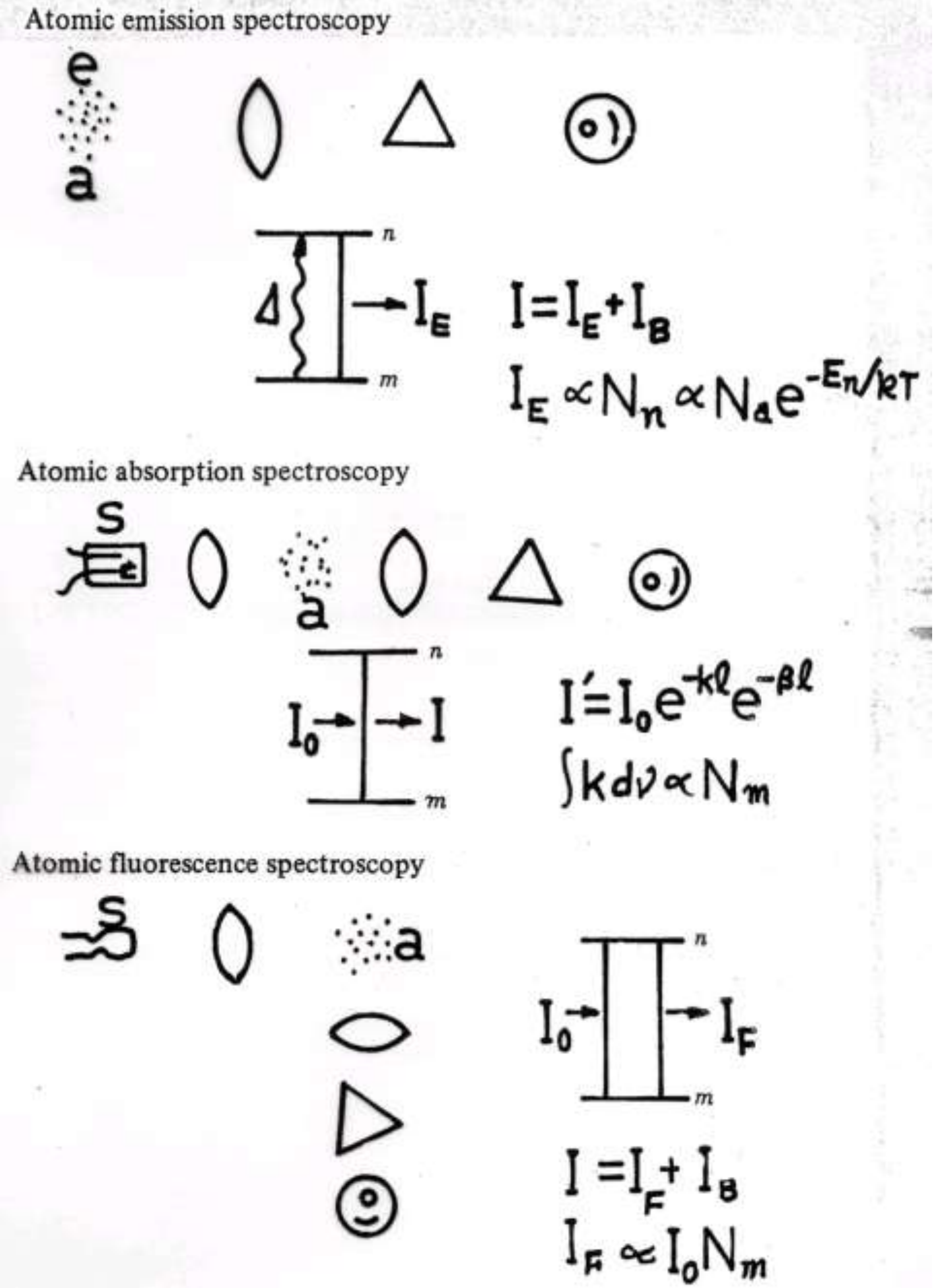

Fig. 2 Schematic diagrams of principle for three kinds of atomic spectroscopy (as for detailed theory, refer to the main text in Chapter 2)

Table 2 Components of analytical atomic spectroscopy

Spectroscopy	Atomization/excitation source
Atomic emission spectroscopy	Chemical flames (air-C_2H_2, air-H_2 etc.)
Flame photometry	Electric discharges
Arc/spark emission	Spark
Inductively coupled plasma	Arc — DC, AC, RF, microwave
	Glow discharge
	Inductively coupled plasma
Atomic absorption spectrometry	Capacitively coupled plasma
	Microwave induced plasma etc.
	Electrothermal atomizer
Zeeman AAS	
	Cold vapor
Atomic fluorescence spectroscopy	Dispersion systems
	Detectors
	Electronics
Atomic magneto-optical rotation spectroscopy	Light sources (hollow cathode lamp, electrodeless discharge lamp etc.)
Multi-line method	

Table 3 Brief chronology of analytical atomic spectroscopy

AES		AAS		AFS	
1666	Light dispersion (Newton)				
		1802	Reversal line (Wollaston)		
		1815	Fraunhofer line (Fraunhofer)		
1860	Flame photometry (Bunsen & Kirchhoff)				
1890s-1930s	Spark/arc-AES, various types of monochromator	1896	Zeeman effect (Zeeman)	1924	Atomic fluorescence (Nicho
		1955	AAS concept (Walsh & Alkemade et al.)		
1961	Prototype of ICP (Reed)	1955-62	Basic development/many patents in Australia and New Zealand		
		1961	ETA (L'vov)	1963	Prediction of AFS (Alkemade)
1962-69	Basic development, detection limit (Fassel et al.)	1962-69	Explosive growth, commercially available systems	1964-69	Theory and basic development (Winefordner et al.)
1965-70	Optimization for low inter-element effect	1969-76	Standardization	1970-	A commercial available non-dispersive instrument, many instrumental improvements
1970-	Mechanism study	1970-	Commercially available EAT's, mechanism study		
		1971	ZAAS (Prugger, Hadeishi)		
1975-80	Explosive growth, commercially available ICP's, standardization	1976-	Commercial available ZAAS, microprocessor	1975-	Dye-laser AFS
1981	ICP-AFS	1982-	New types of (separative) ETA? , trace characterization?	1981	ICP-AFS
1982-	Small sample size, minituarization, detailed mechanism study, other types of plasmas?			1982-	Removal of background scattering, ZAFS? , time-resolved AFS?

PHILOSOPHICAL TRANSACTIONS.

February 19. 16$\frac{71}{72}$.

The CONTENTS.

A Letter of Mr. Isaac Newton, *Professor of the Mathematicks in the University of Cambridge; containing his New Theory about* Light *and* Colors: *sent by the Author to the Publisher from Cambridge, Febr.* 6. 16$\frac{71}{72}$; *in order to be communicated to the* R. Society.

SIR,

TO perform my late promise to you, I shall without further ceremony acquaint you, that in the beginning of the Year 1666 (at which time I applyed my self to the grinding of Optick glasses of other figures than *Spherical*,) I procured me a Triangular glass-Prisme, to try therewith the celebrated *Phænomena* of

about three foot radius (suppose a broad Object-glass of a three foot Telescope,) at the distance of about four or five foot from thence, through which all those colours may at once be transmitted, and made by its Refraction to convene at a further distance of about ten or twelve feet. If at that distance you intercept this light with a sheet of white paper, you will see the colours converted into whiteness again by being mingled. But it is requisite, that the *Prisme* and *Lens* be placed steddy, and that the paper, on which the colours are cast, be moved to and fro; for, by such motion, you will not only find, at what distance the whiteness is most perfect, but also see, how the colours gradually convene, and vanish into whiteness, and afterwards having crossed one another in that place where they compound Whiteness, are again dissipated, and severed, and in an inverted order retain the same colours, which they had before they entered the composition. You may also see, that, if any of the Colours at the *Lens* be intercepted, the Whiteness will be changed into the other colours. And therefore, that the composition of whiteness be perfect, care must be taken, that none of the colours fall besides the *Lens*.

In the annexed design of this Experiment, A B C expresseth the Prism set endwise to sight, close by the hole F of the window

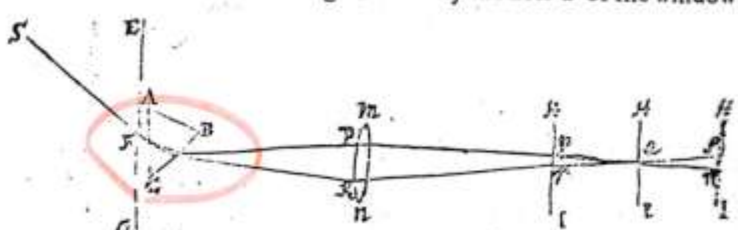

E G. Its vertical Angle A C B may conveniently be about 60 degrees: *M N* designeth the *Lens*. Its breadth 2$\frac{1}{2}$ or 3 inches. S F one of the streight lines, in which difform Rays may be conceived to flow successively from the Sun. F P, and F R two of those Rays unequally refracted, which the *Lens* makes to converge towards Q, and after decussation to diverge again. And H I the paper, at divers distances, on which the colours are projected: which in Q constitute *Whiteness*, but are *Red* and *Yellow* in R, r, and ρ, and *Blew* and *Purple* in P, p, and π.

Phil. Trans. R. S., 92, 365 (1802)

XII. *A Method of examining refractive and dispersive Powers, by prismatic Reflection.* By William Hyde Wollaston, *M. D. F. R. S.*

Read June 24, 1802.

In examining the power with which various substances refract and disperse light, I have for some time past employed a method unnoticed by writers on optical subjects; and, as it is not only convenient in common cases of refraction, but also capable of affording results not attainable by other means, I have been induced to draw up a short account of the method itself, and of the most remarkable instances of its application.

This method was suggested by a consideration of Sir Isaac Newton's prismatic eye-glass, the principle of which depends on the reflection of light at the inner surface of a dense refracting medium.

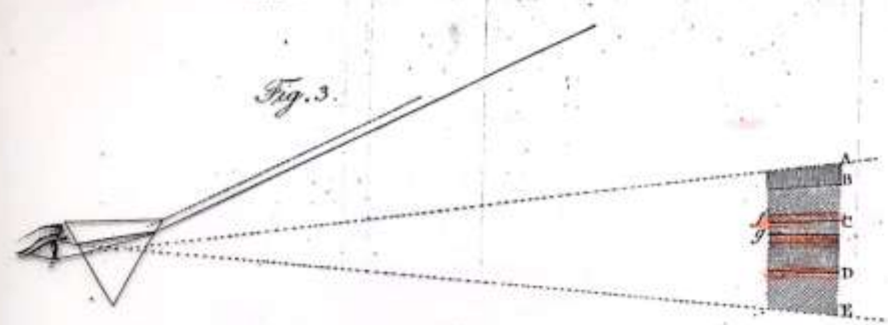

Fig. 3.

Basire Sc.

Ann. phys. Chem., 109, 148 (1860)

XIV. *Ueber die Fraunhofer'schen Linien; von G. Kirchhoff.*

(Aus d. Monatsbericht. d. Berl. Acad. October 1859.)

Fraunhofer
Kirchhoff

Ann. Phys., 110, 160 (1860)

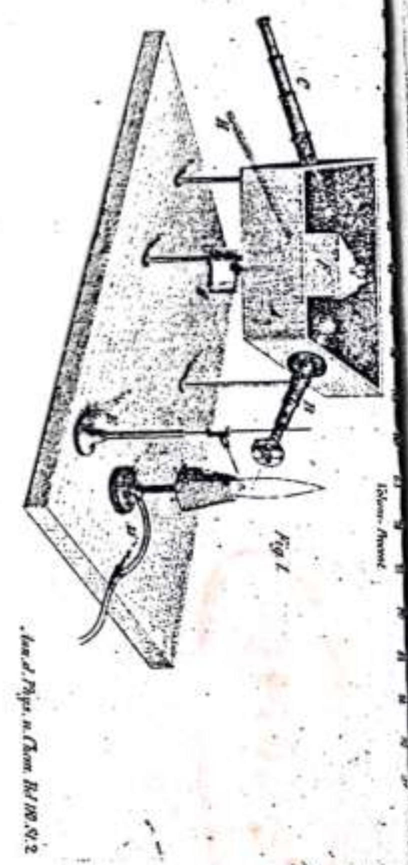

I. Chemische Analyse durch Spectralbeobachtungen; von G. Kirchhoff und R. Bunsen.

Es ist bekannt, dafs manche Substanzen die Eigenschaft haben, wenn sie in eine Flamme gebracht werden, in dem Spectrum derselben gewisse helle Linien hervortreten zu lassen. Man kann auf diese Linien eine Methode der qualitativen Analyse gründen, welche das Gebiet der chemischen Reactionen erheblich erweitert und zur Lösung bisher unzugänglicher Probleme führt. Wir beschränken uns hier zunächst nur darauf, diese Methode für die Metalle der Alkalien und alkalischen Erden zu entwickeln und ihren Werth an einer Reihe von Beispielen zu erläutern.

Die erwähnten Linien zeigen sich um so deutlicher, je höher die Temperatur und je geringer die eigene Leuchtkraft der Flamme ist. Die von Einem von uns angegebene Gaslampe [1]) liefert eine Flamme von sehr hoher Temperatur und sehr kleiner Leuchtkraft, dieselbe ist daher vorzugsweise geeignet zu Versuchen über die jenen Substanzen eigenthümlichen hellen Linien.

Auf Taf. V sind die Spectren dargestellt, welche die genannte Flamme giebt, wenn die so rein als möglich dargestellten Chlorverbindungen von Kalium, Natrium, Lithium, Strontium, Calcium, Baryum in ihr verflüchtigt werden. Das Sonnenspectrum ist, um die Orientirung zu erleichtern, beigefügt.

Die zu den Versuchen benutzte Kaliumverbindung wurde durch Glühen von chlorsaurem Kali, welches zuvor sechs bis achtmal umkrystallisirt war, dargestellt.

1) Diese Annal. Bd. 100, S. 85.

Die Spectren der Alkalien und alkalischen Erden.

Von

G. Kirchhoff und R. Bunsen.

In Taf. I. Fig. 1. haben wir die Metallspectren, welche von uns in zwei Abhandlungen (Pogg. Ann. Bd. 110 und Bd. 113) veröffentlicht sind, in der Ordnung zusammengestellt, welche nach dem chemischen Verhalten der Metalle die angemessenste zu sein scheint. Die Zeichnungen sind unverändert geblieben bis auf eine blaue Linie im Calciumspectrum, die wir früher nicht aufgenommen haben, da sie, den vorzugsweise characteristischen Linien dieses Spectrums an Lichtstärke weit nachstehend, bei unvollkommeneren Apparaten schwer sichtbar ist. Bei der Vollkommenheit des in unserer letzten Abhandlung von uns angegebenen, bereits vielfach verbreiteten, Spectral-Apparates schien es uns indessen geboten, sie nicht zu übergehen, um so mehr, als man sich wiederholt versucht gefühlt hat, dieselbe einem neuen Elemente zuzuschreiben. Andere, schwächere, Linien, welche der neue Apparat in den in Rede stehenden Spectren ausser den dargestellten zeigt, haben wir nachzutragen unterlassen, weil sie bei dem practischen Gebrauch, zu dem die Tafel bestimmt ist, nur wenig Nutzen gewähren, die Auffassung des Eigenthümlichen der einzelnen Spectren aber erschweren würde.

Wir erwähnen bei dieser Gelegenheit ein Verfahren, welches bei spectral-analytischen Untersuchungen wesentlich fördernd ist. Bei dem, in Pogg. Ann. Bd. 113 von uns beschriebenen, Spectralapparate zeigt sich im Gesichtsfelde des Beobachtungsfernrohrs zugleich mit dem zu betrachtenden Spectrum eine Skale. Die einer gewissen hellen Linie entsprechende Skalenablesung ist bei demselben Apparate immer dieselbe, vorausgesetzt, dass an der Stellung der Skale und des Prismas nichts geändert wird, und abgesehen von den nur sehr kleinen Aenderungen, die durch Aenderungen der Temperatur des Prismas hervorgebracht werden. Bei verschiedenen Apparaten ist aber eine Uebereinstimmung

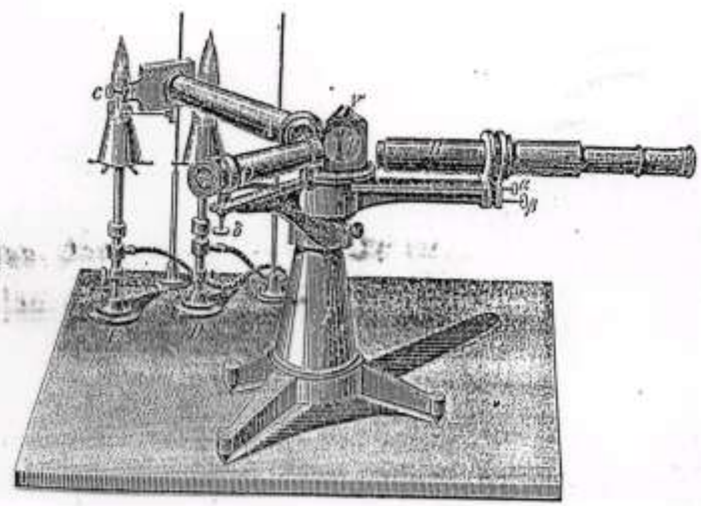

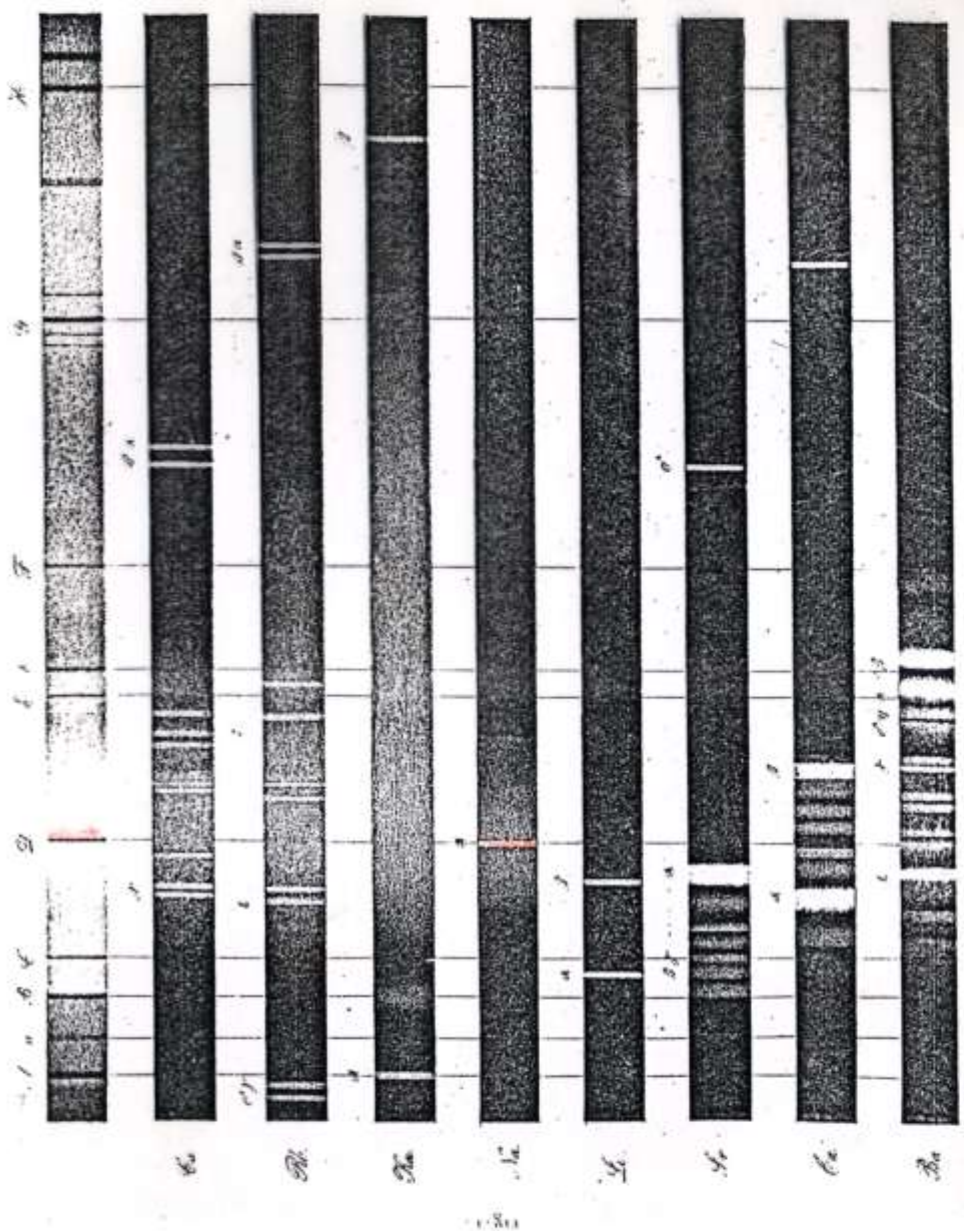

Fresenius' Z. Anal. Chem. 1, 1 (1862).

Die Spectren der Alkalien und alkalischen Erden.

Von

G. Kirchhoff und **R. Bunsen.**

In Taf. I. Fig. 1. haben wir die Metallspectren, welche von uns in zwei Abhandlungen (Pogg. Ann. Bd. 110 und Bd. 113) veröffentlicht sind, in der Ordnung zusammengestellt, welche nach dem chemischen Verhalten der Metalle die angemessenste zu sein scheint. Die Zeichnungen sind unverändert geblieben bis auf eine blaue Linie im Calciumspectrum, die wir früher nicht aufgenommen haben, da sie, den vorzugsweise characteristischen Linien dieses Spectrums an Lichtstärke weit nachstehend, bei unvollkommeneren Apparaten schwer sichtbar ist. Bei der Vollkommenheit des in unserer letzten Abhandlung von uns angegebenen, bereits vielfach verbreiteten, Spectral-Apparates schien es uns indessen geboten, sie nicht zu übergehen, um so mehr, als man sich wiederholt versucht gefühlt hat, dieselbe einem neuen Elemente zuzuschreiben. Andere, schwächere, Linien, welche der neue Apparat in den in Rede stehenden Spectren ausser den dargestellten zeigt, haben wir nachzutragen unterlassen, weil sie bei dem practischen Gebrauch, zu dem die Tafel bestimmt ist, nur wenig Nutzen gewähren, die Auffassung des Eigenthümlichen der einzelnen Spectren aber erschweren würde.

Wir erwähnen bei dieser Gelegenheit ein Verfahren, welches bei spectral-analytischen Untersuchungen wesentlich fördernd ist. Bei dem, in Pogg. Ann. Bd. 113 von uns beschriebenen, Spectralapparate zeigt sich im Gesichtsfelde des Beobachtungsfernrohrs zugleich mit dem zu betrachtenden Spectrum eine Skale. Die einer gewissen hellen Linie

本の線からなることがわかる。波長の長い方をD_1線、短かい方をD_2線と呼ぶ。

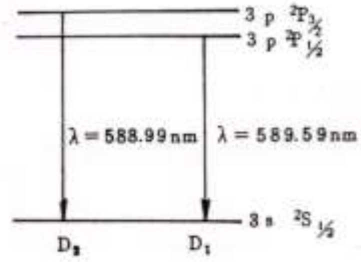

図　3

3．装　置

炎光光度分析と原子吸光分析が行える簡単な組み立て装置が図4に示されている。

光源用電源（実験A3の原子吸光分光計のサイドパネルのスイッチNo.2をHVにする。）

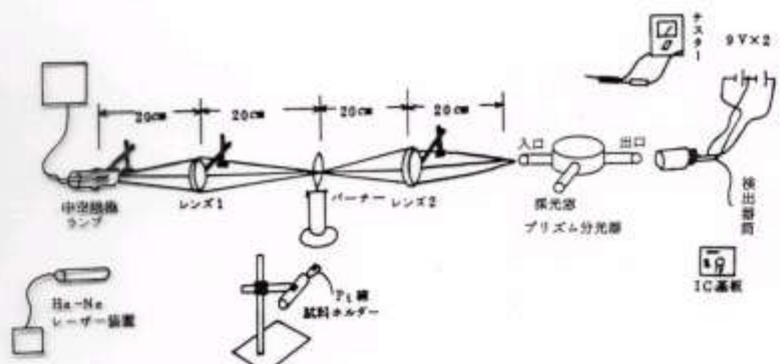

図　4

4．実　験

4－1　試薬の調製……Na_2CO_3、Li_2CO_3を正確にはかりビーカーで希塩酸に溶解し、100mℓメスフラスコに移し標準溶液5％Na、5％Liを調製する。

（Na＝22.99，　Li＝6.941，　Cl＝35.45）

5％Na標準溶液を希釈し50mℓメスフラスコで1，2.5％Naの標準溶液を調製する。

自分の尿、唾液をビーカーに採取する。

4－2　光学調整……図4のように各光学素子を配置する際、光軸が合っていないと光が観測されない。まず中空陰極ランプの位置にクランプでレーザ管を取り付け（中空陰極ランプ、レーザー管共に振動に弱いので絶対落としてはいけない。）電源を入れレーザービームが水平になっているかを、ものさしで調べる（レーザー光は直接見ると目に悪影響を与えるので絶対

g resolving powers up to 15 lines per mm were made.

The spot diagrams were computed from some results[2] of inter-rometer and photographic resolving power tests obtained for a -inch focal length $f/5.5$ Celer type lens, the interferograms ed being for off-axis positions from 8° to 16°. It was decided at sufficient rays (about 750) would be given by a square array f spacing 0.5 mm on the original interferogram of 10 mm diame-r. For convenience, the original interferograms were enlarged 4 mes and printed through a graticule of spacing 2 mm.

For a wave front aberration W, the transverse ray aberration given by $\partial W/\partial(\text{N.A.})$, where N.A. is the numerical aperture. he wave fronts were measured in the sagittal and tangential irections every 2 mm across the enlargement and plotted against merical aperture. The transverse ray aberrations for each plot f the wave front were then obtained by graphical differentiation d plotted against numerical aperture. The spot diagrams were otted from this latter set of graphs.

The photographic plates used at D were prefogged to give a ensity of 1.0 and the exposure time adjusted until the contrast tween a resolved synthesised unit and the background was the as the average contrast given for an easily resolved unit on ving power test film obtained for the lens. The gamma of plates used was very nearly the same as the aerial film used for e resolving power tests. The exposure time had to be redeter-ined for each spot diagram since vignetting caused the number f spots to decrease as the off-axis angle increased.

Then the normal photographic resolving power test may be mulated by printing the spot diagram through each of the test-nit masks in turn onto a separate prefogged plate.

From the results it is hoped to gain some knowledge of the in-ence of the emulsion upon photographic resolving power. It ould also be possible to determine whether diffraction can be nored for the large aberrations shown by this type of lens.

J. Opt. Soc. Amer., 45, 583 (1955)

Double-Beam Method of Spectral Selection with Flames

C. T. J. Alkemade and J. M. W. Milatz
Physisch Laboratorium der Rijksuniversiteit te Utrecht, Utrecht, Holland

(Received December 27, 1954)

A NONDISPERSIVE, optic-electrical filter instrument has been developed that combines good luminosity with high spectral resolving power (~0.1 A), at wavelengths which are of practical interest in spectrochemistry. Use was made of the double-beam method, which is well known in i.r. spectroscopy. In our instrument this method was applied with a flame containing vapor of some element as a specific absorber. This flame (A in Fig. 1) was placed in one of the two light beams (I and II) which

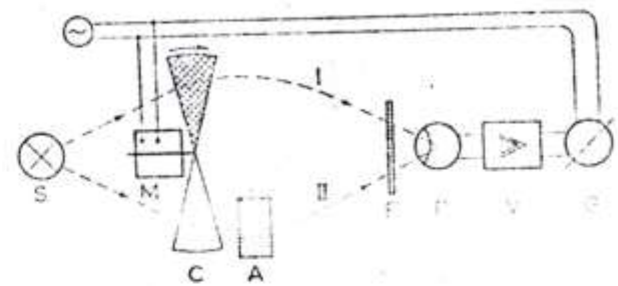

FIG. 1. S = light source to be analyzed; C = rotating disk chopping light-beams I and II in opposite phase; A = specific absorbing medium; F = auxiliary color filter; P = photomultiplier tube; G = synchronous ac measuring device.

are periodically chopped in opposite phase by chopper C. The balance of the double beam, which is detected by a photomultiplier (P) connected to a synchronous measuring device (G) is disturbed for wavelengths that are specifically absorbed by the vapor in the

Spectrochimica Acta, 1955, Vol. 7, pp. 108 to 117. Pergamon Press Ltd., London

The application of atomic absorption spectra to chemical analysis

A. WALSH
Chemical Physics Section, Division of Industrial Chemistry,
Commonwealth Scientific and Industrial Research Organization, Melbourne, Australia

(*Received 18 January 1955*)

Summary—The theoretical factors governing the relationship between atomic absorption and atomic concentration are examined and the experimental problems involved in recording atomic absorption spectra are discussed. On the basis of the discussions, it is shown that such spectra provide a promising method of chemical analysis with vital advantages over emission methods, particularly from the viewpoint of absolute analysis. It is also suggested that the absorption method offers the possibility of providing a simple means of isotopic analysis.

1. Introduction

The application of atomic spectra to chemical analysis has proved so successful over such a wide field that there is a tendency to overlook some of the basic limitations of existing methods. In spite of the remarkable advances in technique which have resulted in press-button analyses of high precision at fantastic speeds, there has been practically no progress whatsoever in solving the fundamental problem of devising an absolute method, i.e., a method which will provide an analysis without comparison with chemically analyzed standards or synthetic samples of known composition. In routine analysis for production control this problem is of little consequence, since it is only necessary to have a limited number of standards, and in such work modern direct-reading methods leave little to be desired, except on the score of complexity of equipment and associated expense. When analyses of miscellaneous materials are required, the task of providing the required range of standards becomes insurmountable and the spectrochemical method then loses its accuracy, since accurate analyses generally necessitate the use of standards which are closely similar in composition to the sample for analysis. In some analyses it is also essential that the sample and standards be similar as regards physical condition. For example, the intensity of the spectrum of a metal or alloy may vary with the metallurgical history of the sample. This difficulty may be overcome by taking the sample into solution, but accurate and sensitive methods of analyzing solutions are only available for the limited range of elements, having a low excitation potential, which can be estimated by flame photometry. In this method, also, it is necessary to use standard solutions having compositions closely similar to that of the test solution.

The possibility of adapting any of the existing methods to absolute analysis does not appear to be promising. In the first place, there seems to be little prospect of developing a light source which is such that the emission spectrum of a given element is not affected by the presence in the atomic vapour of atoms of other elements. Secondly, even if these interelement effects were eliminated, there remains the problem of absolute intensity measurement and the associated problem

Atomic Magneto-optical Rotation (AMOR)

OPTIQUE. — *Sur une nouvelle action subie par la lumière traversant certaines vapeurs métalliques dans un champ magnétique*. Note de MM. D. MACALUSO et O.-M. CORBINO, présentée par M. Lippmann.

« 1. Un faisceau de lumière solaire polarisée par un premier nicol traverse le champ magnétique fourni par un électro-aimant Ruhmkorff, puis un second nicol, une lentille cylindrique, et est reçu sur un réseau concave de Rowland. Avec un oculaire muni d'un micromètre, on observe le second

Compt. Rend. Séance, 127, 548 (1898).

meter and height 15 mm). Along the central axis, a cavity in a circular truncated cone (the upper aperture 2.5 mm diameter, the lower aperture 10 mm diameter and height 15 mm) is bored to conduct the radiation from the light source to the monochromator via the atoms evolving on the glassy carbon strip atomizer. The directions of the magnetic field and the radiation are made to coincide with the Faraday configuration. The magnetic field strength can be altered by changing the distance between the pole pieces. A maximum magnetic field strength of ca. 3 kG was attainable with a gap of 5 mm between the pole pieces.

Fig. 3. The first and second authors holding the cylinder and the constructed AMORS, respectively, the two car batteries and a second author's motor car (Mitsubishi Lancer) to carry them

the intervals between measurements by swit solenoid valve (Chukyo Denki). A small cylin 0°C and 1 atm was used to carry the whole in car. The contents in such a small cylinder we ca. 1,000 measurements.

The overall size of the constructed $60 \times 30 \times 17$ cm and its weight is 15 kg. Figur first and second author holding the cylir constructed AMORS, the car batteries and a se motor car (Mitsubishi Lancer) to carry them, building of our Department. Figure 4 shows the car batteries and the cylinder accommodat of the motor car. Wires connecting the batt AMORS are to be seen. When used, the connected in series to generate 24 V. Two fu connected in a parallel are mounted in the er the motor car and charged during car runn pairs of the car batteries are alternately charged car and discharged by the AMORS.

2.2 Electronic System

Figures 5 and 6 show the block diagram of system constructed and the relevant time c sequences produced by timing circuits, resp photocurrents from the photomultiplier tube ½ inch compact type) are amplified and c corresponding voltages by the preamplifier amplifier IC Intersil LF356) and sent to the f circuits.

During a short period when a hole on the c intersecting the optical axis, a blank volta sponding to the photocurrents induced by t

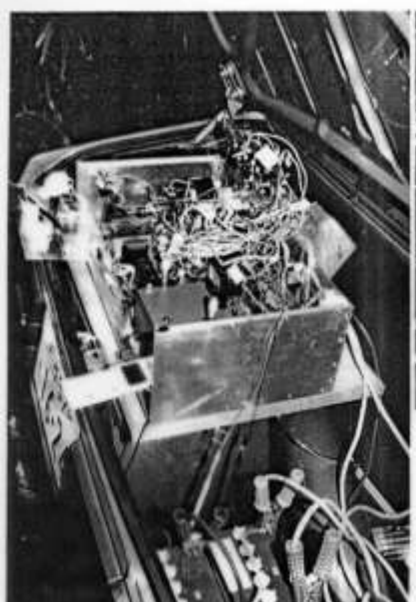

Fig. 4. AMORS accommodated in the trunk of the motor car. The tw batteries, the connecting wires and the cylinder are also seen in the photograph and the components in the AMORS, involving the he atomizer, in the right photograph

K.Kitagawa , Y.Yasui ,
Fresenius' Zeitschrift
fur Analytische Chemie ,
Vol.321 , No.6 , pp.563-571 (1985)

図5-11 車載用小型原子磁気旋光計（ファラデー配置）[11]

In situ analysis

Table 3 Brief chronology of analytical atomic spectroscopy

AES		AAS		AFS	
1666	Light dispersion (Newton)				
		1802	Reversal line (Wollaston)		
		1815	Fraunhofer line (Fraunhofer)		
1860	Flame photometry (Bunsen & Kirchhoff)				
1890s-1930s	Spark/arc-AES, various types of monochromator	1896	Zeeman effect (Zeeman)	1924	Atomic fluorescence (Nichols)
		1955	AAS concept (Walsh & Alkemade et al.)		
1961	Prototype of ICP (Reed)	1955-62	Basic development/many patents in Australia and New Zealand		
		1961	ETA (L'vov)	1963	Prediction of AFS (Alkemade)
1962-69	Basic development, detection limit (Fassel et al.)	1962-69	Explosive growth, commercially available systems	1964-69	Theory and basic development (Winefordner et al.)
1965-70	Optimization for low inter-element effect	1969-76	Standardization	1970-	A commercial available non-dispersive instrument, many instrumental improvements
1970-	Mechanism study	1970-	Commercially available EAT's, mechanism study		
		1971	ZAAS (Prugger, Hadeishi)		
1975-80	Explosive growth, commercially available ICP's, standardization	1976-	Commercial available ZAAS, microprocessor	1975-	Dye-laser AFS
1981	ICP-AFS	1982-	New types of (separative) ETA , trace characterization	1981	ICP-AFS
1982-	Small sample size, minituarization, detailed mechanism study, other types of plasmas			1982-	Removal of background scattering, ZAFS , time-resolved AFS

ICP-MS, LEI, AMOR (CFS) PAS

ADR

原子吸光分光法の登場 (Appearance of AAS)

1955年、Walsh[10]と Alkemade[118]らは別々に、原子蒸気を通過するとき共鳴光が吸収され

discharge
Oh, plasma

flames

somethin[illegible]id
blood pl[illegible]asma(原形質)

Why are you plasma?
(πλασμα)

Masaki

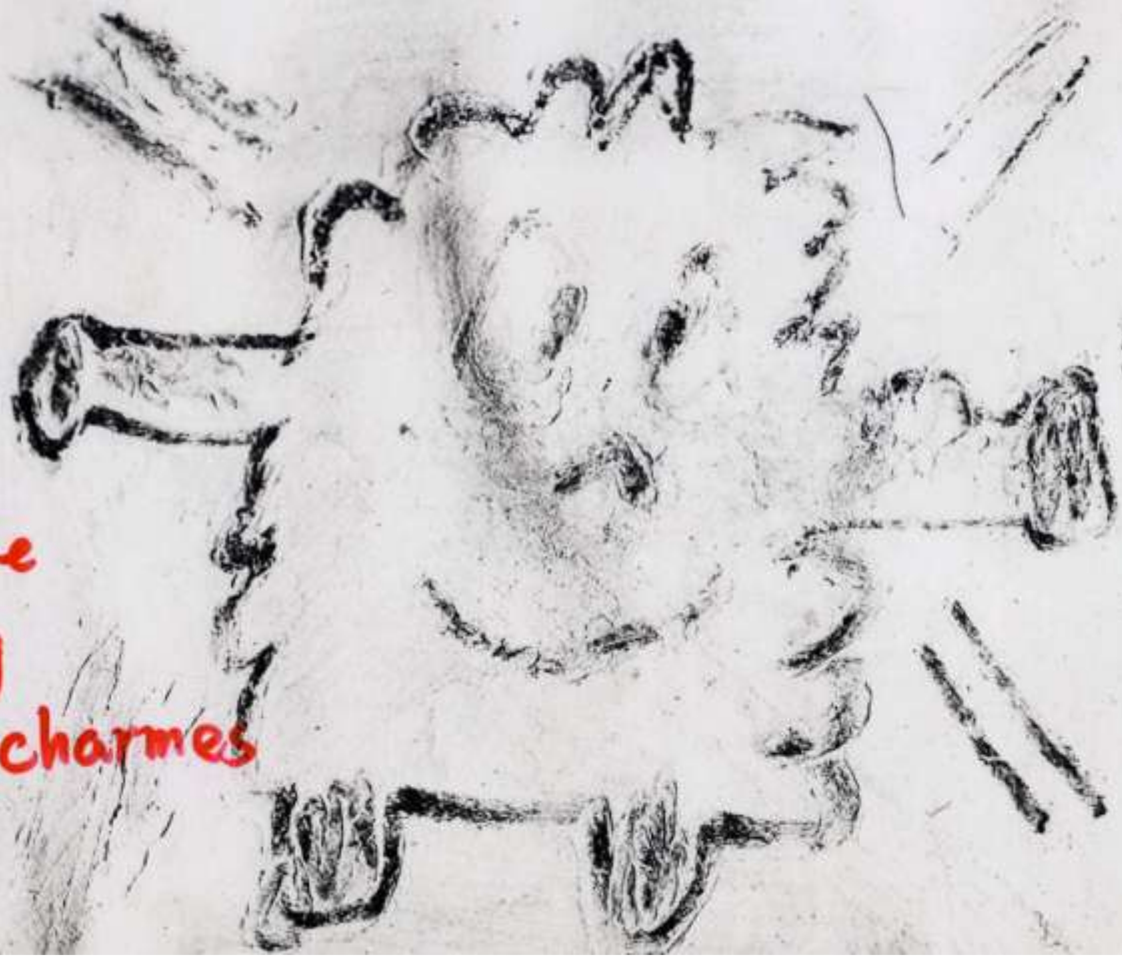

Subtle
thing
but charmes
me!

Flame

Plasma--subtle thing like [?]!

cf. a Japanese traditional saying

"Woman's mind & autumn sky"

Therefore, she charms me.

原子分光分析のための原子化器・励起源

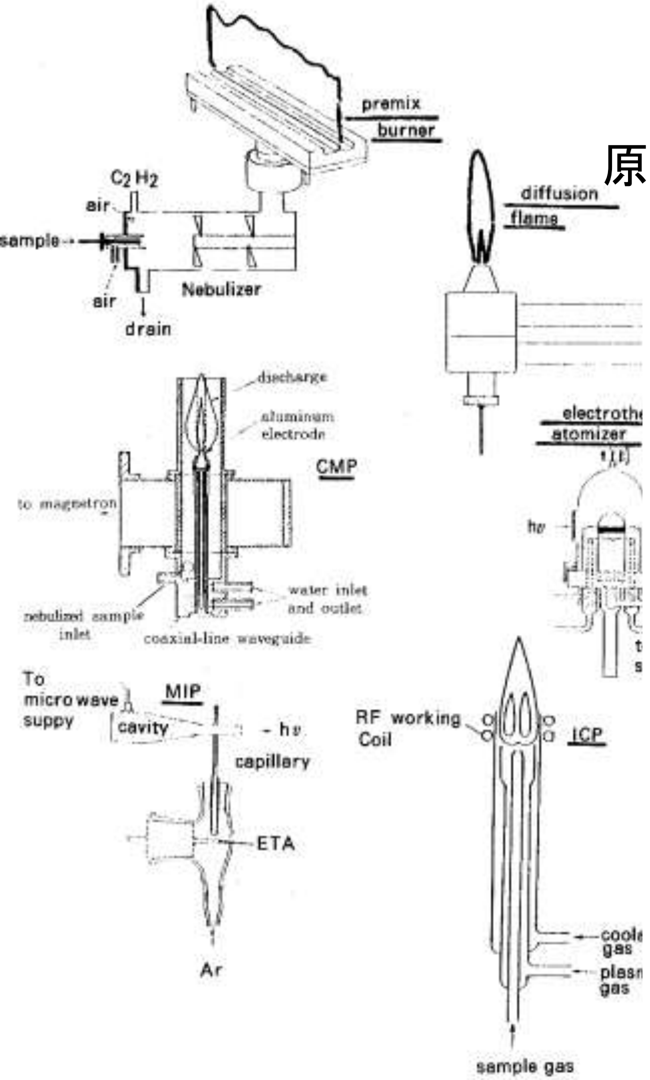

Fig. 1. Various types of atomizers and excitation sources

the air-acety
For the atc
suitable bec
care must b

stable leve
analysis of
at atmospl
high sensit

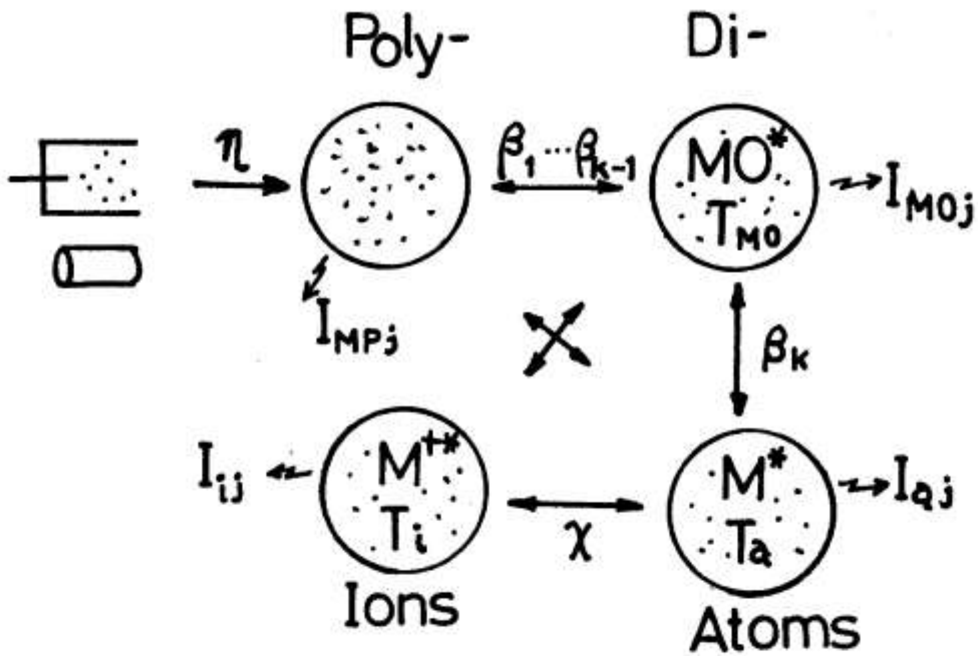

Fig. 2. Model system of atomizers and excitation sources

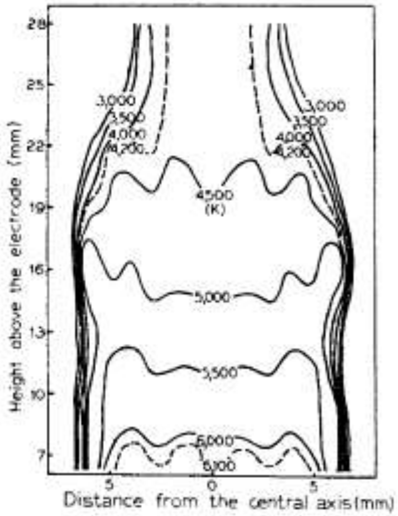

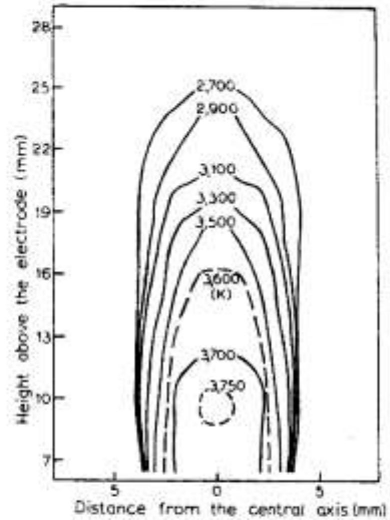

Fig. 5. Profile of excitation temperature of manganese atoms in argon plasma torch.

Fig. 6. Profile of excitation temperature of manganese atoms in nitrogen plasma torch.

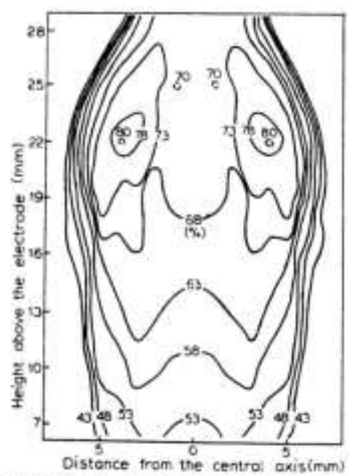

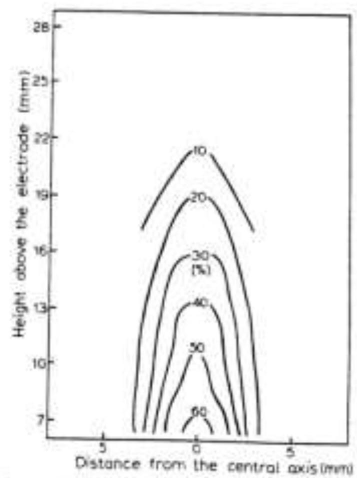

Fig. 7. Profile of degree of ionization of manganese atoms in argon plasma.

Fig. 8. Profile of degree of ionization of manganese atoms in nitrogen plasma.

K.Kitagawa , T.Takeuchi ,
Analytica Chimica Acta ,
Vol.60 , pp.309-318 (1972)

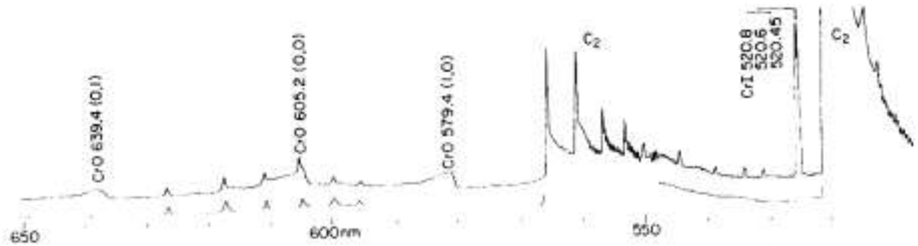

Fig. 4. Typical emission spectrum of CrO displayed on the oscillograph.

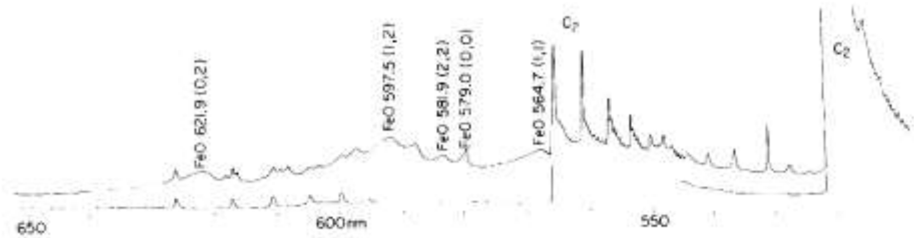

Fig. 5. Typical emission spectrum of FeO displayed on the oscillograph.

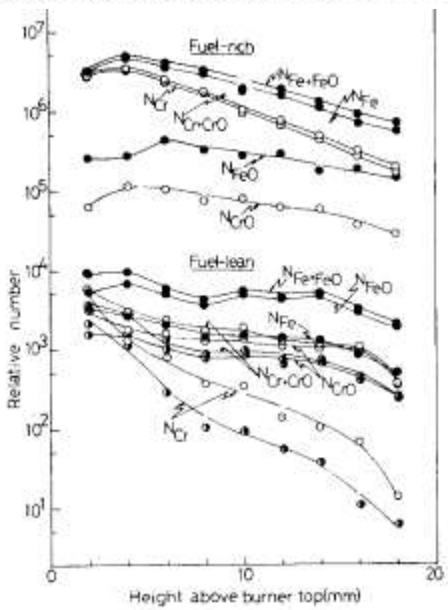

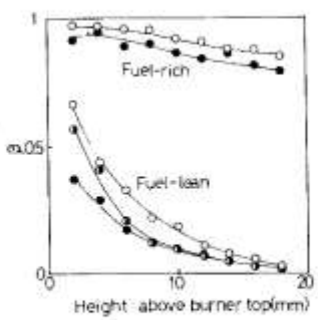

Fig. 8. Distribution of the relative number of species in fuel-rich and lean flames. The relative numbers of iron species are divided by the molar concentration ratio 20:80. (○) Cr(III); (◑) Cr(VI); (●) Fe(III).

Fig. 9. Distribution of the β values. (○) Cr(III); (◑) Cr(VI); (●) Fe(III).

K.Kitagawa , T.Takeuchi ,
Analytica Chimica Acta ,
Vol.60 , pp.309-318 (1972)

- ＜社会人時代＞（昭和48 - 50年）
- 日立製作所 那珂工場勤務：旋盤工として半年の勤務を経て、保田和雄先生や小泉英明先生とZeeman原子吸光分析装置の開発や販売に従事した。水銀、直接分析のためにランプに磁場を印加し、サイドに分裂するσ成分をバックグラウンド吸光、変化しないπ成分を原子吸光に利用し、バックグラウンド補正を行った。後に、原子化器に磁場を印加する、逆ゼーマンへ展開した。（これは今なお販売されるヒット商品となるが、新規開発されない現状に嬉しくもあり悲しくもあり・・）他に、開発部のトラブルターミネーターとして全国各地を回った。

図1　501形日立ゼーマン水銀分析計

日立評論　VOL. 56　No. 11(1974-11)　1124

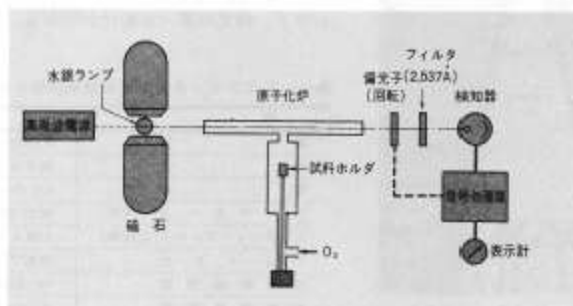

図2　501形日立ゼーマン水銀分析計構造図

- 直接分析

Laser-assisted HF-heated cup glow discharge lamp for direct solid sample analysis

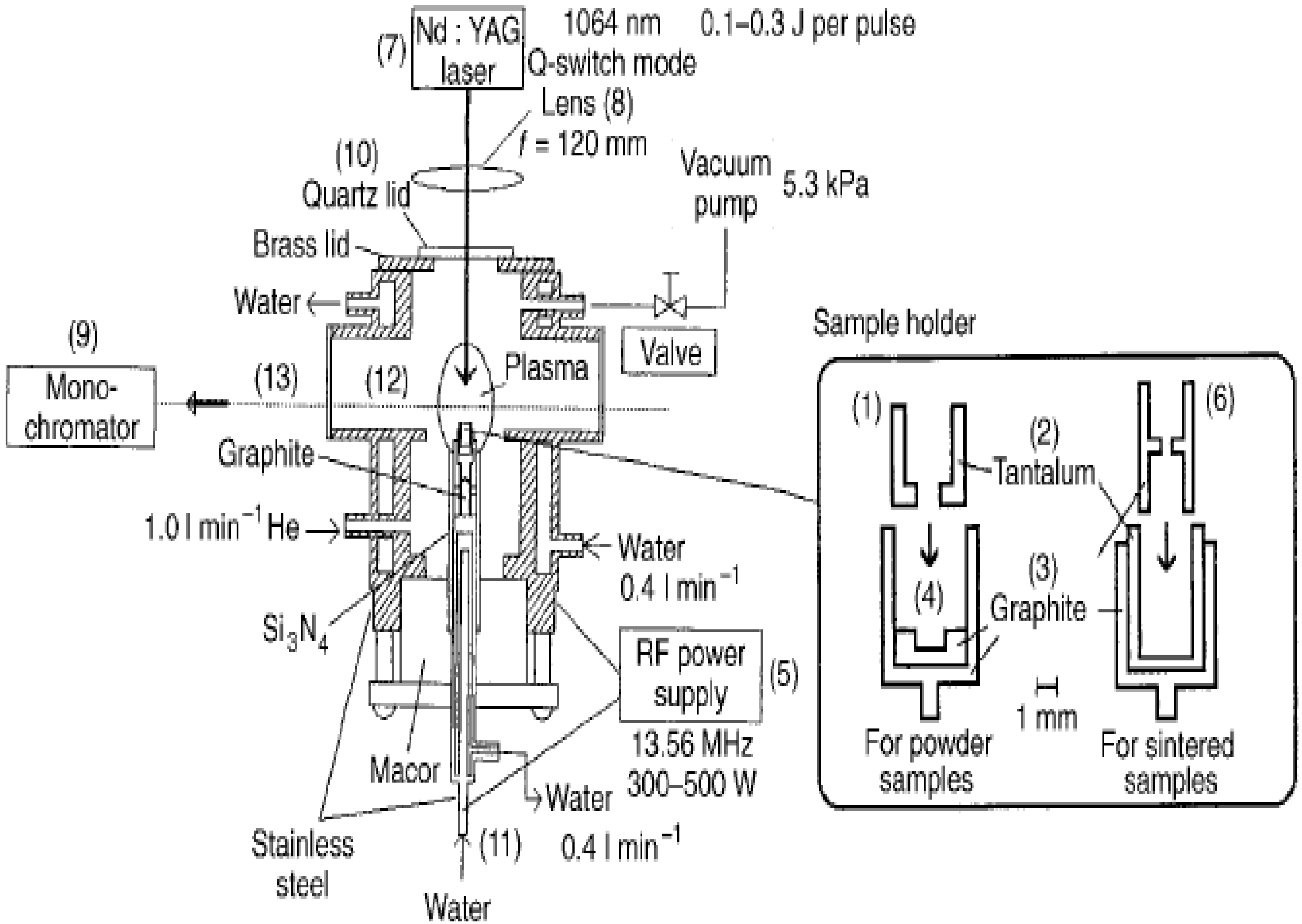

Fig. 1 Schematic diagram of the experimental system: (1) sample holder; (2) tantalum lid; (3) graphite cup; (4) graphite disk; (5) rf power source; (6) different type of sample holder for sintered ceramics; (7) Nd:YAG laser; (8) laser beam-focusing lens; (9) spectrometer; (10) quartz window for laser irradiation; (11) central electrode; (12) discharge chamber; and (13) quartz window for optical observation.

T.Ogura , H.Inoue , S.Tsuge , K.Kitagawa , N.Arai , Journal of Analytical Atomic Spectrometry , Vol.12(8) , pp.823-826 (1997)

Table 1 Experimental conditions

Rf power	500 W (2100 °C),* or 350 W (1800 °C),† SWR = 1.5–3
Laser pulse	10 pulses s^{-1}, 124 mJ per pulse,* 270 mJ/pulse,† Q-switch mode
He pressure	5.3 kPa
He flow rate	1.0 l min^{-1} (NTP)
Bandpass of spectrometer	0.045 nm
Observation height	0–25 μm above the sample holder top
PMT voltage	− 810 V (max.)
Flow rate of coolant water	0.4 l min^{-1}

* For powdered samples.
† For sintered samples.

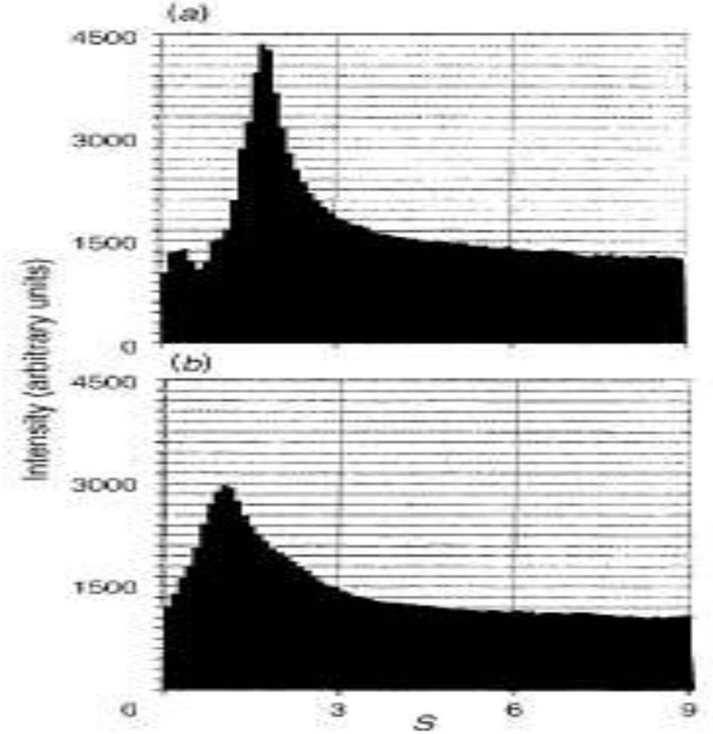

Fig. 2 Effect of laser irradiation on the emission peak in direct excitation of powder ceramics (*a*) with and (*b*) without laser irradiation. Sample, silicon nitride powder (SN-BL, Japan Fine Ceramics Center).

Table 2 Effect of laser irradiation on Al emission peak in direct excitation of powder ceramics ($n = 4$). The sample and the conditions are the same as in Fig. 1.

	Without laser	With laser	Ratio
Average peak area (arbitrary units)	930*	1600	2.6
RSD (%)	5.1	2.8	0.55

* Sample powder residue was occasionally found in the cup. This value is based on 100% introduction.

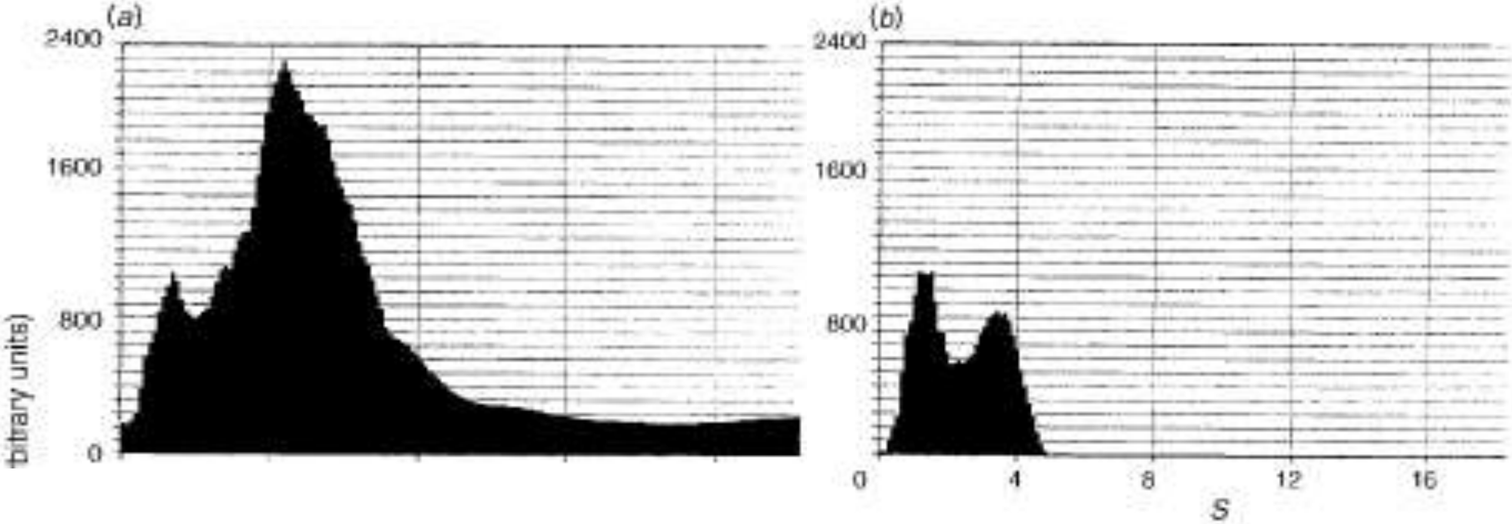

Fig. 3 Effect of laser irradiation on emission peak in direct excitation of sintered ceramics (*a*) with and (*b*) without laser irradiation. Sample, sintered silicon nitride (Japan Fine Ceramics Center) cut to about 1 mm^3 (6–11 mg) with a diamond cutter. Wavelength = Mg I 279.553 nm.

Table 3 Effect of laser irradiation on Mg emission peak in direct excitation of sintered ceramics ($n = 3$)

	Without laser	With laser	Ratio
Average peak area for 1 mg of the initial sample (arbitrary units)	1360	6660	4.9
RSD (%)	22.8	3.6	0.16
Average vaporized mass* (%)	17.7	43.6	2.5
Normalized peak area by ablated mass (arbitrary units)	7680	15300	2.0

* Calculated as 100(1 − residue mass/mass introduced).

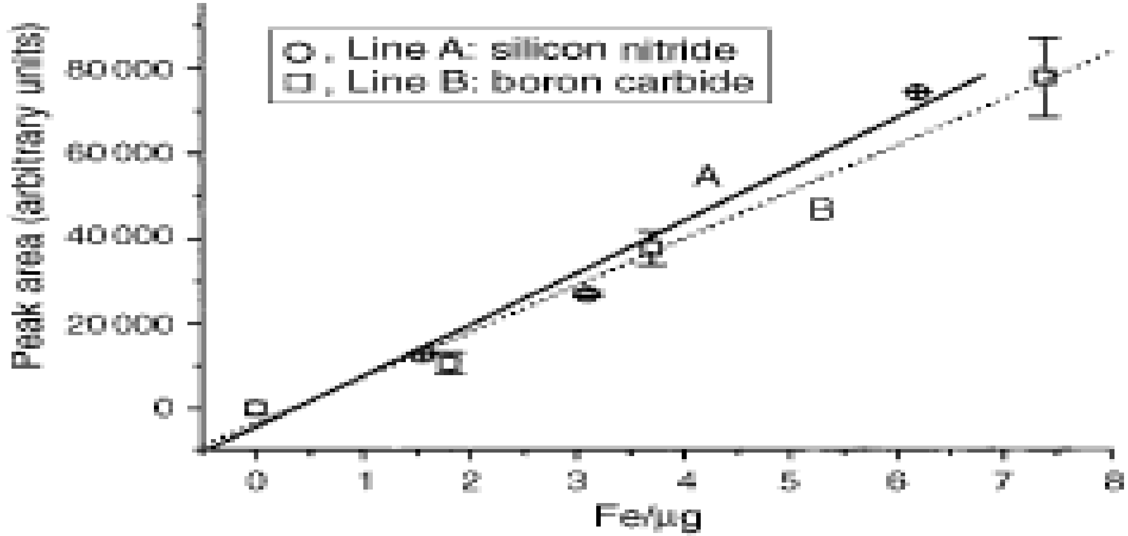

Fig. 4 Calibration curve for direct determination of Fe in silicon nitride using powder standards: ○ and A, with the powdered standard of silicon nitride; □ and B, with the powdered standard of boron carbide.

Table 4 Direct determination of Fe in sintered silicon nitride using powder standards ($n = 3$). Wavelength = Fe II 259.940 nm*

	Powder standard	
	Silicon nitride	Boron carbide
Found (%)	0.039	0.042
Relative error (%) from the reference of 0.048%	23	14
RSD (%)	5.6	18

* The sample of sintered silicon nitride and standards are those available from the Japan Fine Ceramic Center.

直接分析のための分離原子化器

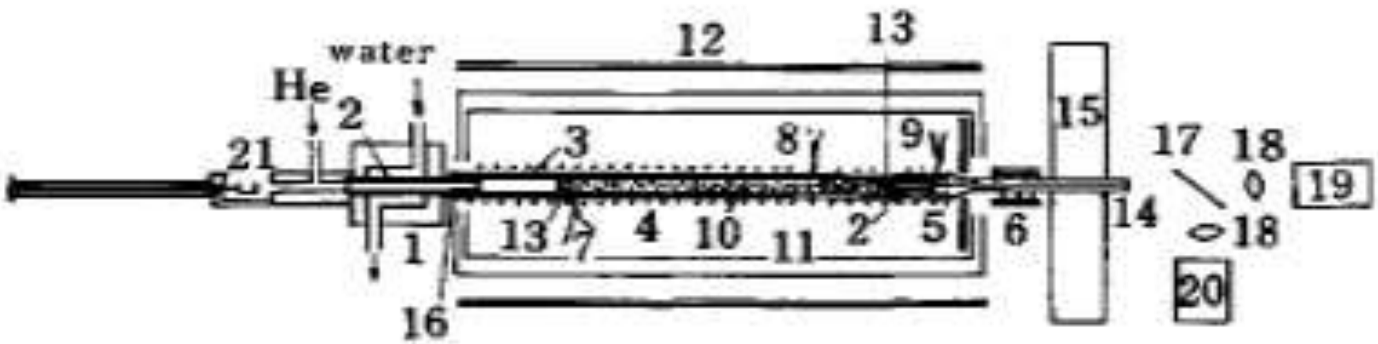

Fig. 1 Schematic diagram of the separative column ato izer/microwave-induced plasma system (SCA-MIP). condenser; 2, recrystallized alumina tube (4 mm i.d., 6 n o.d.); 3, recrystallized alumina tube (6 mm i.d., 10 mm o.c.,, 4, Kanthal wire heater 1; 5, Kanthal wire heater 2; 6, Kanthal

wire heater 3; 7, thermocouple (Pt/PtRh) 1; 8, thermocouple 2; 9, thermocouple 3; 10, activated charcoal (30 – 60 mesh); 11, ceramics case; 12, stainless steel case; 13, silica-alumina wool; 14, MIP discharge tube; 15, TM_{010} microwave cavity;

16, ceramics adhesive (Toa Gosei Aron Ceramics-D); 17, grid mirror; 18, lens; 19, spectrometer 1 (Nippon Jarrell Ash); 20, spectrometer 2 (Jobin Yvon); 21, sample holder (Mo cup).

Table 1 Equipment

Spectrometer
Nippon Jarrell-Ash Model JE–50E, f=0.5 m photomultiplier tube HTV R666
Jobin-Yvon Model H20UV, f=0.2 m, photomultiplier tube R763
Photomultiplier tube power supply
Laboratory-made
Microwave power supply
Electromedical Supply Model Microtron 200 MK–2
Microwave cavity
Laboratory-made silver-plated brass TM_{010} type (92 mm i.d., 122 mm o.d., 15 mm height and 8 mm hole)
X-Ray fluorescence analyzer
Kevex/Rigaku Model Untratrace System 0600
Strip chart recorder
Toa Denpa Model FBR–251A and 252A

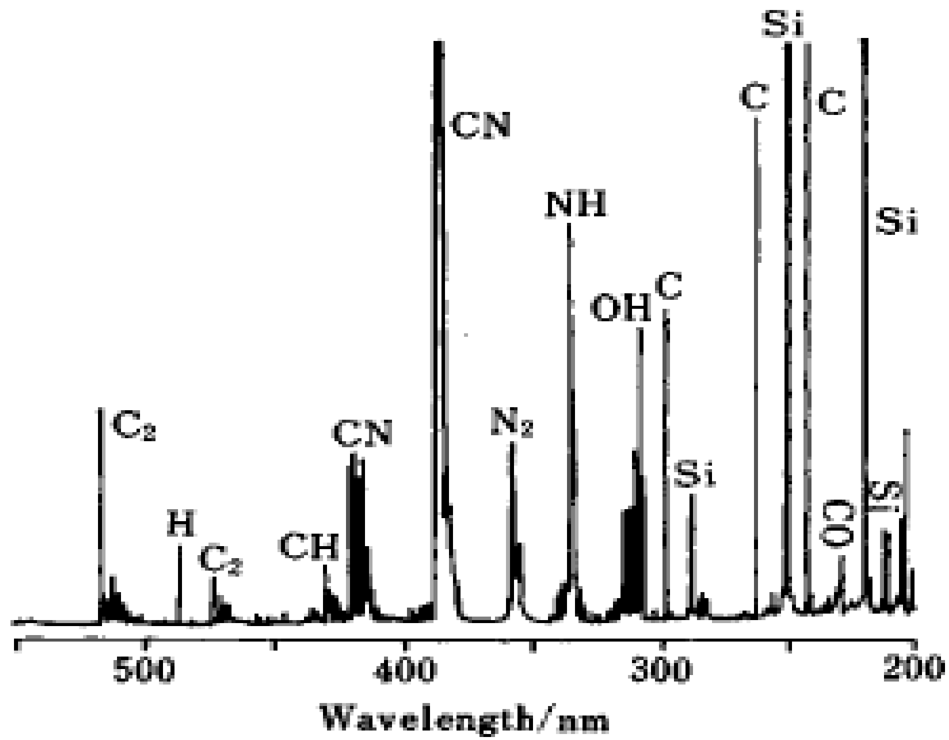

Fig. 2 Background emission spectrum from the SCA–MIP system. Discharge tube, fused silica tube (2 mm i.d., 4 mm o.d.) cooled with air; microwave power, 80 W incident and 5 W reflected; He carrier, 100 ml min^{-1} STP.

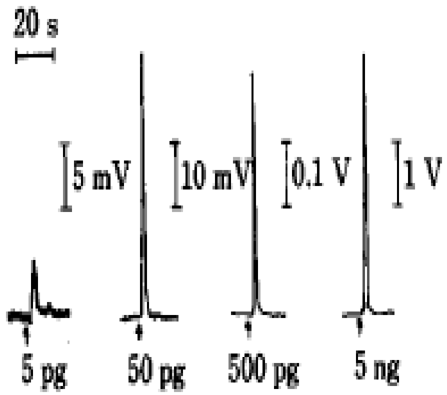

Fig. 3 Typical signal traces of Hg emission. Sample, 5 μl of $HgCl_2$/0.5%EDTA·$2NH_4$; wavelength, 253.65 nm; column temperature, 1100° C (column middle); arrows, sample introduction.

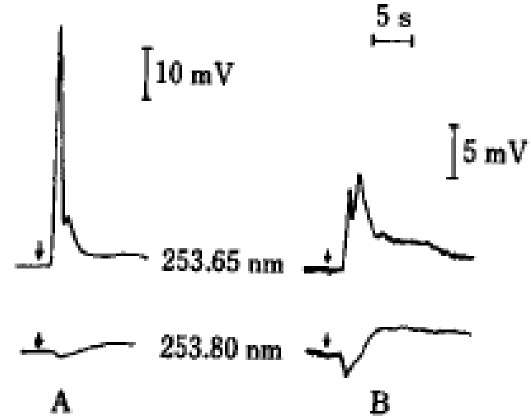

Fig. 4 Typical signal traces of Hg emission with solid samples. A, NBS Orchard Leaves SRM 1571 0.64 mg in 5 μl suspension; B, Bovine Liver SRM 1577 0.68 mg in 5 μl suspension; SCA condition, same as in Fig. 3.

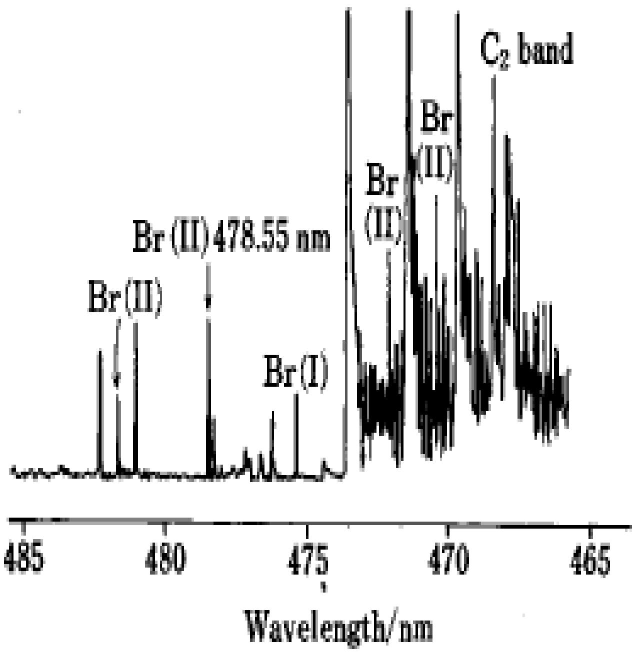

Fig. 5 Emission spectrum of Br from the SCA-MIP. Sample, bromobenzene saturated in the He carrier; SCA condition, same as in Fig. 3.

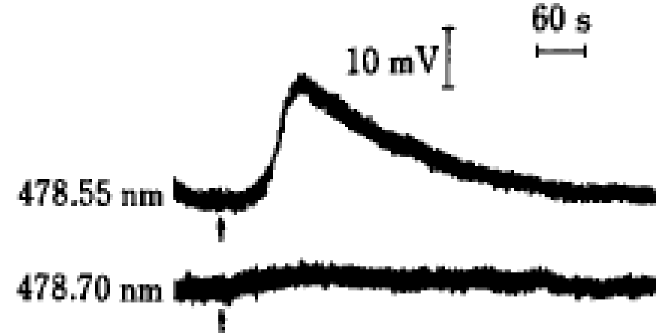

Fig. 7 Typical signal traces of Br and background emissions. Column temperature, 1280°C (column middle); He carrier, 100 ml min^{-1} STP; sample 20 μgBr (5 μl) as NH_4Br.

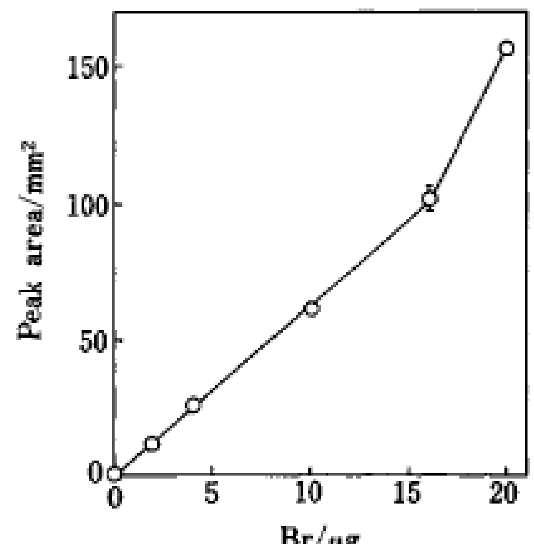

Fig. 8 Calibration curve of Br. Sample, 5 μl as NH_4Br; He carrier, 400 ml min^{-1} STP; column temperature, same as in Fig. 7.

直接分析のための原子磁気旋光分光法

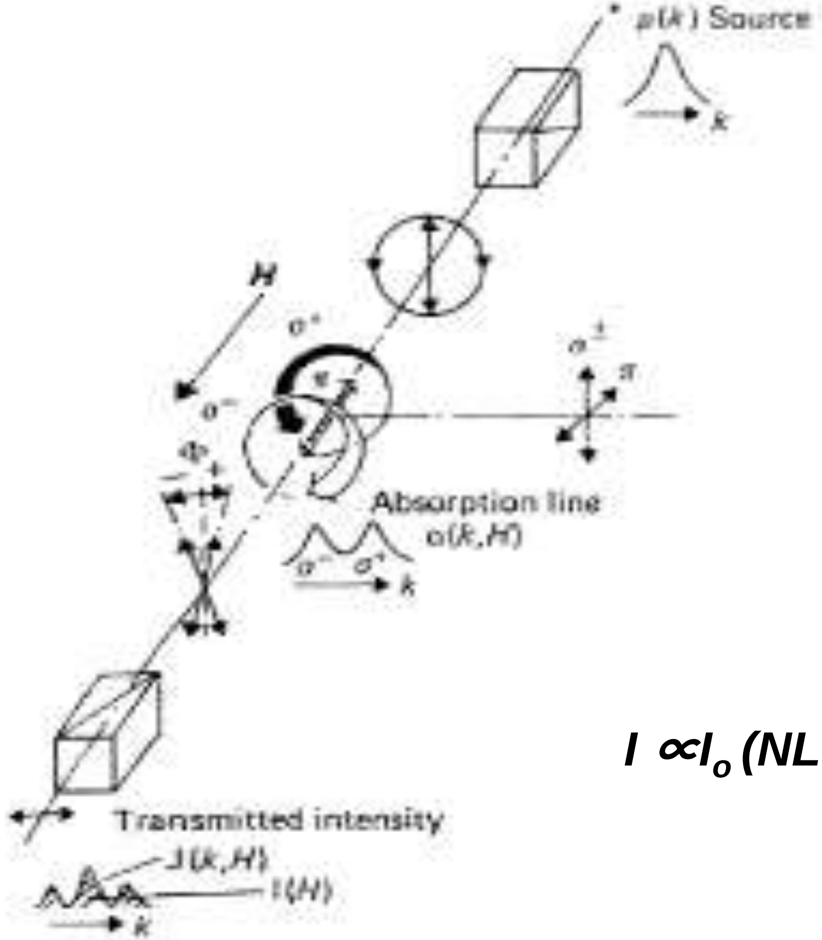

Fig. 2. Relation between the Faraday effect and the Zeeman effect.

$$I \propto I_o (NLf)^2 M(H)$$

K.Kitagawa , T.Shigeyasu , T.Takeuchi , Analyst , Vol.103 (1231) , pp.1021-1030 (l978)

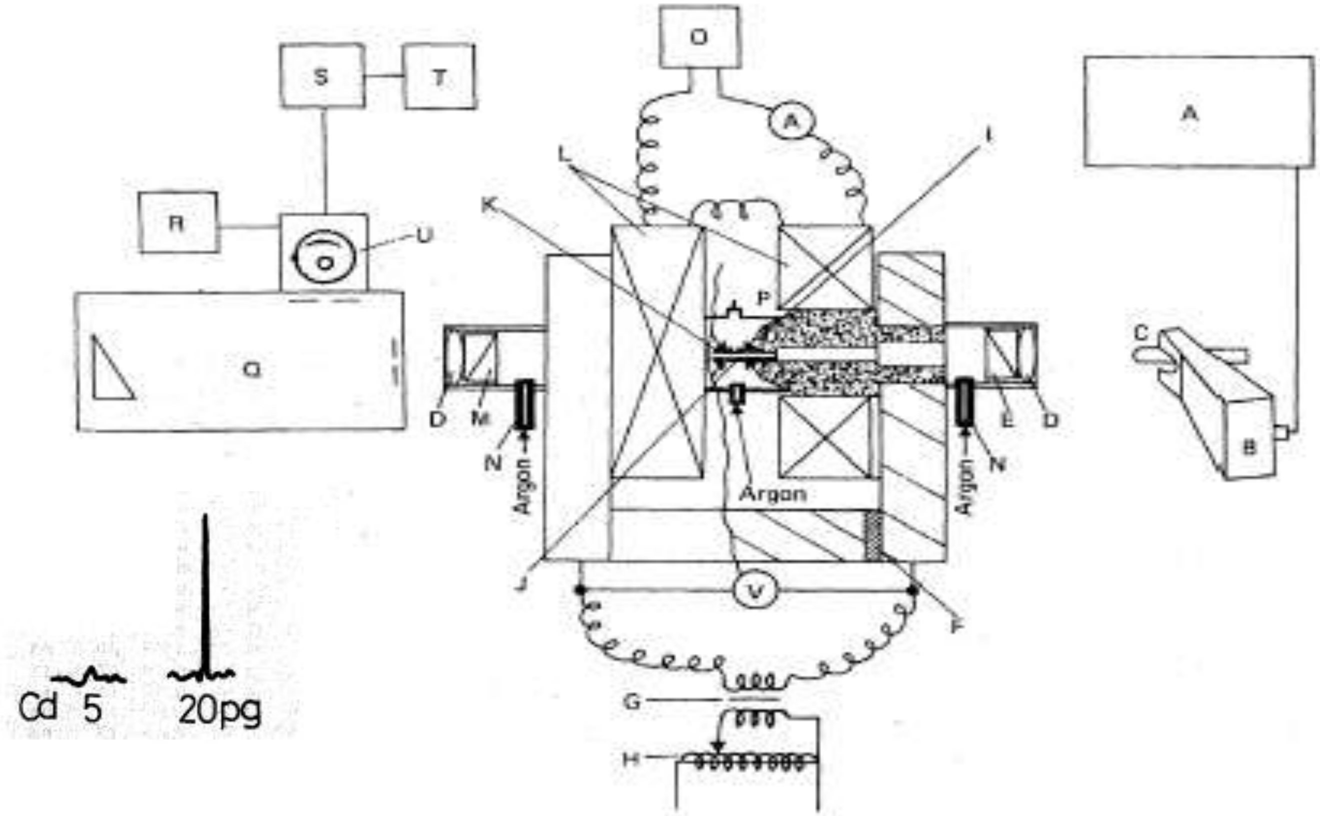

Fig. 4. Schematic diagram of the optical system: A, microwave power supply for the electrodeless discharge lamp; B, microwave cavity; C, electrodeless discharge lamp; D, lens; E, polarizer; F, insulator; G, transformer; H, variable transformer; I, pole piece; J, graphite tube atomizer; K, graphite cone; L, solenoid coil; M, analyzer; N, gas inlet; O, power supply for the solenoid coil; P, chamber; Q, prism monochromator; R, stabilizer for high-voltage supply for the photomultiplier tube; S, d.c. amplifier; T, strip-chart recorder; and U, photomultiplier tube.

K.Kitagawa , T.Shigeyasu , T.Takeuchi , Analyst , Vol.103 (1231) , pp.1021-1030 (l978)

吸光の補正　$I_{corr}=I_{amor}/I_{aas+bga}$

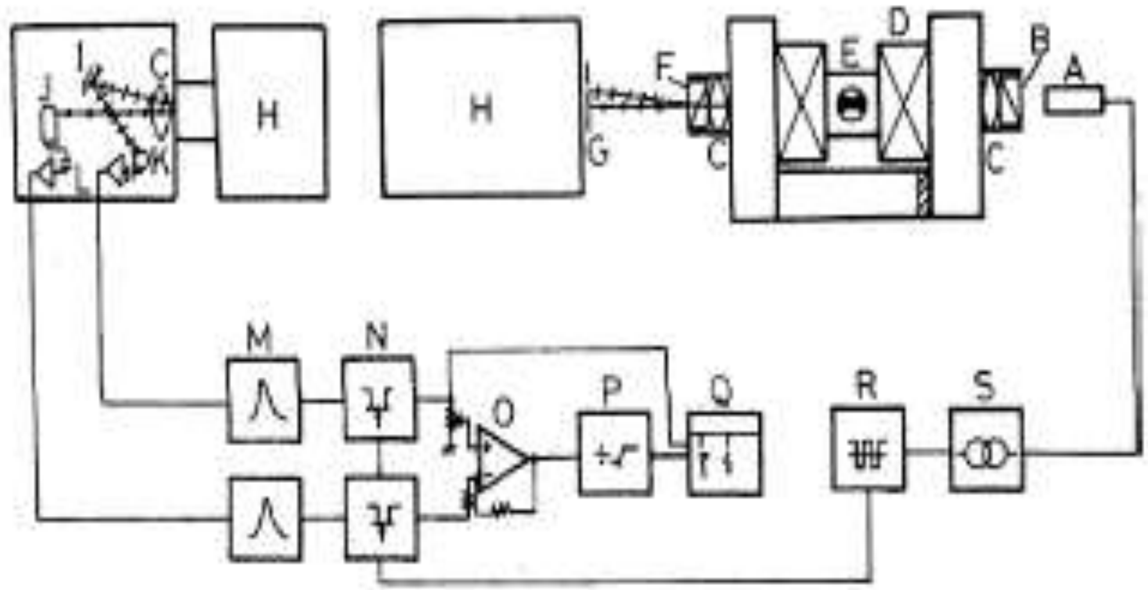

Fig. 8. Schematic diagram of the experimental arrangement. (A) hollow cathode lamp, (B) Glan-type prism, (C) lens, (D) electromagnet, (E) graphite tube atomizer and atomization chamber, (F) Rochon prism, (G) iris diaphragm, (H) prism monochromator, (I) plane mirror, (J) photomultiplier tube (R955), (K) photomultiplier tube (R306), (L) a.c. preamplifier, (M) bandpass filter amplifier, (N) phase-sensitive rectifier, (O) off-set amplifier, (P) operational amplifier for dividing and square root processing, (Q) strip chart recorder, (R) pulse generator and (S) current stabilizing power supply.

K.Kitagawa , T.Koyama , T.Takeuchi , Analyst , Vol.104 (1242) , pp.822-830 (l979)

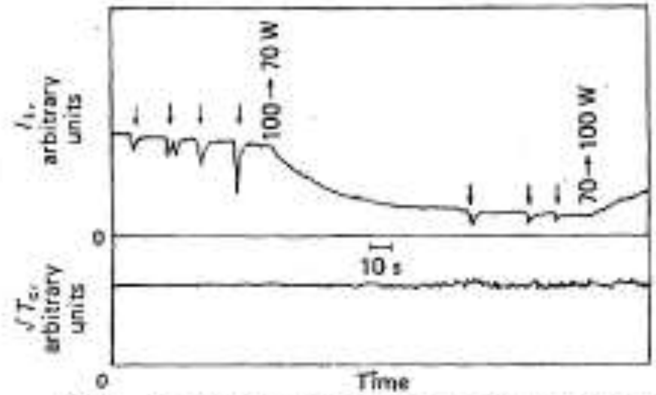

Fig. 9. Traces showing correction for energy loss and variation in intensity of source radiation. Arrows indicate the introduction of cigarette smoke.

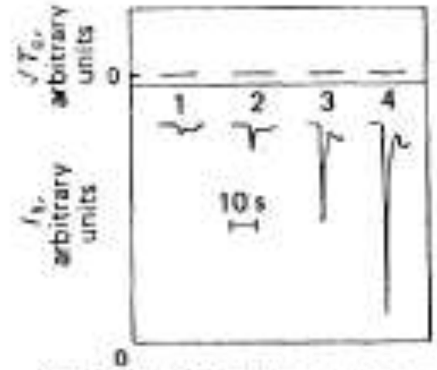

Fig. 10. Oscilloscope traces of the corrected response for pyrolysis of different amounts of starch at the atomization temperature of 1800 °C, showing the background scattering. 1, No starch; 2, 2.5 μg of starch; 3, 5 μg of starch; and 4, 10 μg of starch.

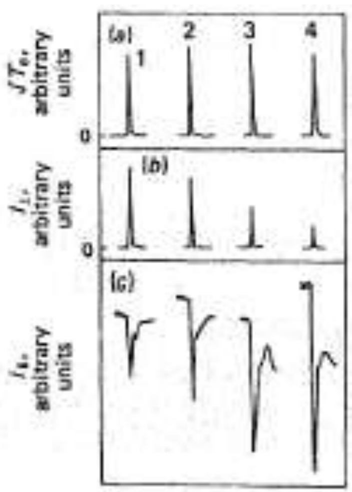

Fig. 11. Correction of energy loss and variation in intensity of source radiation for electrothermal atomization. 1, 50 pg of cadmium; 2, 5 μg of starch added; 3, 10 μg of starch added; and 4, 15 μg of starch added. See text for explanation of (a), (b) and (c).

K.Kitagawa , T.Koyama , T.Takeuchi , Analyst , Vol.104 (1242) , pp.822-830 (l979)

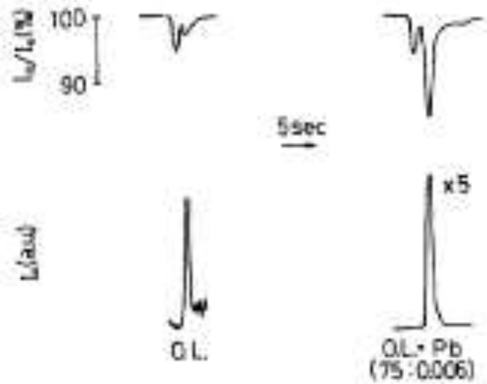

Fig. 12. Typical peaks of I_L and I_B for NBS Orchard Leaves SRM 1571. O.L. = Orchard Leaves.

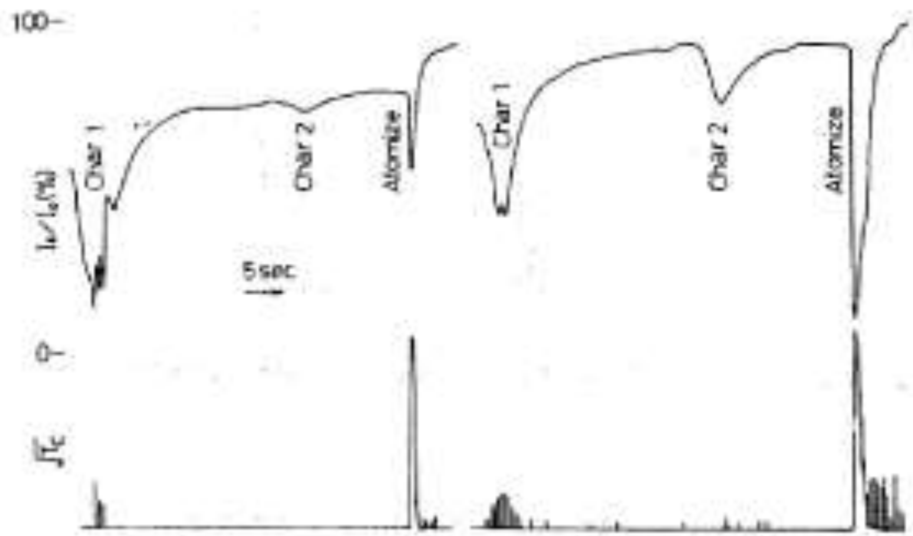

Fig. 14. Two typical cases of correction in the analysis of human blood.

K.Kitagawa , T.Koyama , T.Takeuchi , Analyst , Vol.104 (1242) , pp.822-830 (l979)

Table 1. Results of analysis

Element	Sample		Found* S.A.M.	Found* C.M.	Certificate or reference
Pb	NBS Orchard Leaves SRM 1571 (ppm)		45.3 ± 0.9		45 ± 3
	Human blood (n g ml^{-1})	1	106 ± 19	120 ± 22	90†
		2	100 ± 16	110 ± 21	110†
		3	144 ± 19	138 ± 26	140†
	Volcanic ashes (ppm)	1		3.5 ± 0.7‡	
		2		4.3 ± 0.7§	
		3			5‖
Mn	Volcanic ashes (%)			0.069±0.007	0.07
Cr	Orchard Leaves (ppm)		(350°C)	2.4±0.5	2.6±0.3
			(700°C)	2.3±0.4	
	Volcanic ashes (ppm)	1		28±10‡	29‖
		2		34±5§	

* Results based on at least five replicate determinations.

† Taken from normal persons in December, 1979 and analysed in Public Health Research Laboratory, Medical School, Nagoya City University, Mizuhokawasumi, Mizuho-ku, Nagoya, Japan.

‡ Taken near the 8th station of Ontake Volcano in November, 1979.

§ Taken in Kaida Village, Nagano, Japan, in November, 1979.

‖ Taken in Shinbashi, Nagano, Japan, in November, 1979 and analysed in Nagano Research Institute for Health and Pollution, Kome-mura, Oaza-Amori, Nagano, Japan.

S.A.M. = Standard Addition Method.

C.M. = Calibration Method.

Precisions given in terms of S.D.

Temperatures in parentheses are charring temperature.

K.Kitagawa , T.Koyama , T.Takeuchi ,
Analyst , Vol.104 (1242) ,
pp.822-830 (l979)

No. 18'

車載用小型原子磁

ファラデー配置)(1)

analysis

the car batteries and the cylinder accommodat
of the motor car. Wires connecting the batt
AMORS are to be seen. When used, the
connected in series to generate 24 V. Two fu
connected in a parallel are mounted in the e
the motor car and charged during car run
pairs of the car batteries are alternately charge
car and discharged by the AMORS.

2.2 Electronic System

Figures 5 and 6 show the block diagram of
system constructed and the relevant time c
sequences produced by timing circuits, res
photocurrents from the photomultiplier tube
½ inch compact type) are amplified and c
corresponding voltages by the preamplifier
amplifier IC Intersil LF356) and sent to the f
circuits.

During a short period when a hole on the c
intersecting the optical axis, a blank volta
sponding to the photocurrents induced by

Fig. 3. The first and second authors holding the cylinder and the constructed AMORS, respectively, the two car batteries and a second author's motor car (Mitsubishi Lancer) to carry them

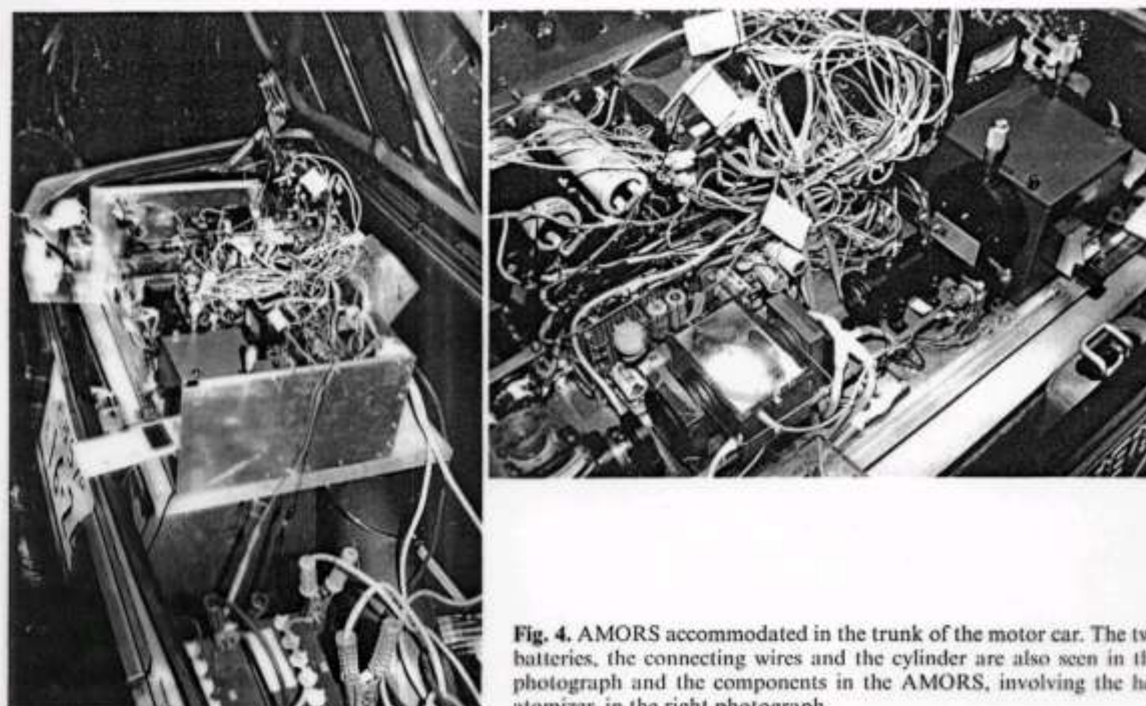

Fig. 4. AMORS accommodated in the trunk of the motor car. The tw batteries, the connecting wires and the cylinder are also seen in the photograph and the components in the AMORS, involving the he atomizer, in the right photograph

K.Kitagawa , Y.Yasui , Fresenius' Zeitschrift fur Analytische Chemie , Vol.321 , No.6 , pp.563-571 (1985)

- ＜助手・講師時代＞（昭和50 - 平成6年）竹内次夫先生、柘植　新先生、柳沢正明先生、Horlick先生らと原子分光分析法研究

*1983年日本分析化学会奨励賞（楠先生、中村先生と）

Institute of Energy Science

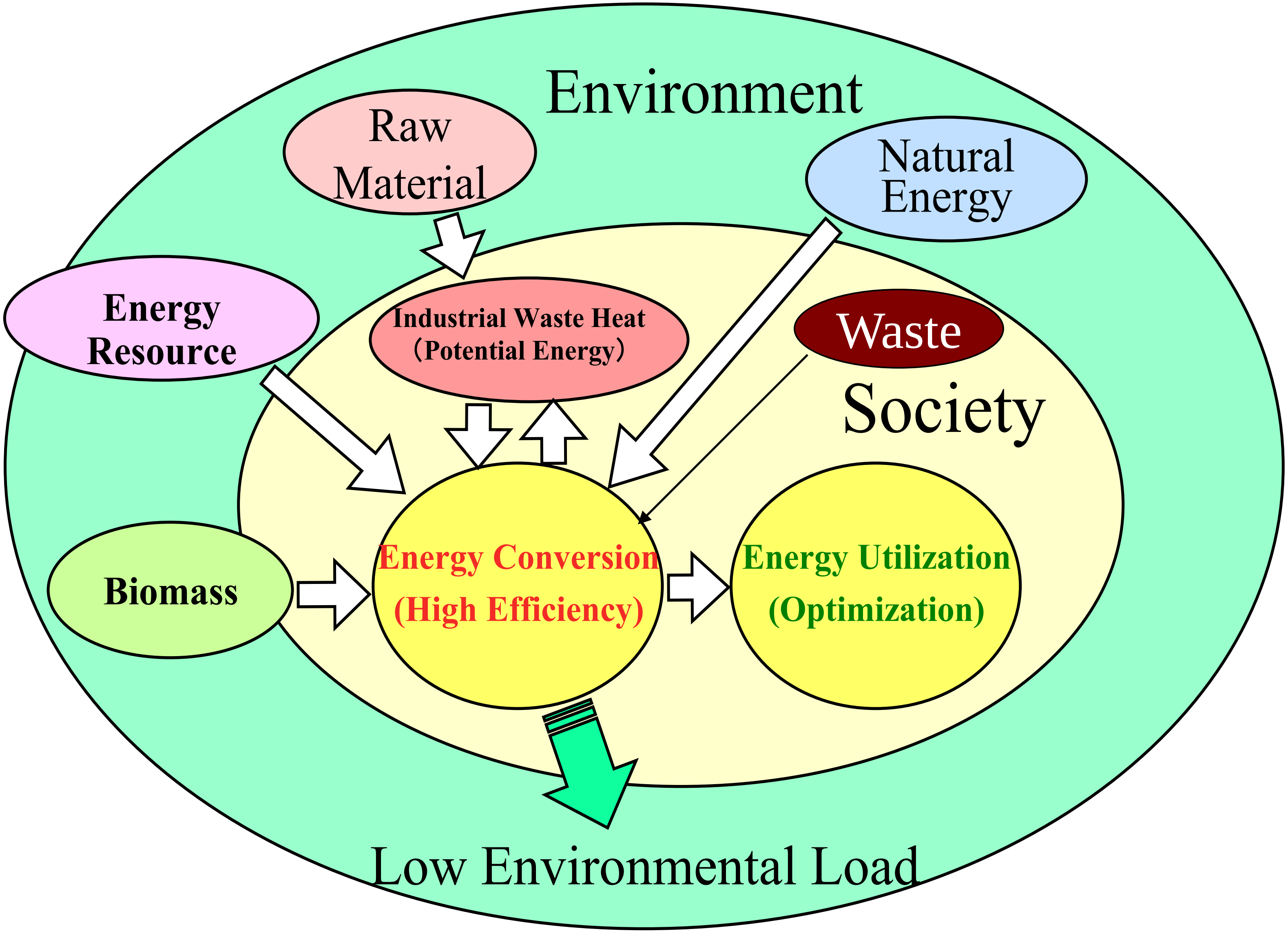

名古屋大学旧高効率エネルギー変換研究センター

Research Center for Advanced Energy Conversion, Nagoya University (RAN)

Division of Energy Science at EcoTopia Science Institute

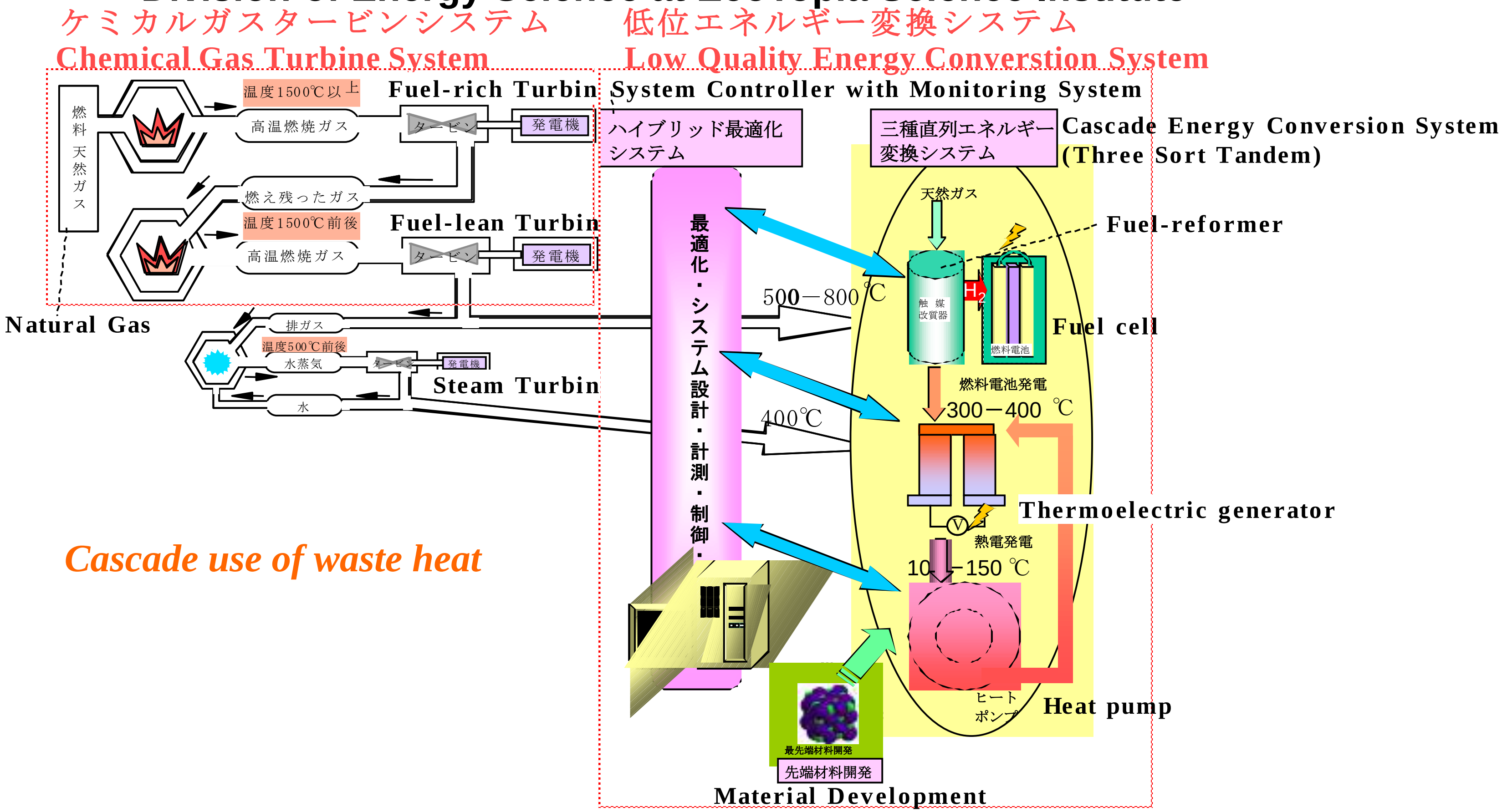

Advanced Energy Conversion Group
Division of Energy Science
EcoTopia Science Institute
Nagoya University

- Prof. Kiatagwa, Assist. Prof. Morita, Dr.Matsumoto & Dr. Nelfa
- Spectroscopic analyses of combustion, Fuel cell, Hydrothermal reforming of
- biomass and biowaste, LED illumination

- Assoc. Prof. Takashi Itoh

  Syntheses and systems of thermoelectric materials

- Prof. Yutaka Hasegawa

  Turbine compressor and wind turbine systems

Assoc. Prof. Kojima

Chemical gas turbine, combustion systems and supersonic fuel reforming

Prof. Kobayashi & Dr. Huan

Heat pump systems and CO_2 issues

Chemicalgas turbine system

Study of combination of fuel-rich and fuel-lean combustions using a two-step gas turbine

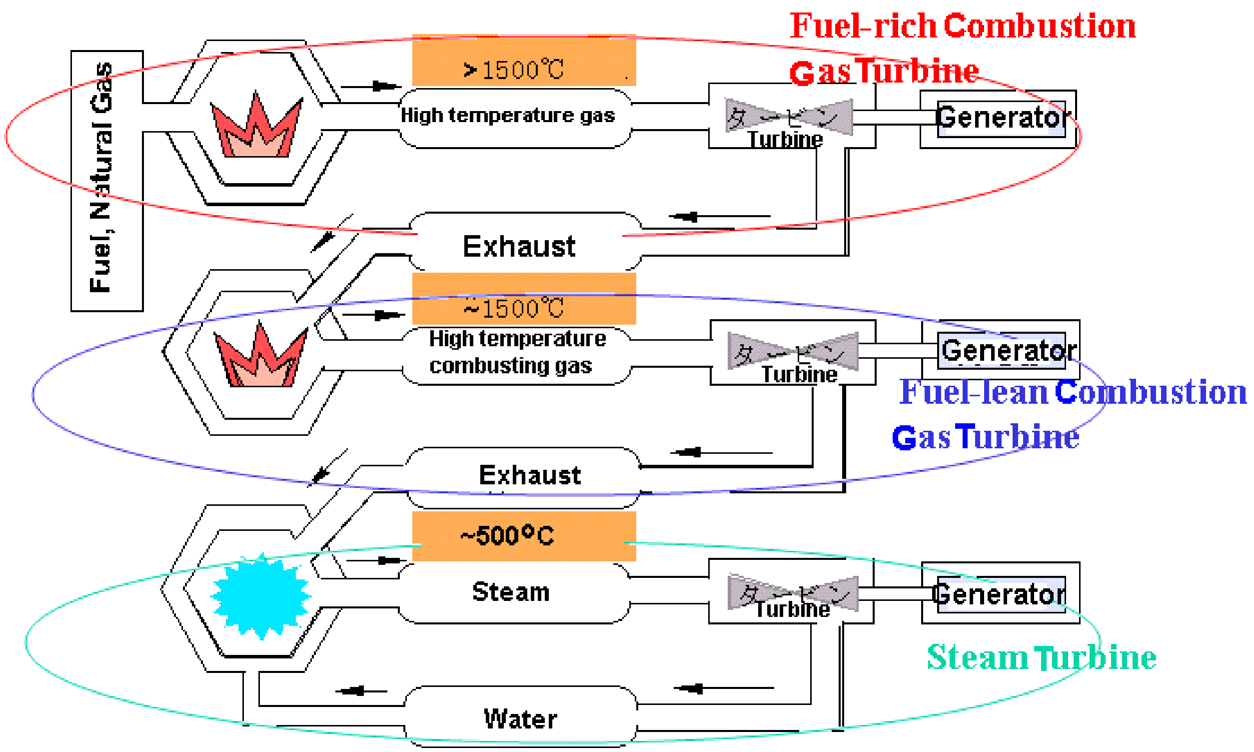

Fig.　Illustration of a chemical gas turbine system

Fuel-rich Combustion Gas Turbine

- Low NOx Emission from Regenerative Industrial Furnace for kira-kira 30% Energy Saving
- Spectroscopic Observation

Two-color method

Planck's law

$$\rho = \varepsilon_\lambda \cdot \frac{8\pi hc}{\lambda^5} \cdot \frac{1}{\exp\left(hc/\lambda k T\right) - 1}$$

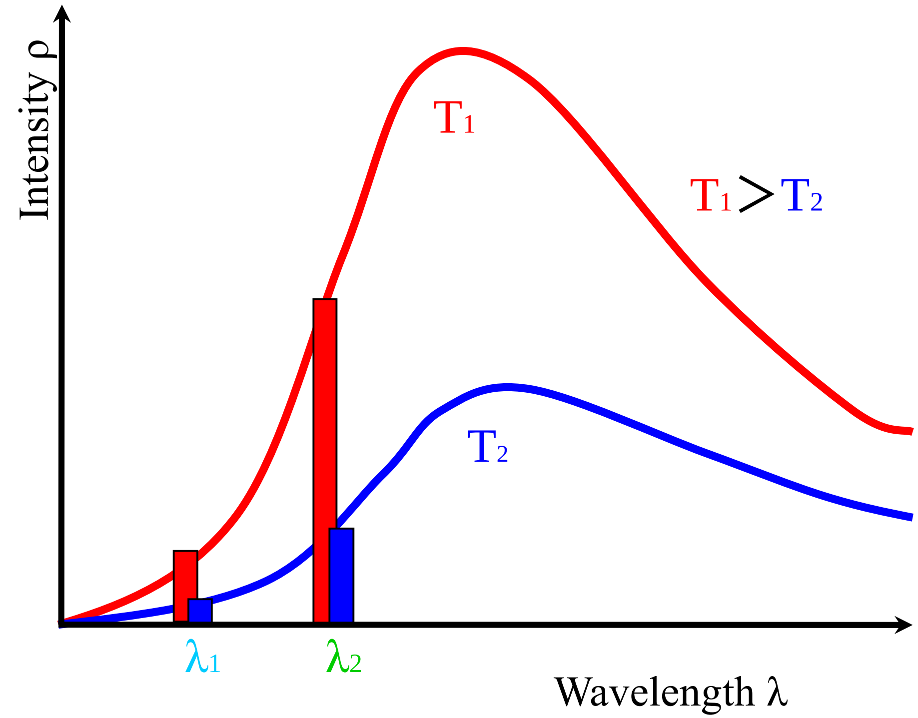

Taking a ratio of intensities at 2 wavelengths,

$$\frac{\rho_2}{\rho_1} = \left(\frac{\lambda_1}{\lambda_2}\right)^5 \cdot \frac{\exp\left(hc/\lambda_1 k T\right) - 1}{\exp\left(hc/\lambda_2 k T\right) - 1}$$

ρ_1

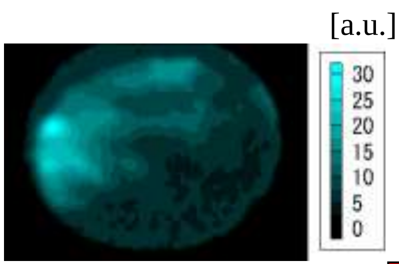

490 nm

ρ_2

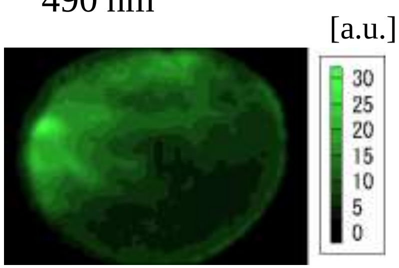

530 nm

→ T

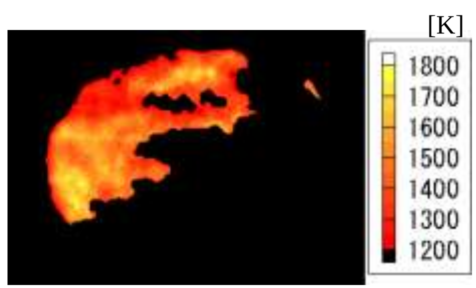

温度

- ρ : Unit radiation energy [Jm^{-4}]
- h : Planck's const 6.62608 × 10^{-34} [Js]
- λ : Wavekength [m]
- c : light velocity 2.99792458 × 10^{8} [ms^{-1}]
- k : Boltzmann const 1.38066 × 10^{-23} [JK^{-1}]
- T : Temperature [K]
- ε_λ : Emissivity [-]

Object :Test Furnace of Keihin Iron Plant, NKK (Currently JFE)

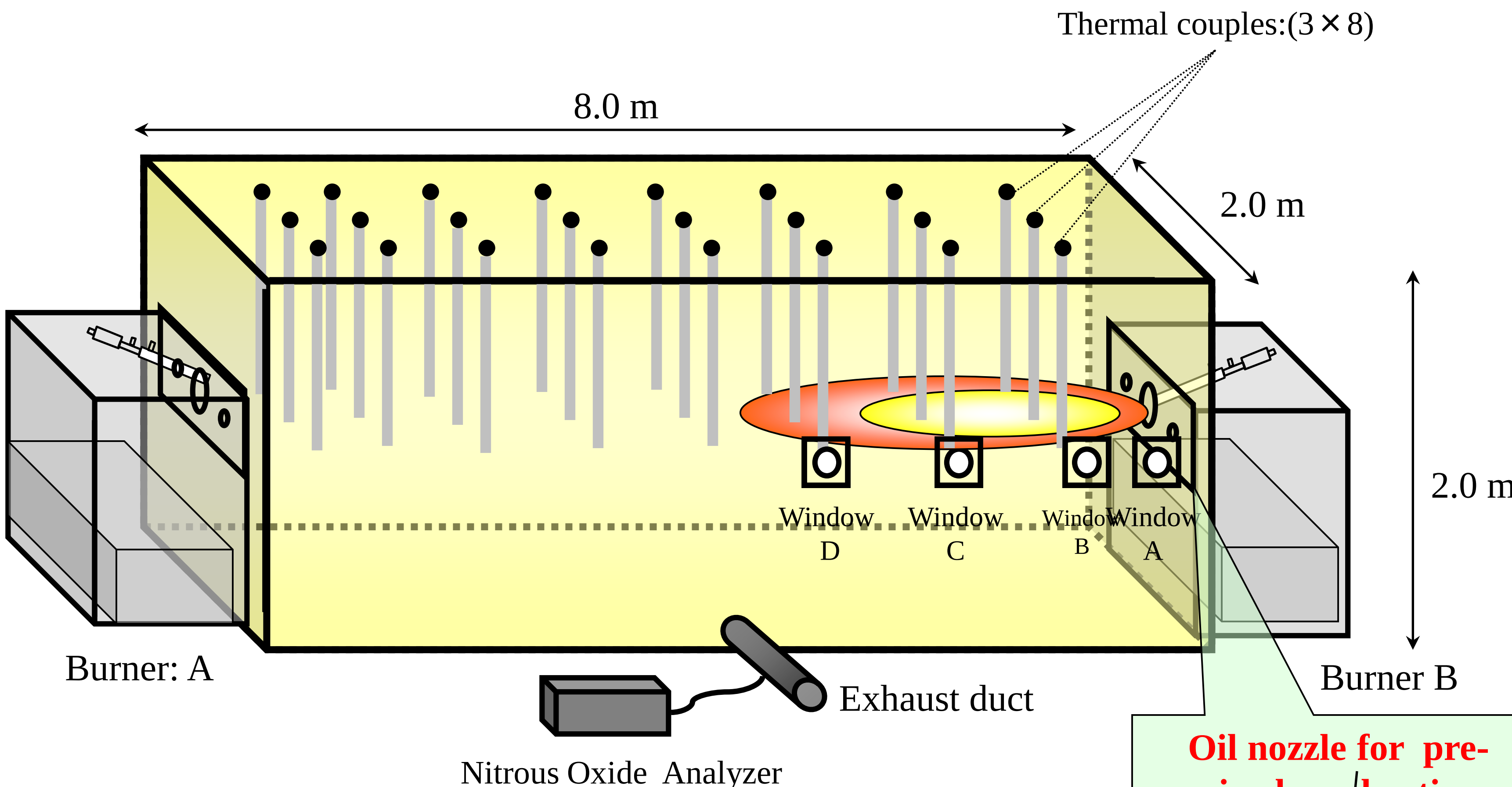

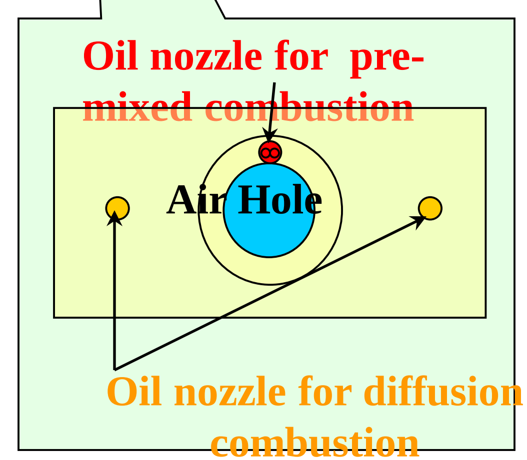

Fuel : Heavy Oil

Combustion:

Pre-mixed combustion : combustion of fully mixed air and fuel takes place in the chamber

Diffusion combustion : Combustion and mix of fuel and air takes place at the same time in the chamber

Measurement Set-up

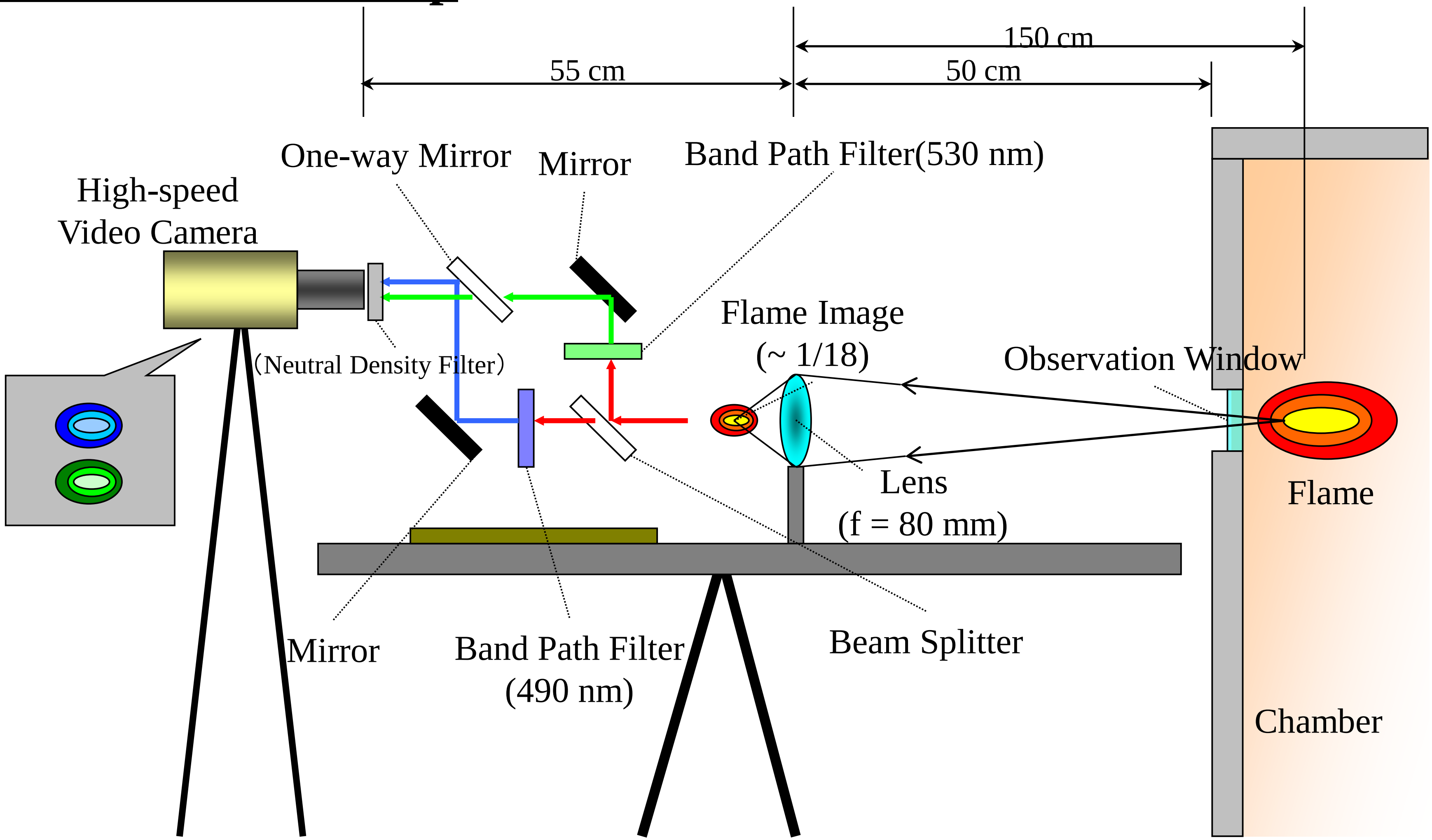

Band Path Filter:

530.88 nm(Half Width 8.77 nm)

490.0 nm (Half Width 28.0 nm)

High-speed video camera (photron,FASTCAM ultima 40K)

Top Speed: 125 frame/sec Exposure Time: 1/125 sec

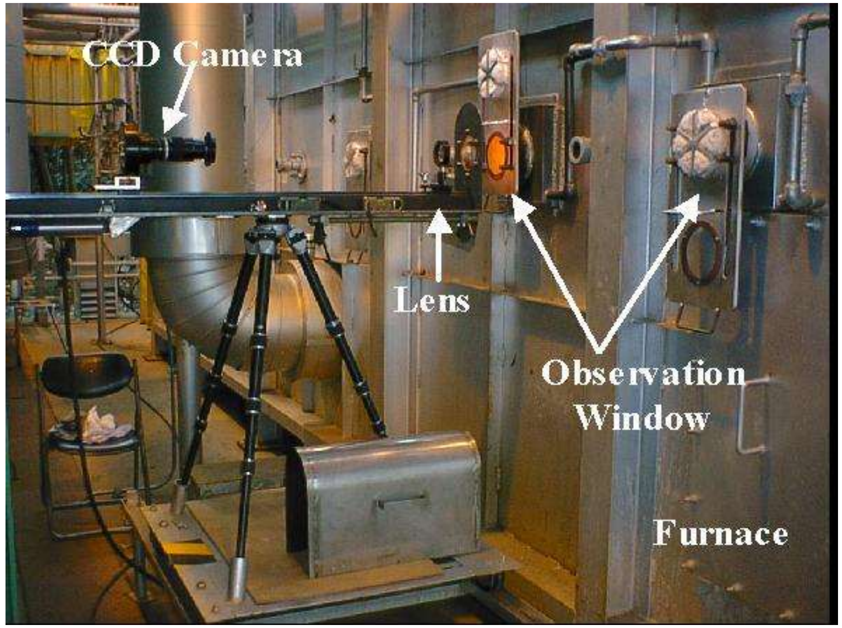
CCD Camera
Lens
Observation Window
Furnace

Temperature profiles (premixed combustion)

（Slow Motion(~1/10)）

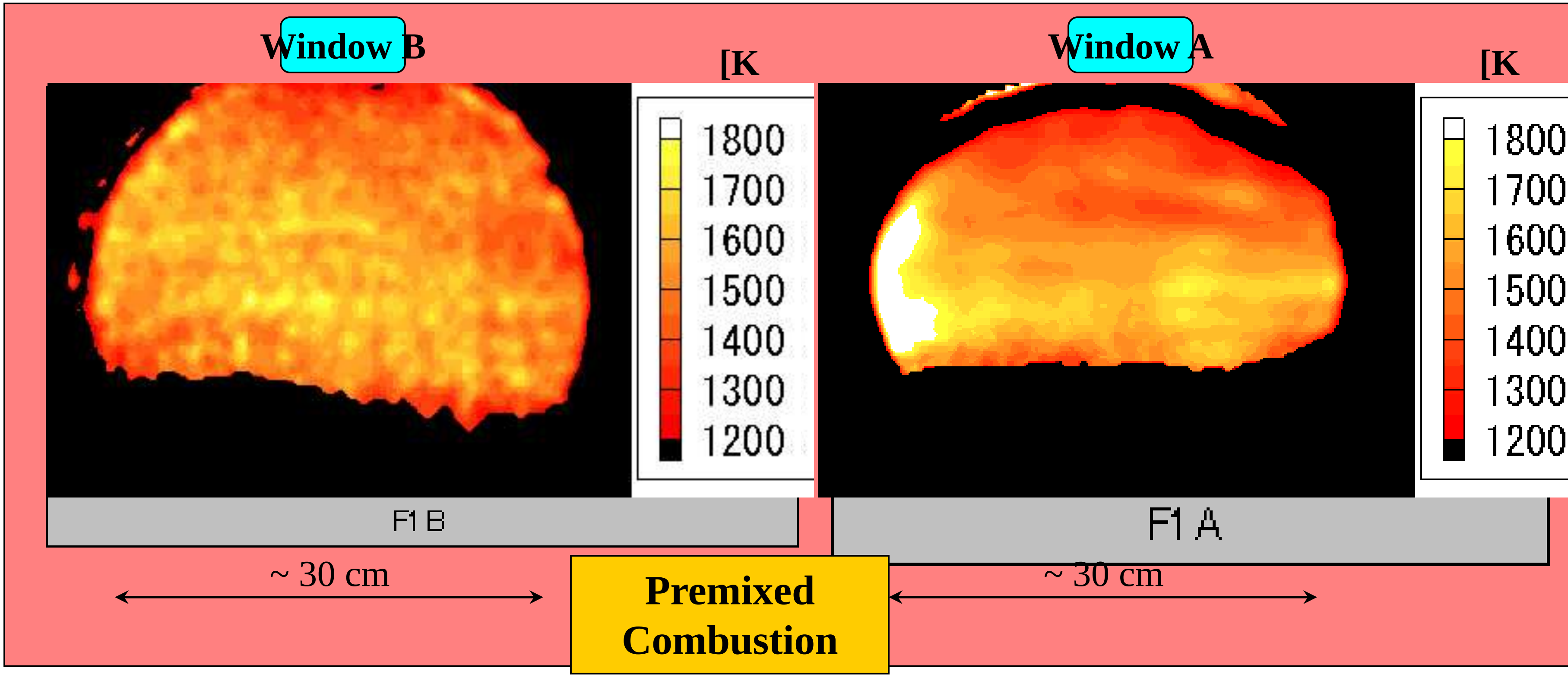

[NO_x] in the exhaust

126～144 ppm

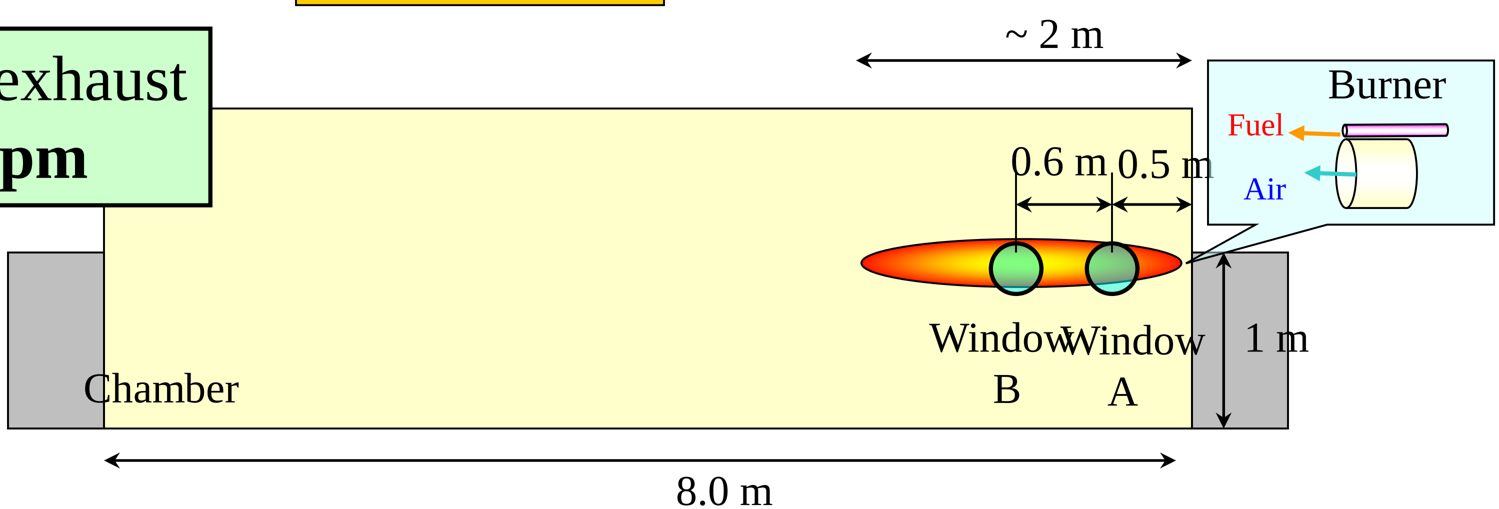

Temperature profiles (diffusion combustion)

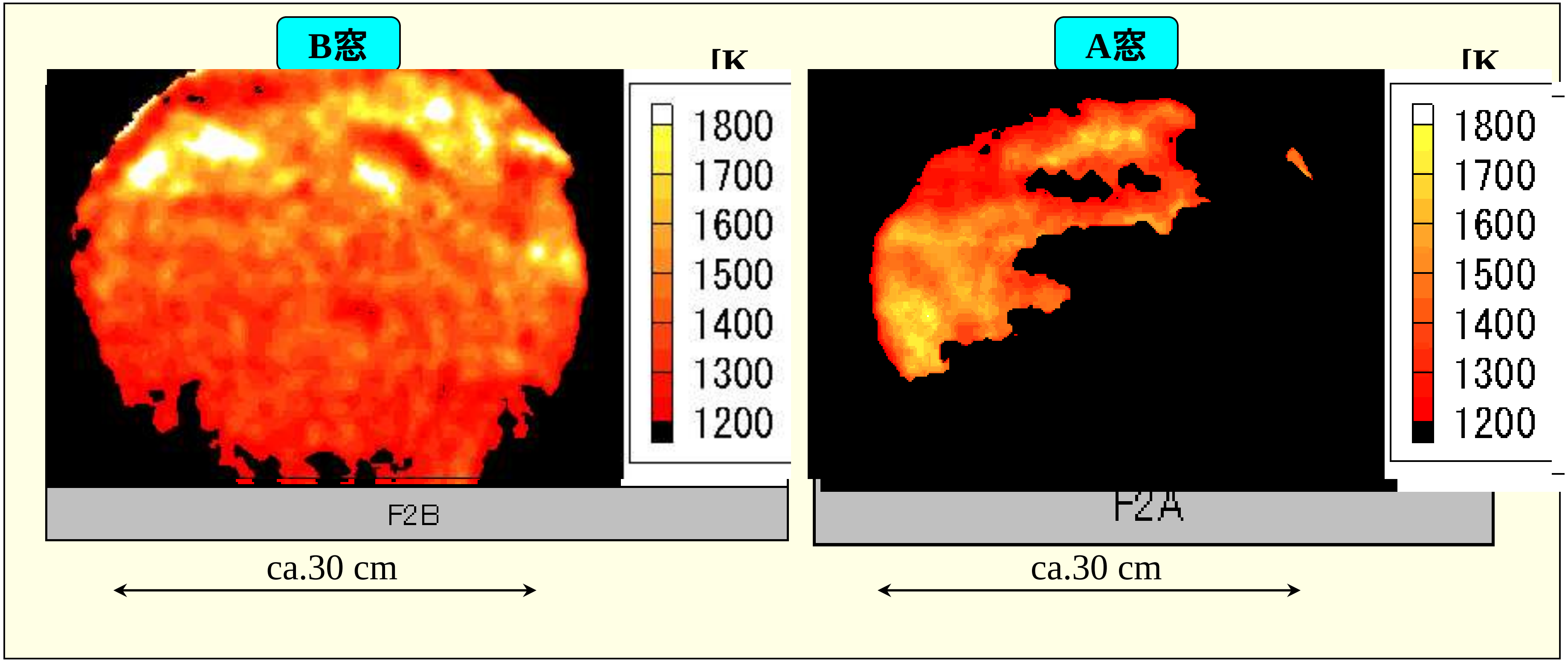

[NO_x] in the exhaust
24～33 ppm

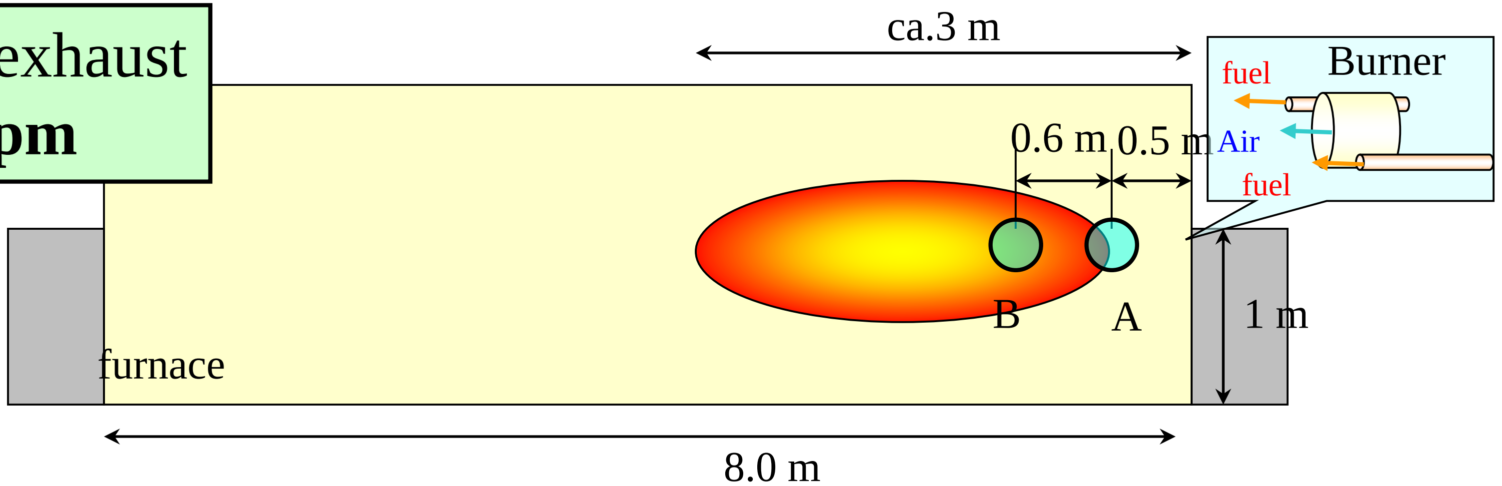

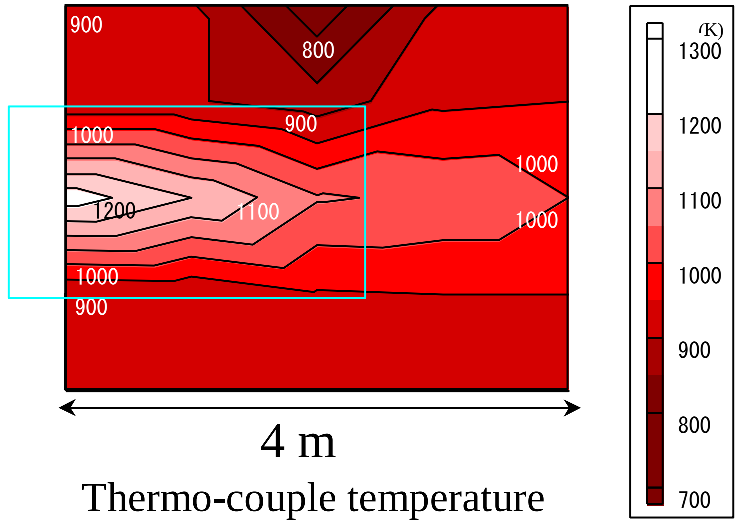

Thermo-couple temperature

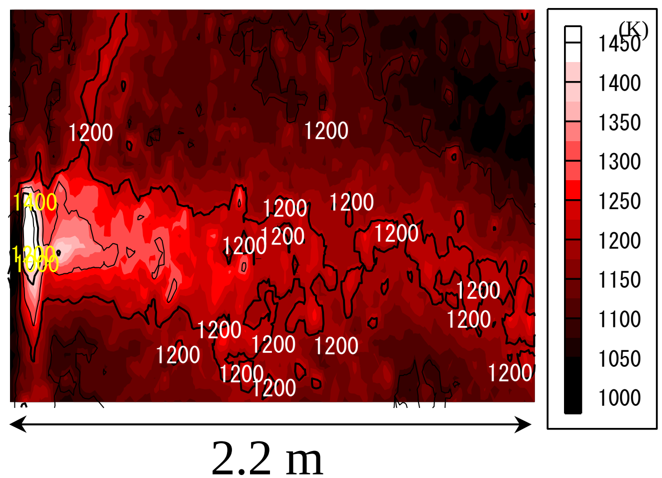

C_2 vibrational temperature

Premixed flame Exposure time 0.01[s]

Figure 5 Temperature distribution

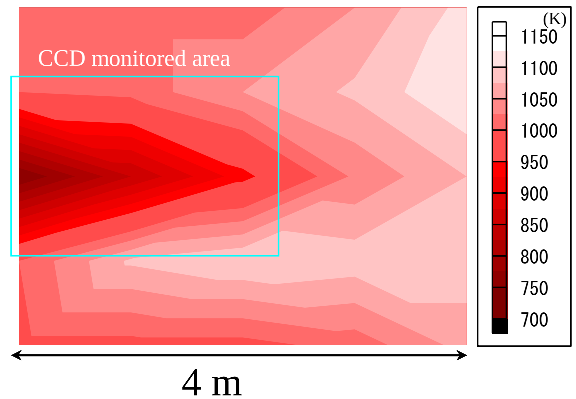

Thermo-couple temperature

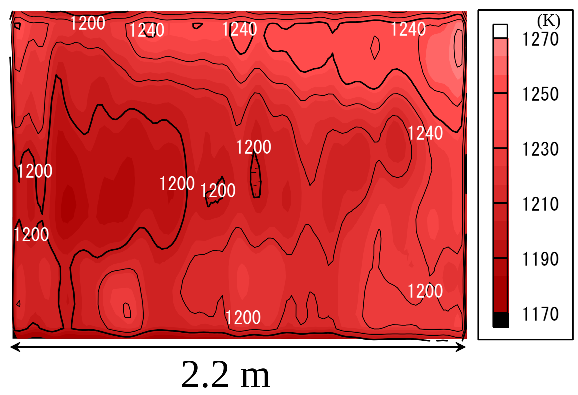

C_2 vibrational temperature

Diffusion flame Exposure time 0.01[s]

Figure 4 Temperature distribution

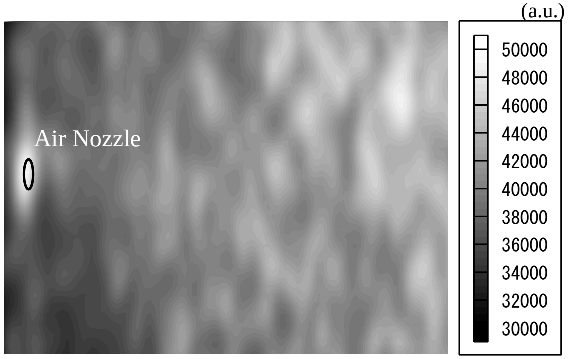

Premixed flame

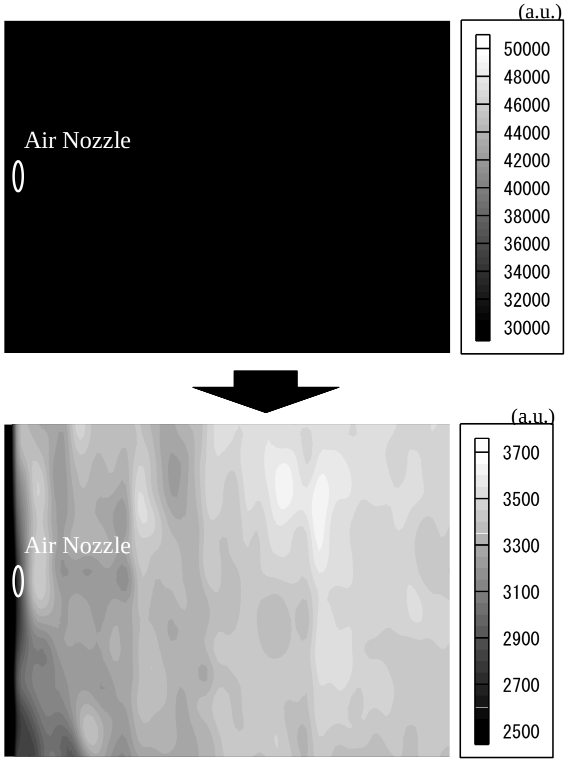

Diffusion flame

Figure 8 NO Emission Intensity

ICP Inductive coupled plasma

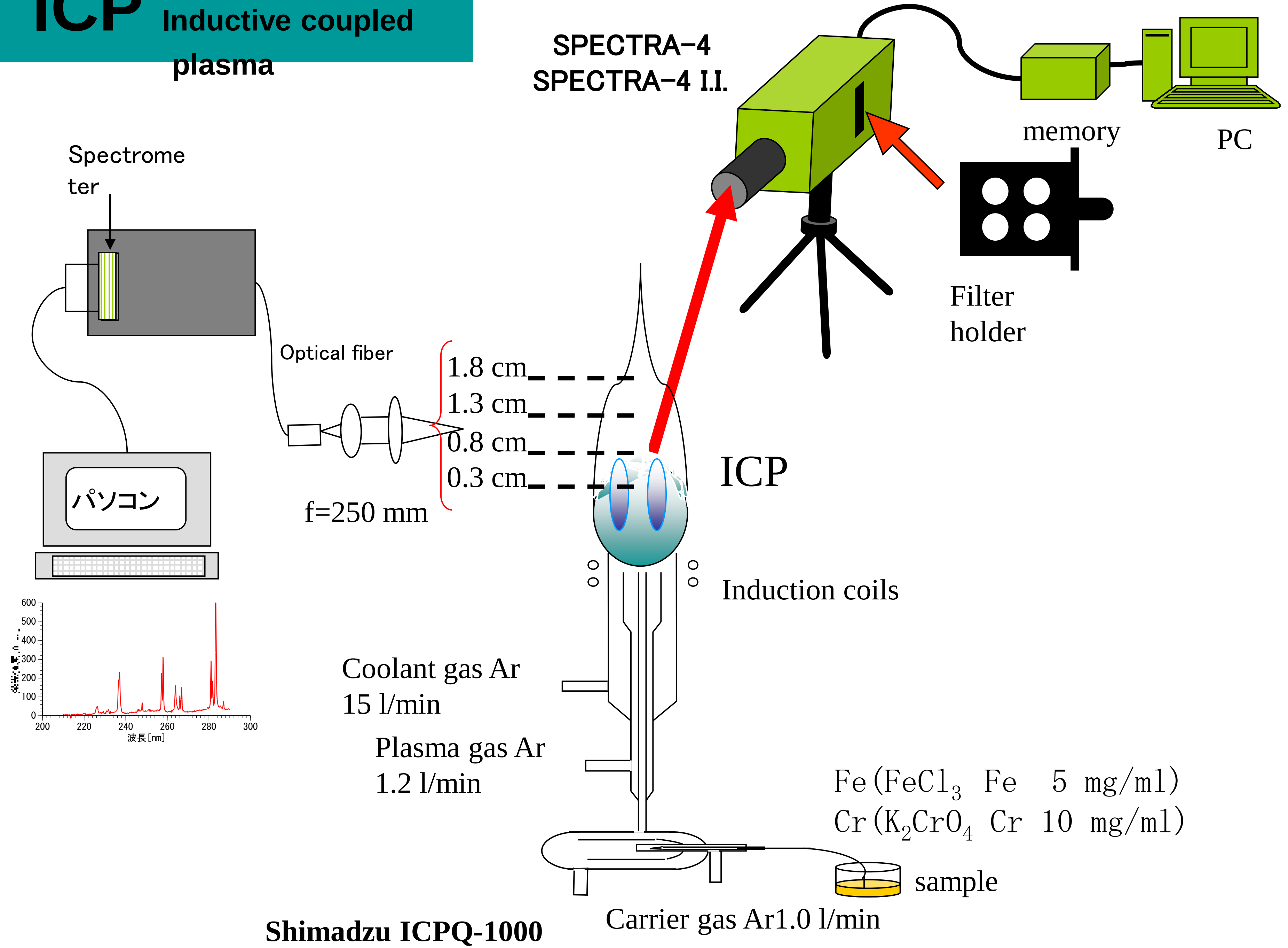

Excitation temperature

H=0.8cmICPプラズマの発光スペクトル

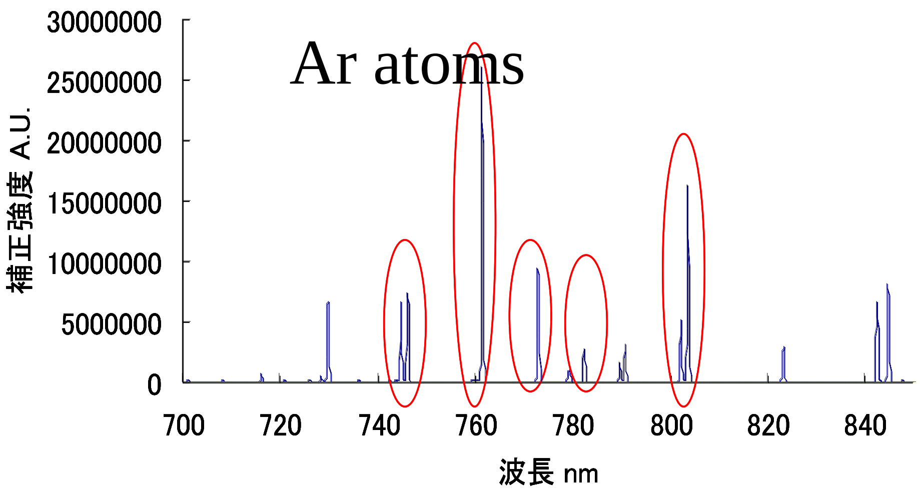

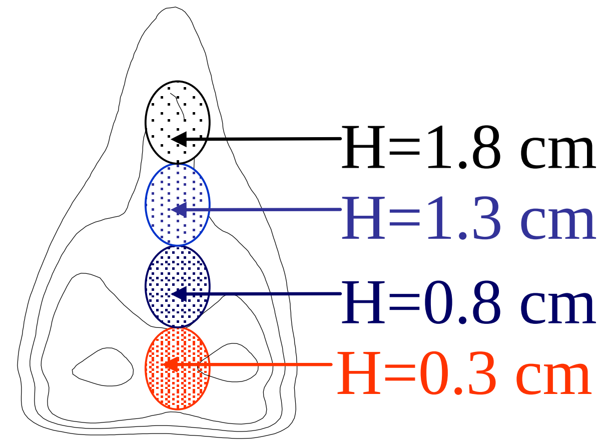

H=0.8cmICPプラズマの発光スペクトル

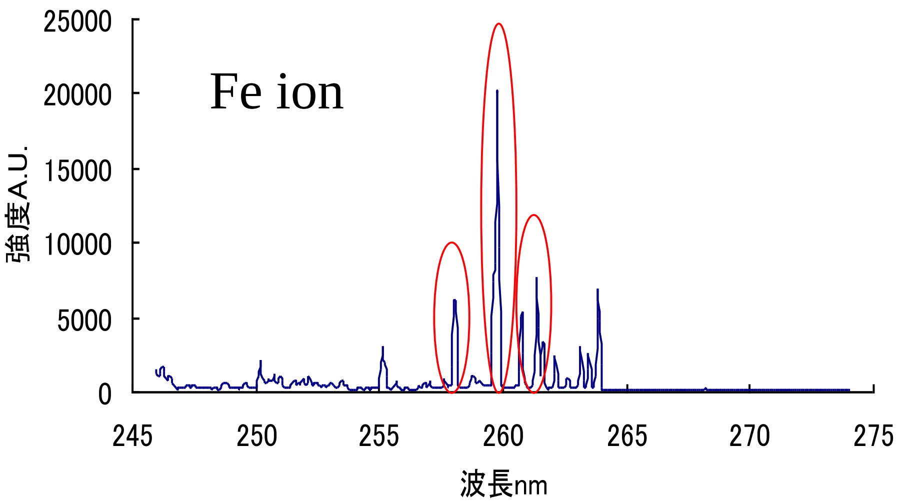

H=0.8 cm
Ar Boltzmann Plot

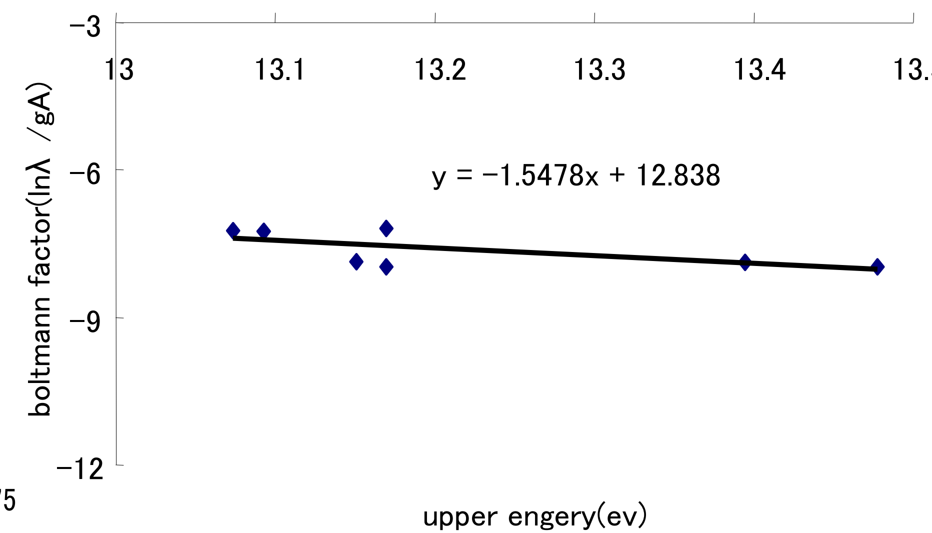

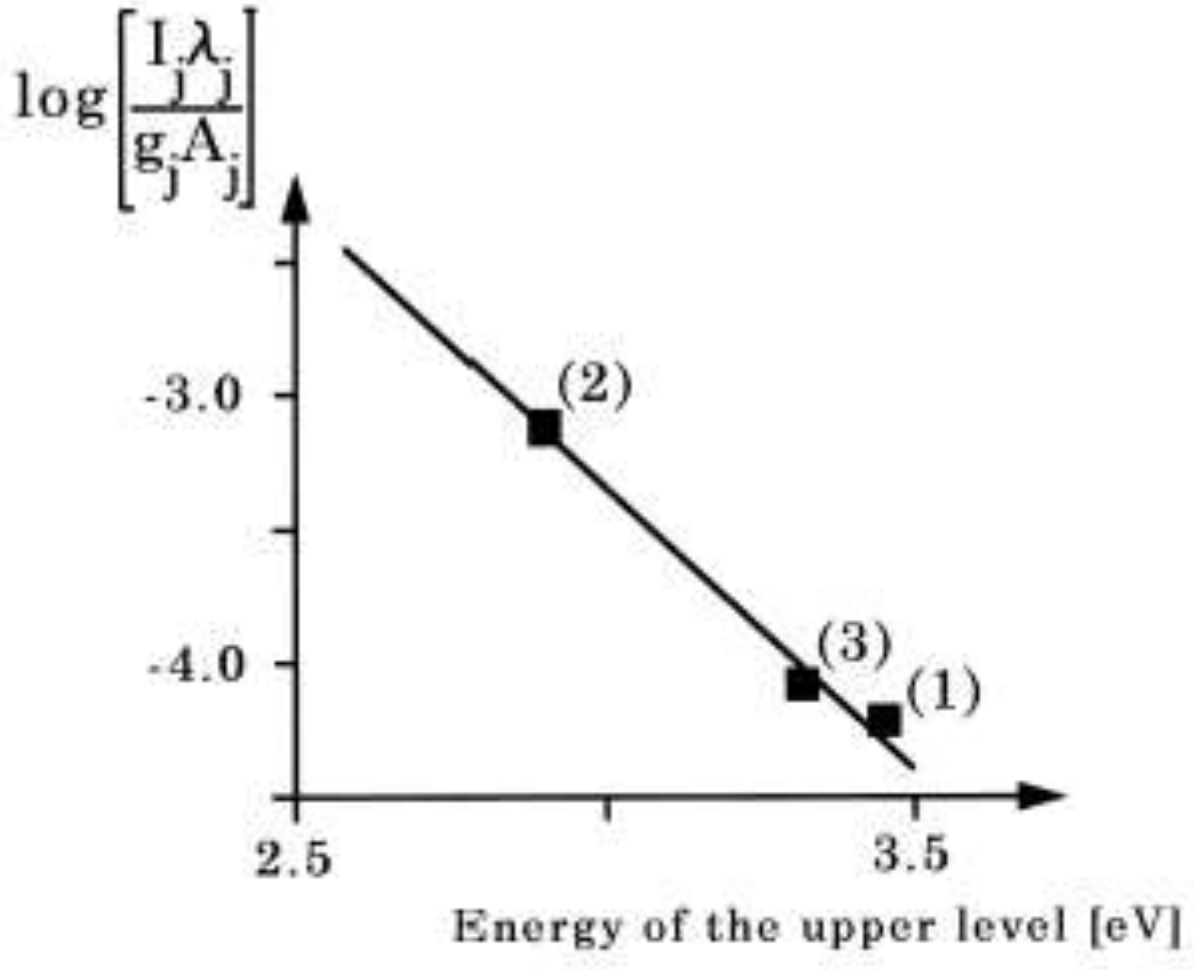

Boltzmann plot of Chromium triplets

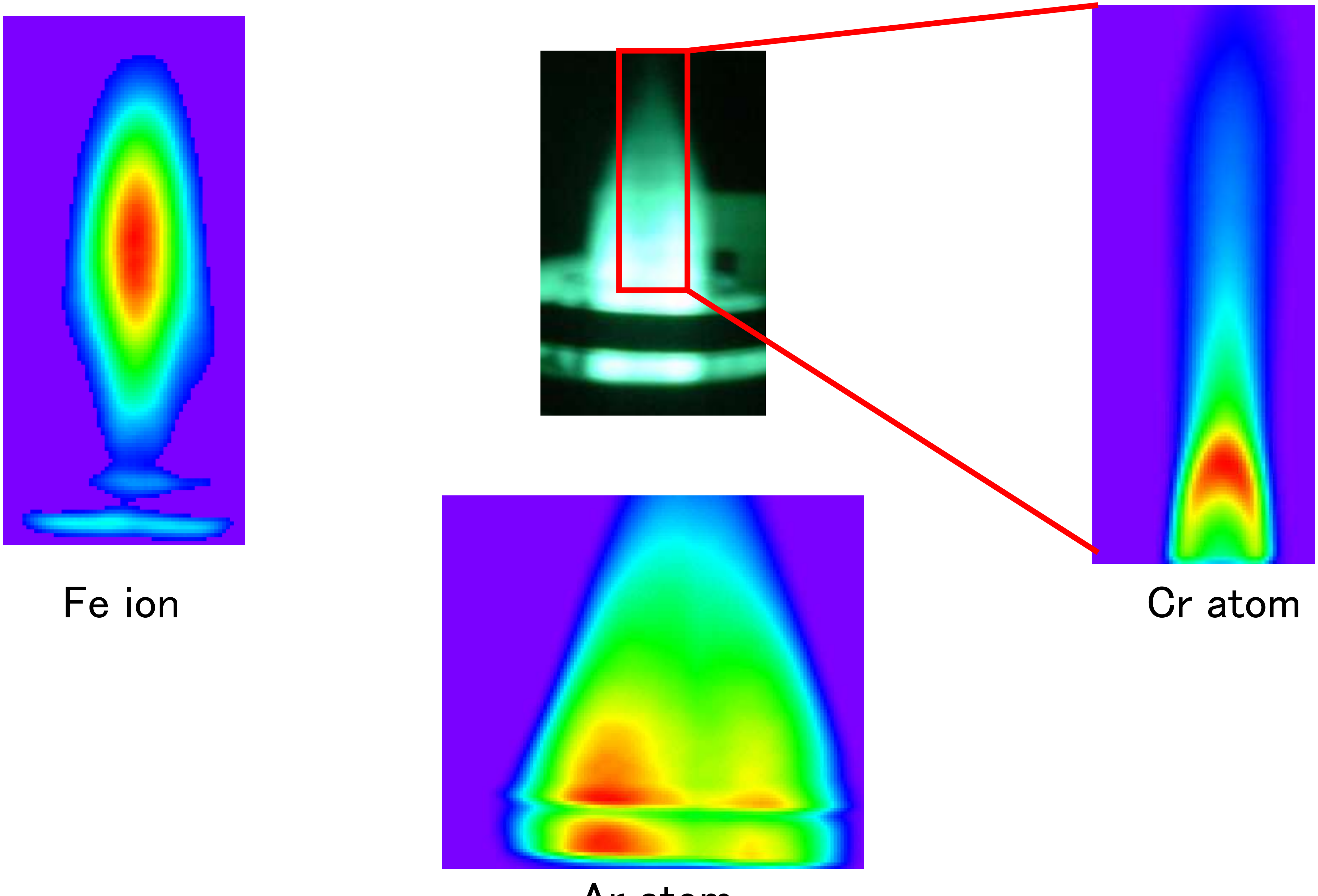

Fe ion
Cr atom
Ar atom

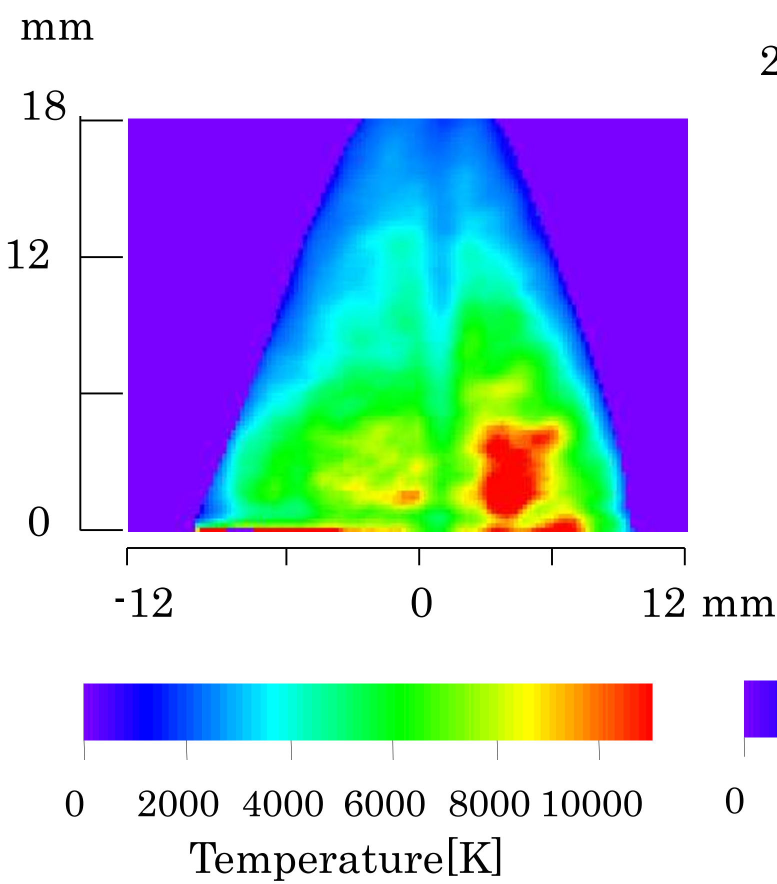

Ar Excitation T

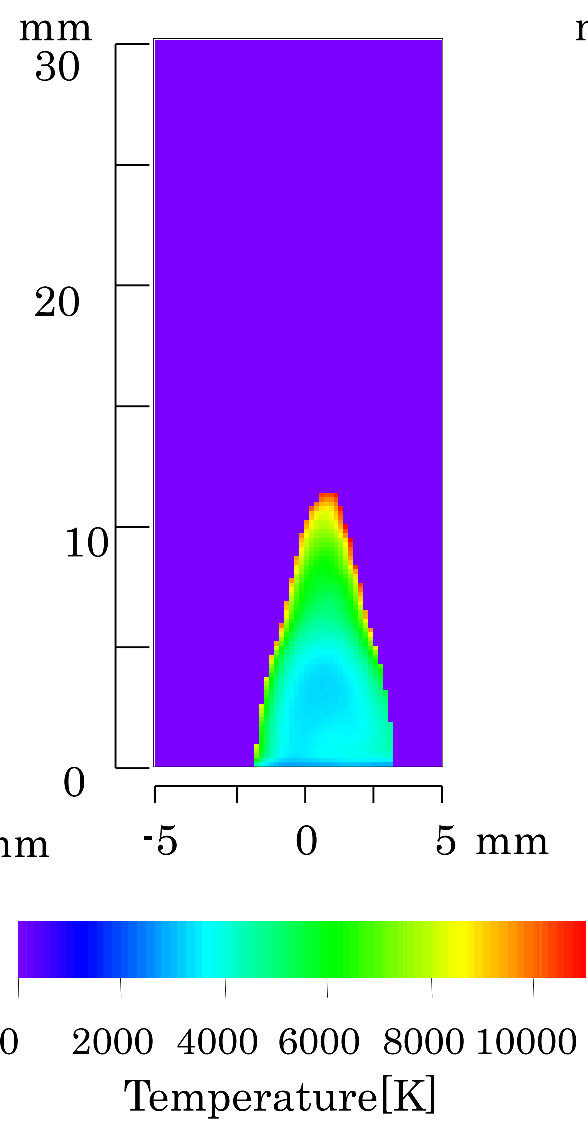

Cr atoms

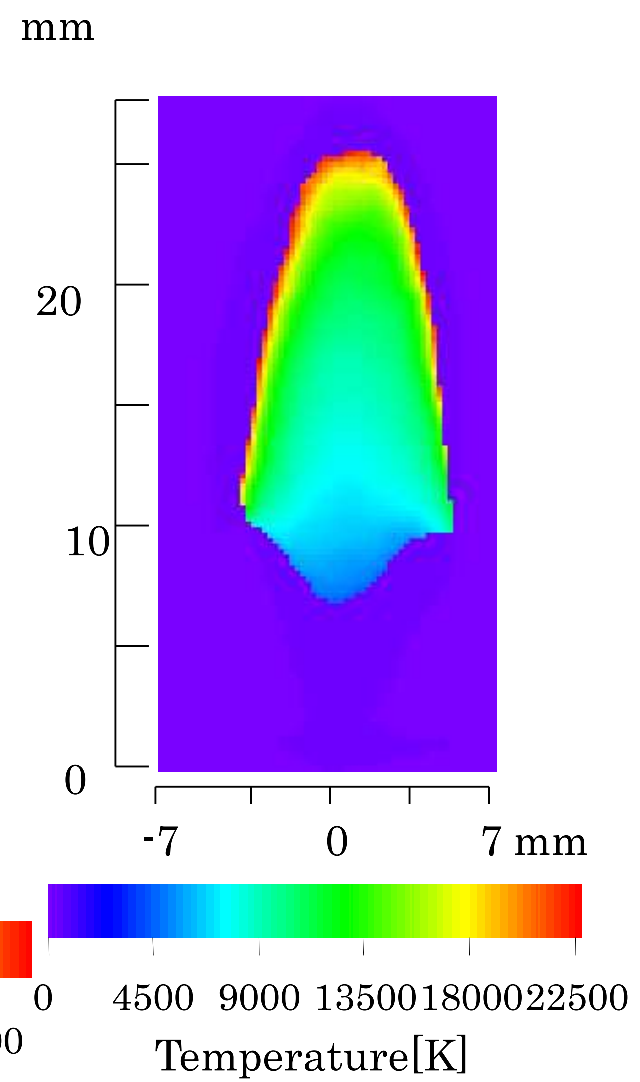

Fe ions

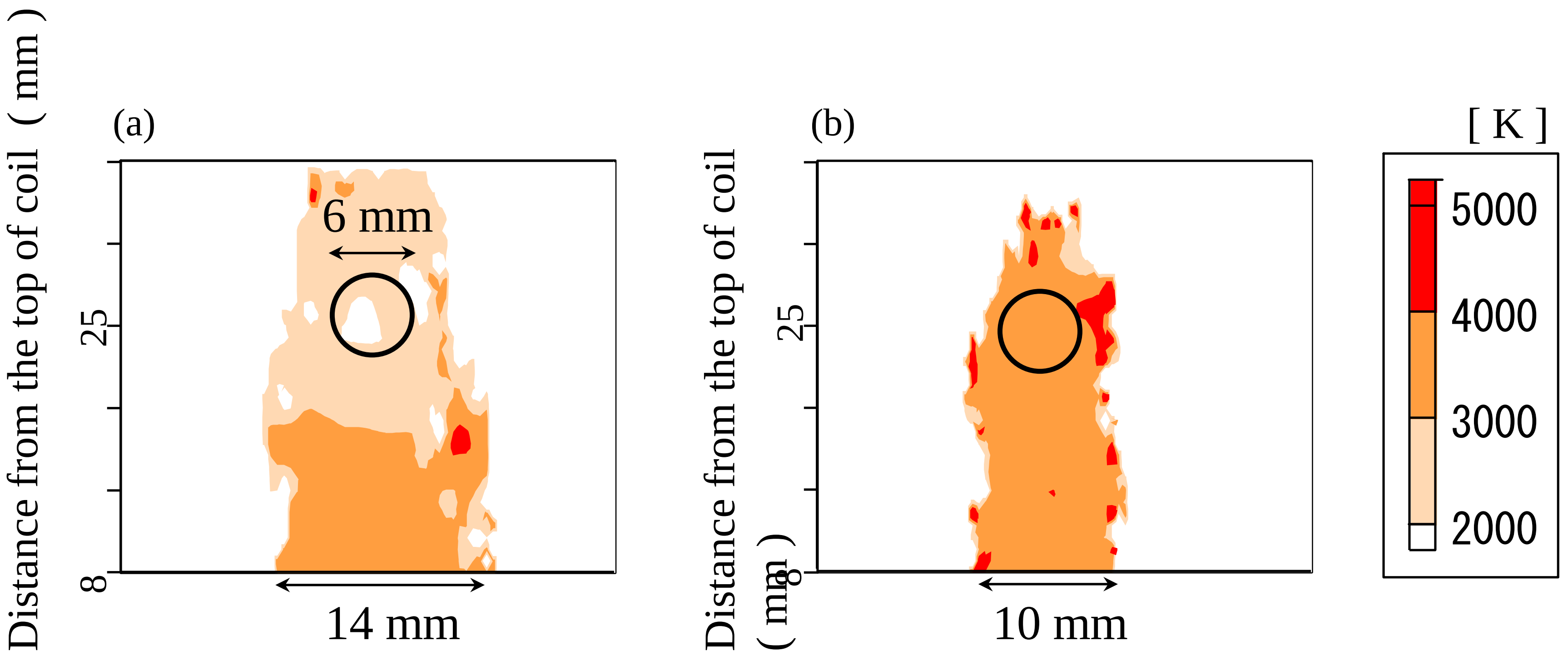

(a) inactive (b) oxidative

Spatial distribution of Fe excitation temperature with a graphite disk in plasmas under inactive and oxidative conditions.

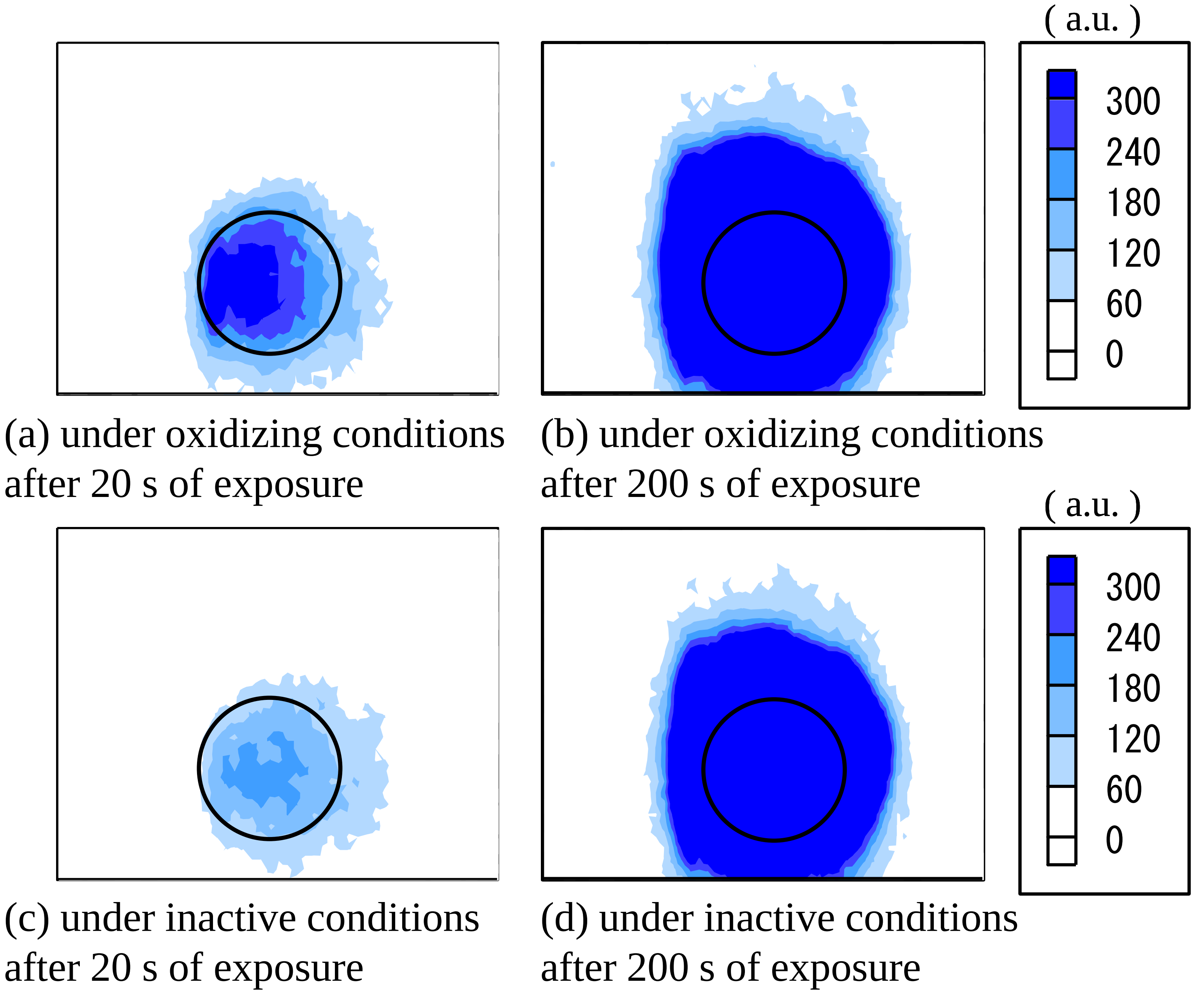

Spatial distribution of spectral intensities of C emission around the C/C composite surface. 흑연 디스크의 주위의 탄소 원자 발광의

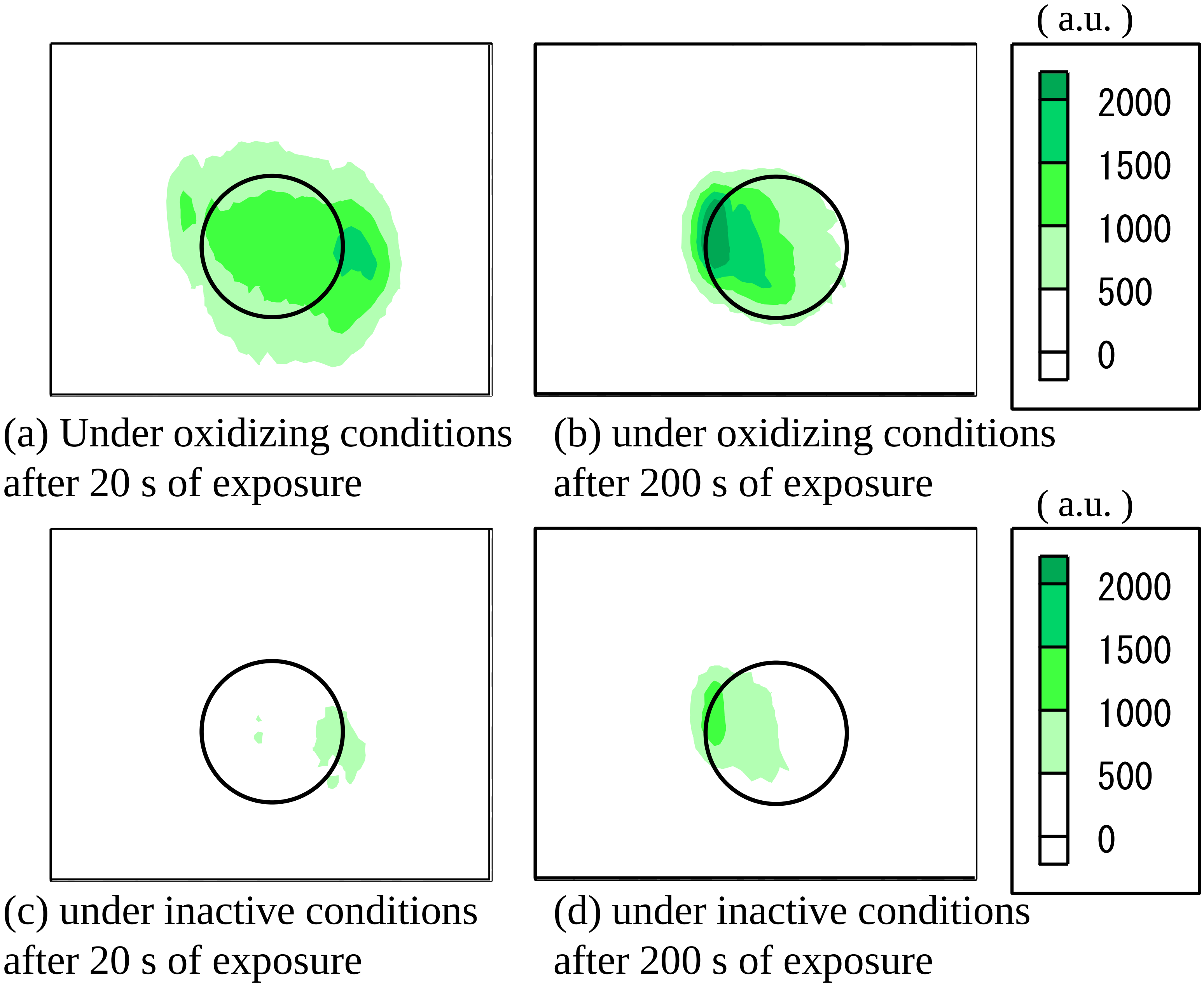

Fig. 5. Spatial distribution of spectral intensities of Si emission around the C/C composite surface with the double layer coating surface.

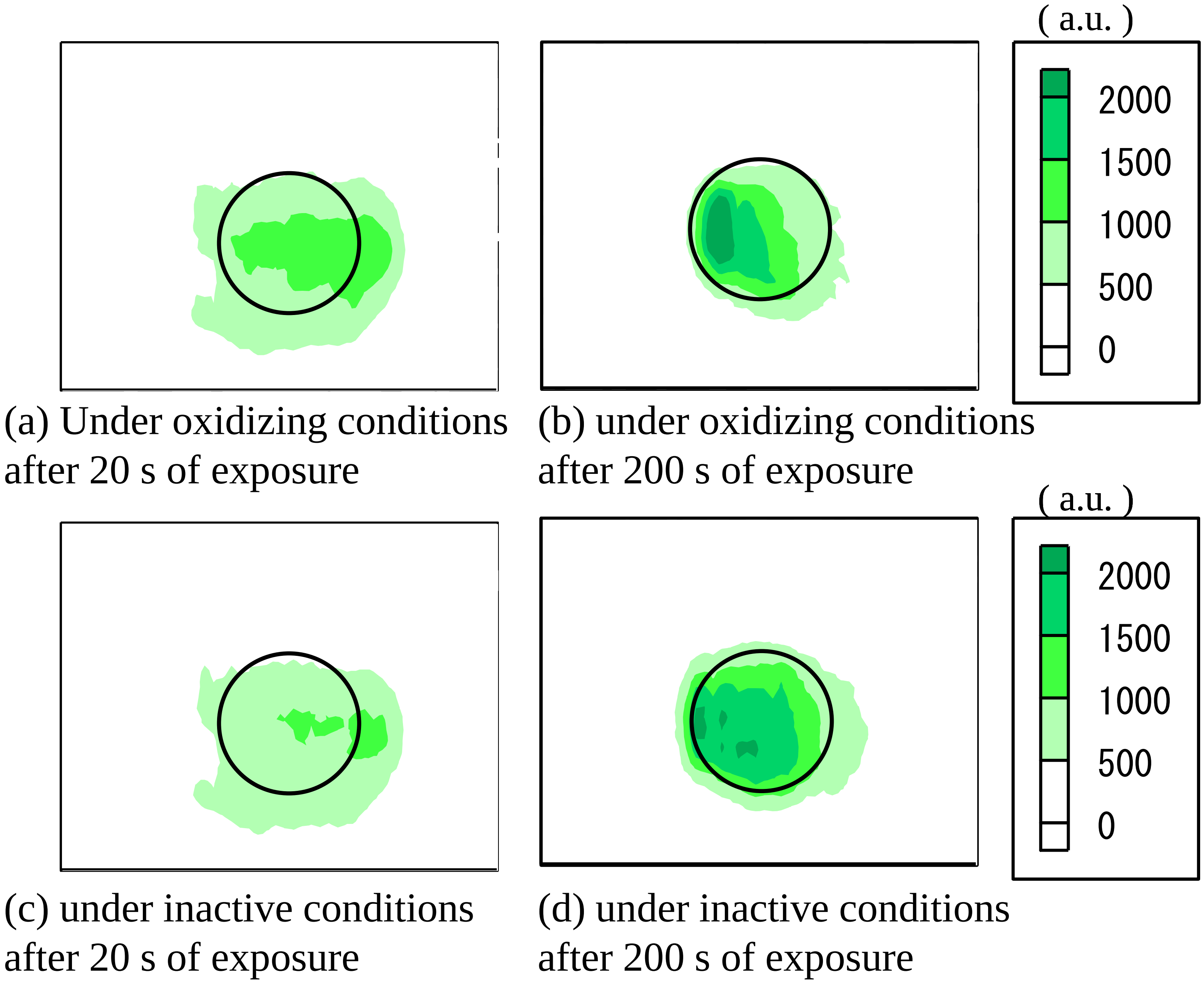

Fig. 6. Spatial distribution of spectral intensities of Si emission around the SiC disk surface.

Nuclear Fusion Plasmas

D + D or D + T -> He + Energy

No CO_2 emission

⇩

Issues

1.Ingintion

2.Damage on Reactor
Carbon Linings:
Chemical Sputtering

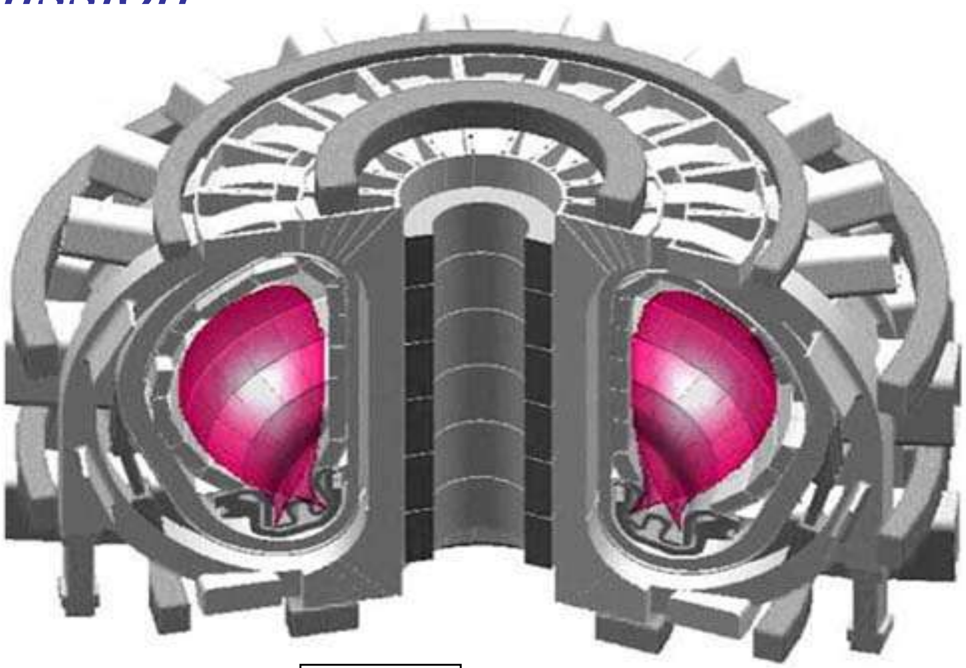

Reactor

http://www.naka.jaea.go.jp/ITER/iter/index7.html

HYBTOK-Ⅱ

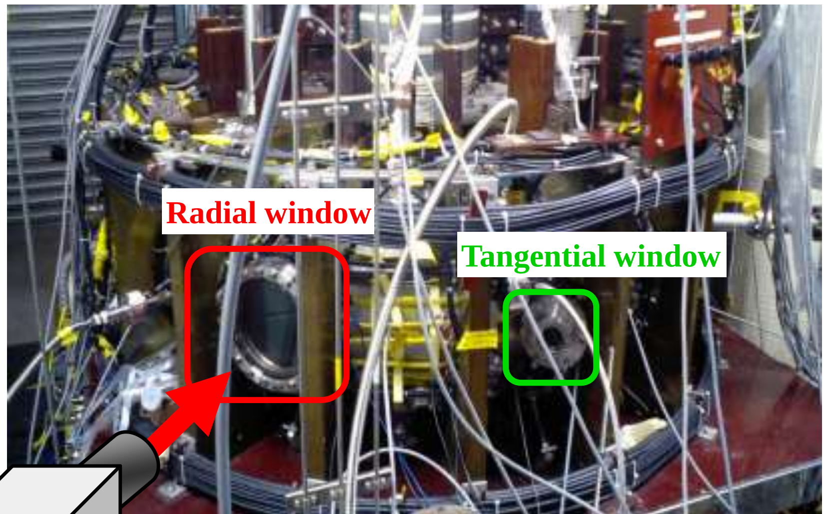

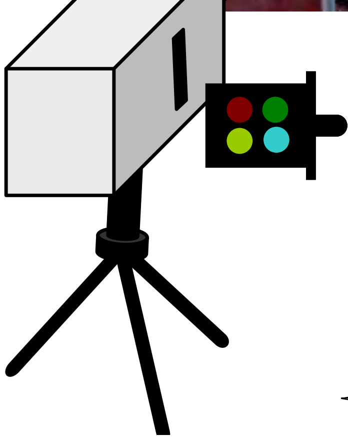

High speed 4-Ch Video camera

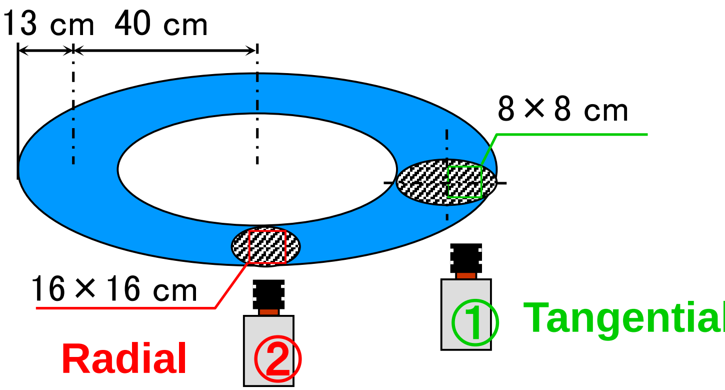

HYBTOK-II physical properties

L. d.	40 cm	Plasma gas	He
S.d	13 cm	Discharge duration	~20 ms

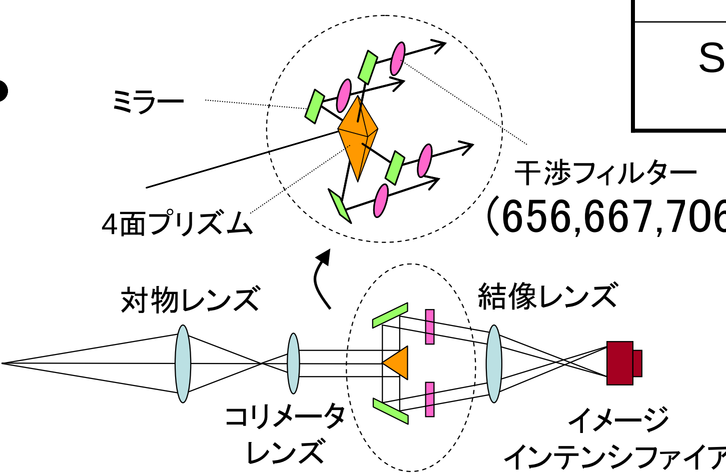

カメラの光学系

Video Camera Conditions

frame rate	2000,6000 fps
Intensifier gain	1.2 ～ 4.6
Focus length	50 mm
F	1.2

Spectrum for a plasma for helium atoms and ions

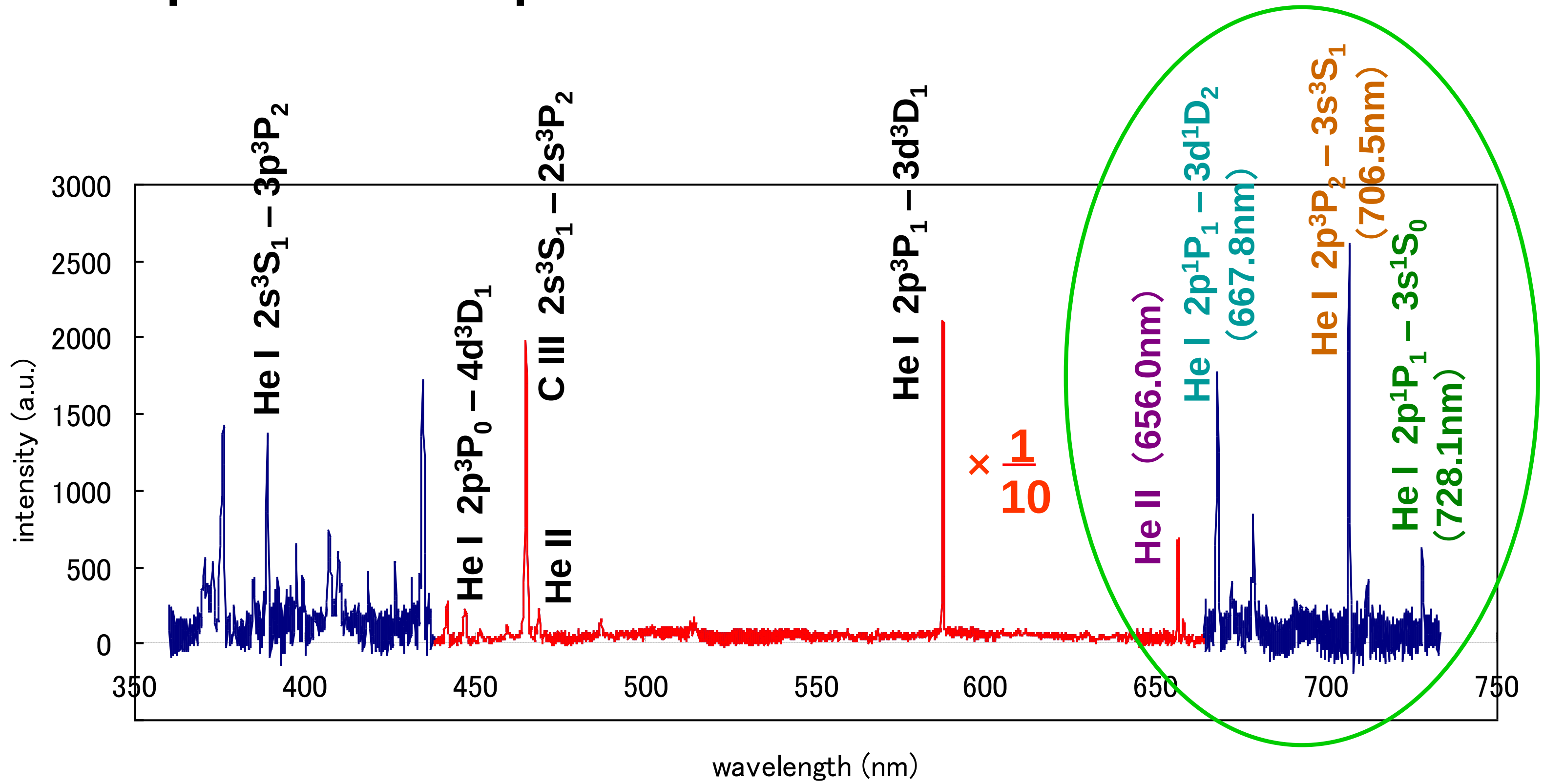

Hydrothermal Process

- Biomass sample : 0.1 g
- Distilled H_2O / D_2O : 3 ml
- Additives :
  - Sodium carbonate (Na_2CO_3)
  - Nickel catalyst (Ni / SiO_2)

- Reaction Temp. : 400ºC
- Pressure : ca. 25 MPa

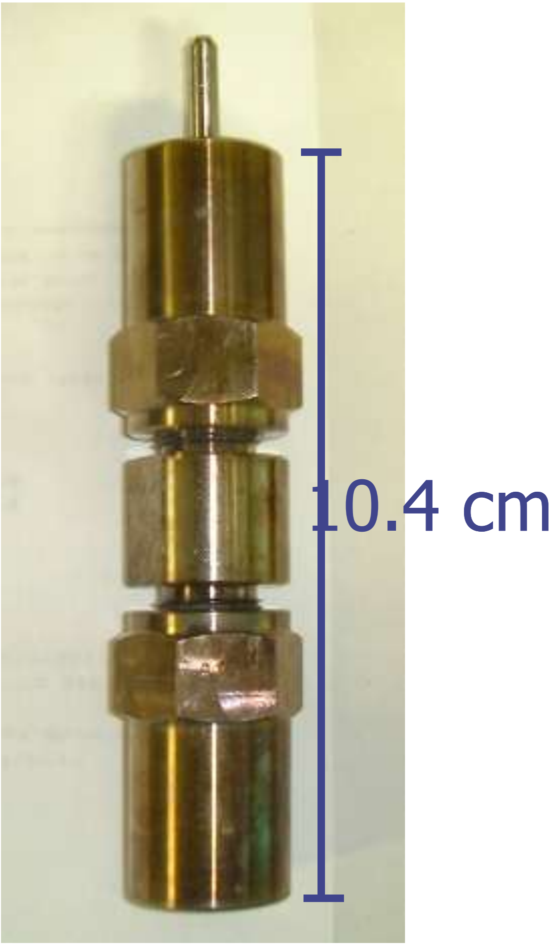

Microtube reactor
(10.5 ml)

Hydrothermal gasification of biowaste

- Cellulose

(Model biomass sample)

◈ Real biomass

Wasted wood

C: 46.1 wt% H: 6.1 wt%
N: 1.5wt% S: 0.7 wt%

"Okara"

C:46.2 wt% H: 6.7 wt%
N: 6.1 wt% S: 0.9 wt%

Fertilizer

C: 34.8 wt% H: 5.3 wt%
N: 7.6 wt% S: 1.3 wt%

Peat

C: 46 wt% H: 5 wt%
N: 1 wt% O: 38 wt%

Effect of Na_2CO_3 and Ni Catalyst on Hydrothermal Reaction of Cellulose

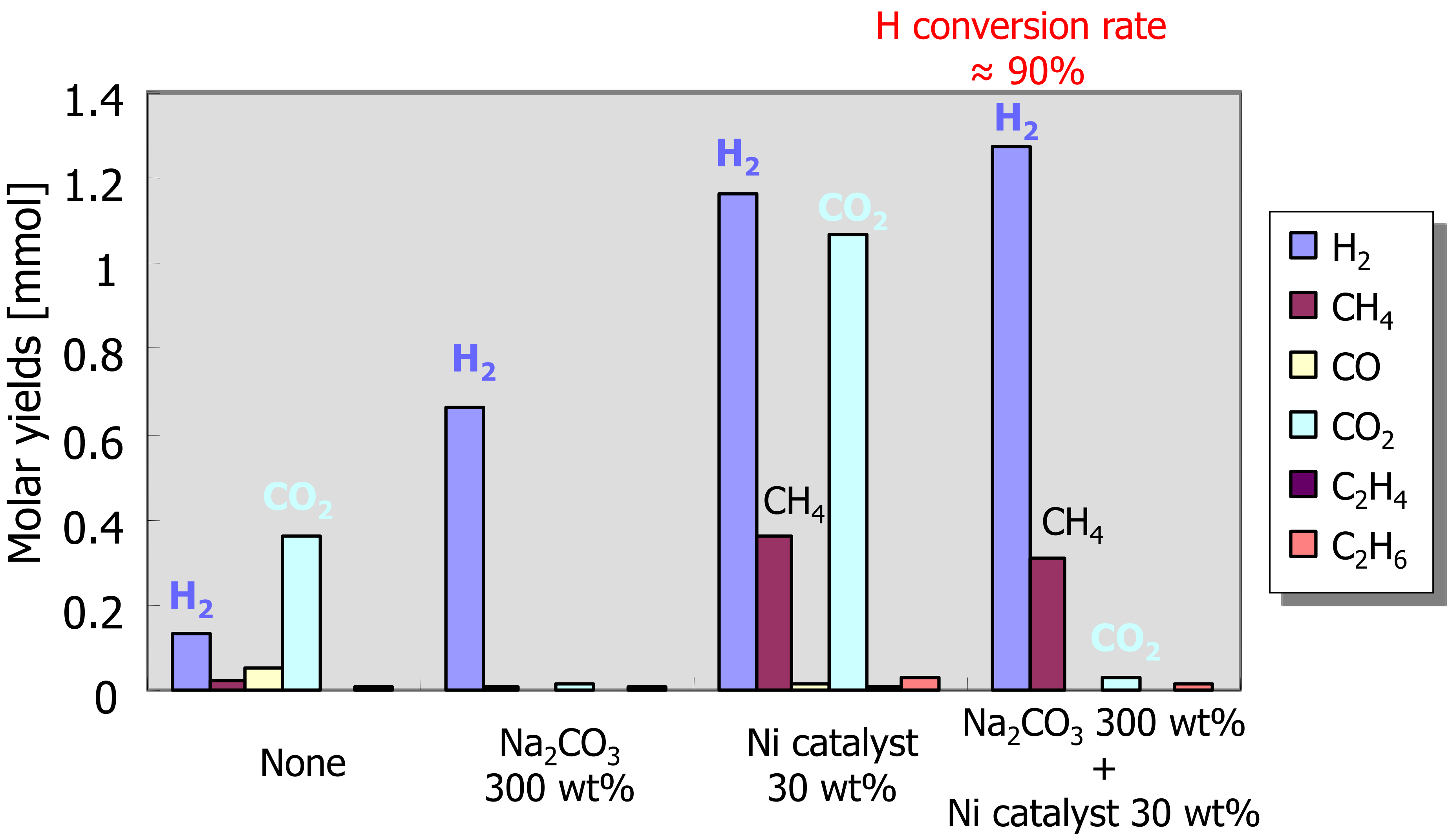

Effect of Additives on Hydrothermal Reaction of Wasted Wood

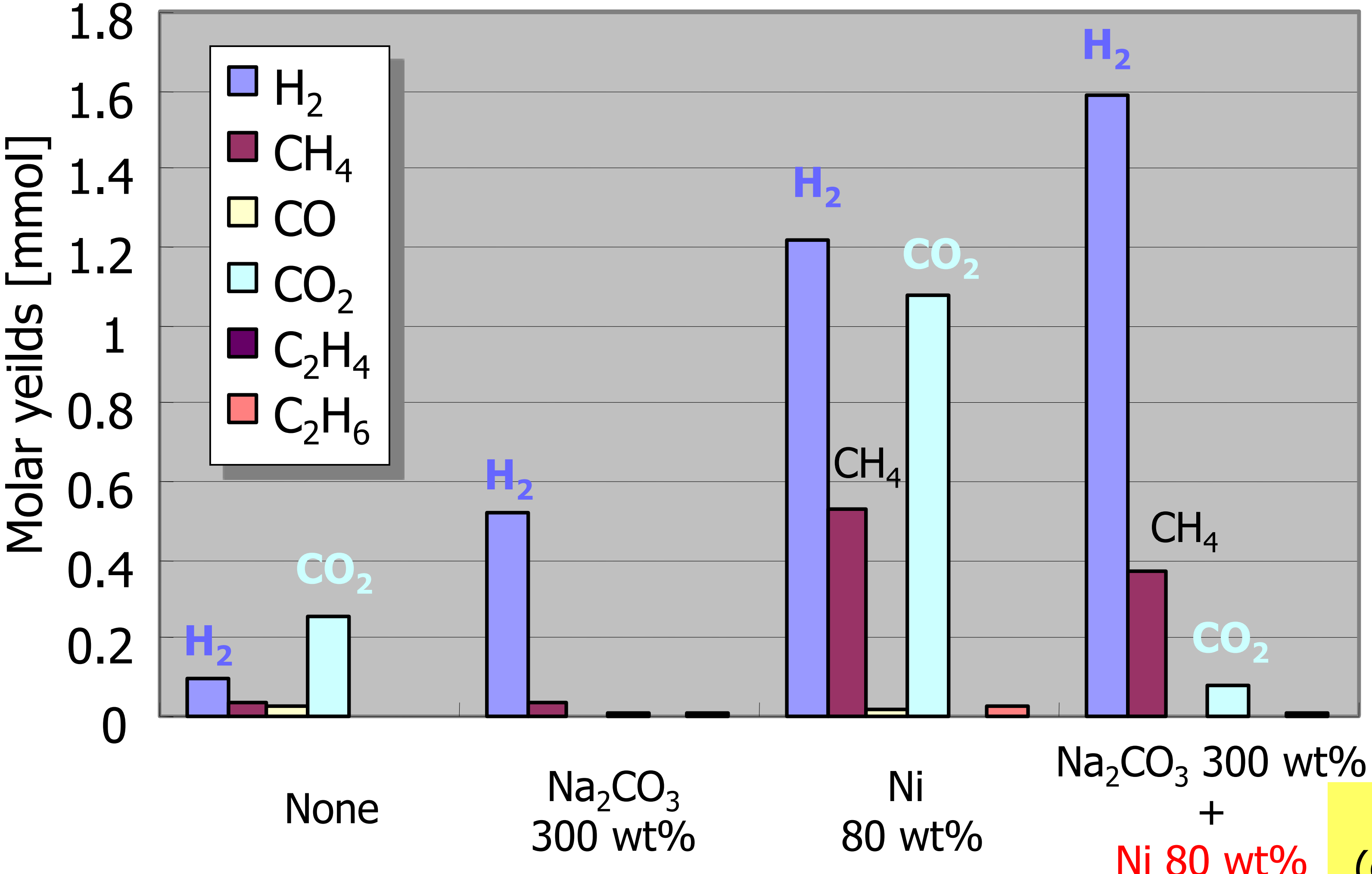

30 wt% (cellulose)

Effect of Additives on hydrothermal Reaction of Okara and Organic Fertilizer

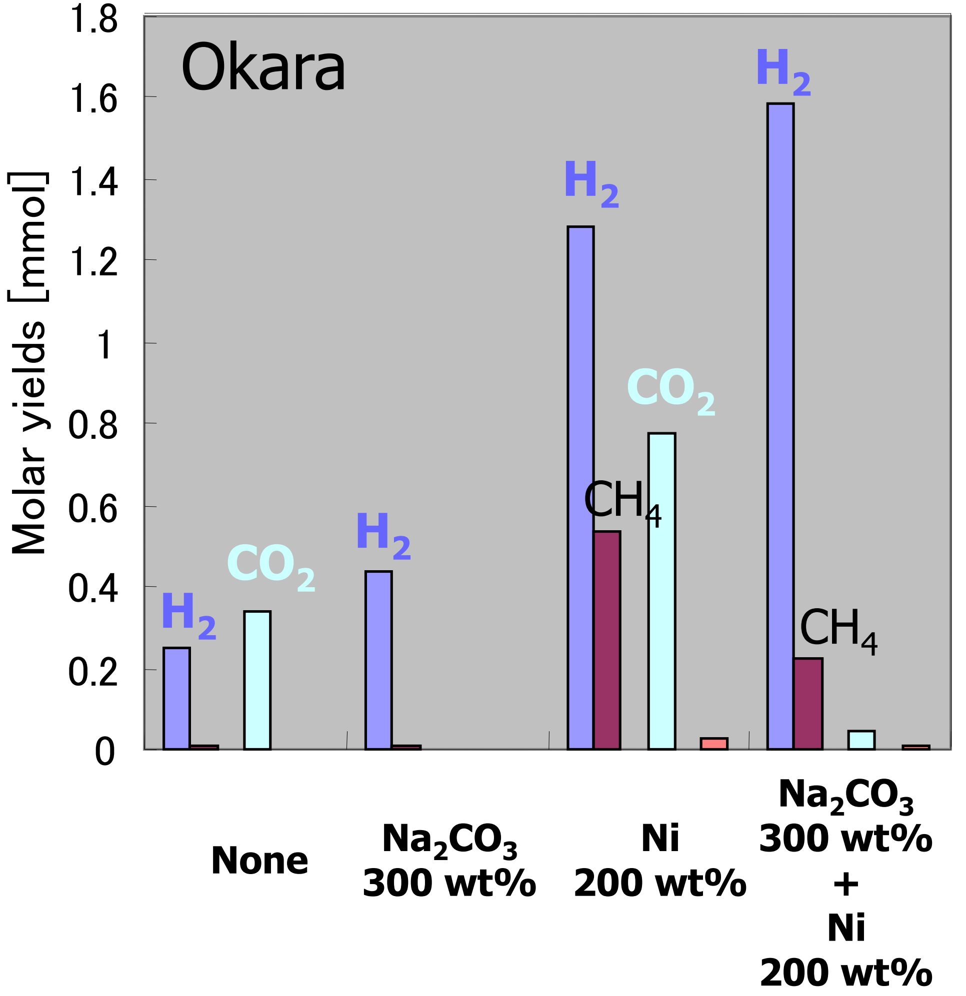

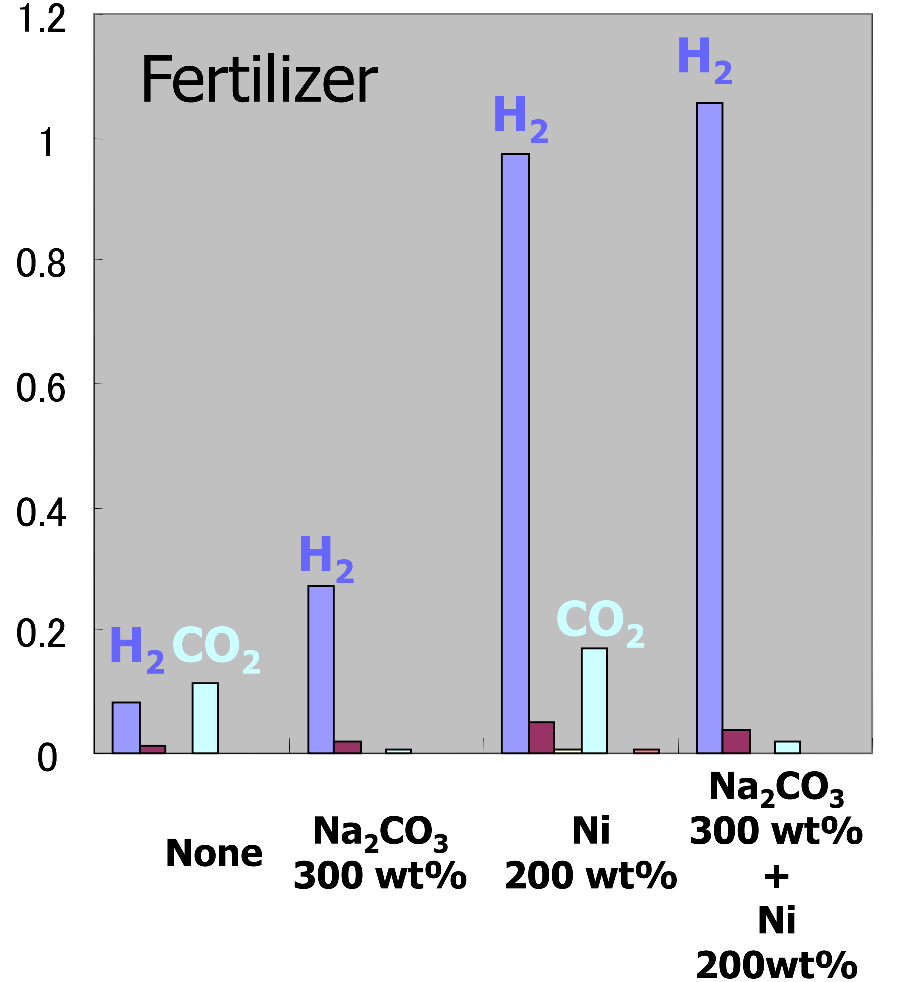

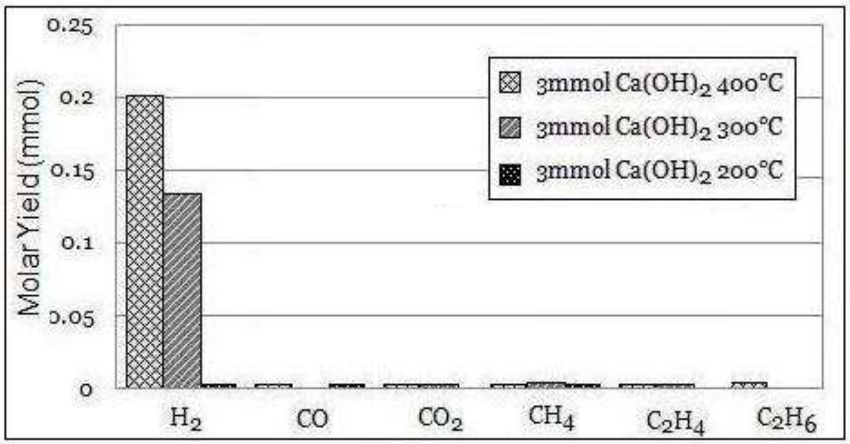

0.25
0.2
0.15
0.1
0.05
0
Molar Yield (mmol)
3mmol Ca(OH)2 400°C
3mmol Ca(OH)2 300°C
3mmol Ca(OH)2 200°C
H2
CO
CO2
CH4
C2H4
C2H6

(a)

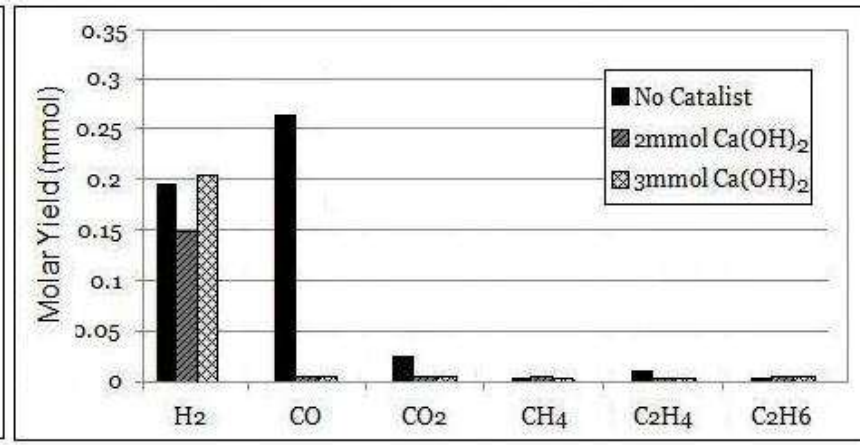

0.35
0.3
0.25
0.2
0.15
0.1
0.05
0
Molar Yield (mmol)
No Catalist
2mmol Ca(OH)2
3mmol Ca(OH)2
H2
CO
CO2
CH4
C2H4
C2H6

(b)

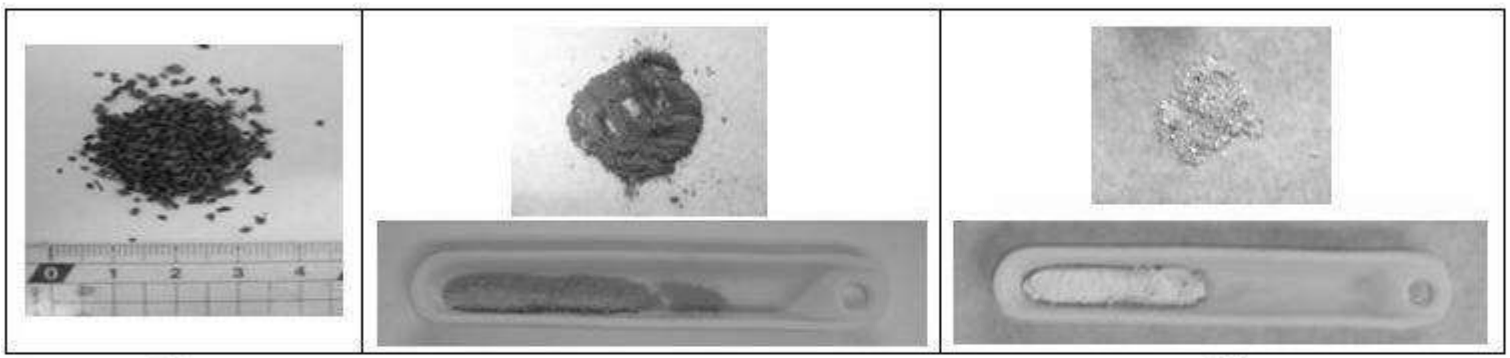

(a) (b) (c)

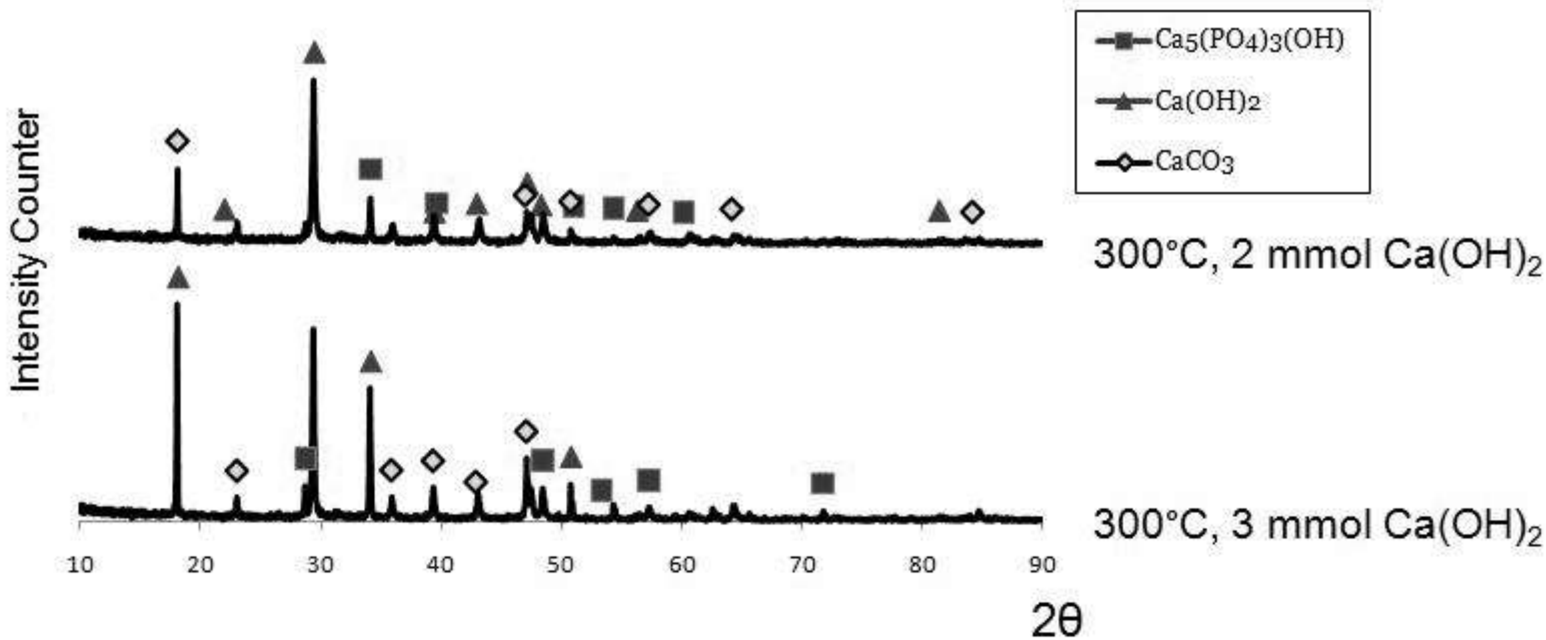
Ca5(PO4)3(OH)
Ca(OH)2
CaCO3
Intensity Counter
300°C, 2 mmol Ca(OH)2
300°C, 3 mmol Ca(OH)2
10
20
30
40
50
60
70
80
90
2θ

In situ monitoring of water in a PEM

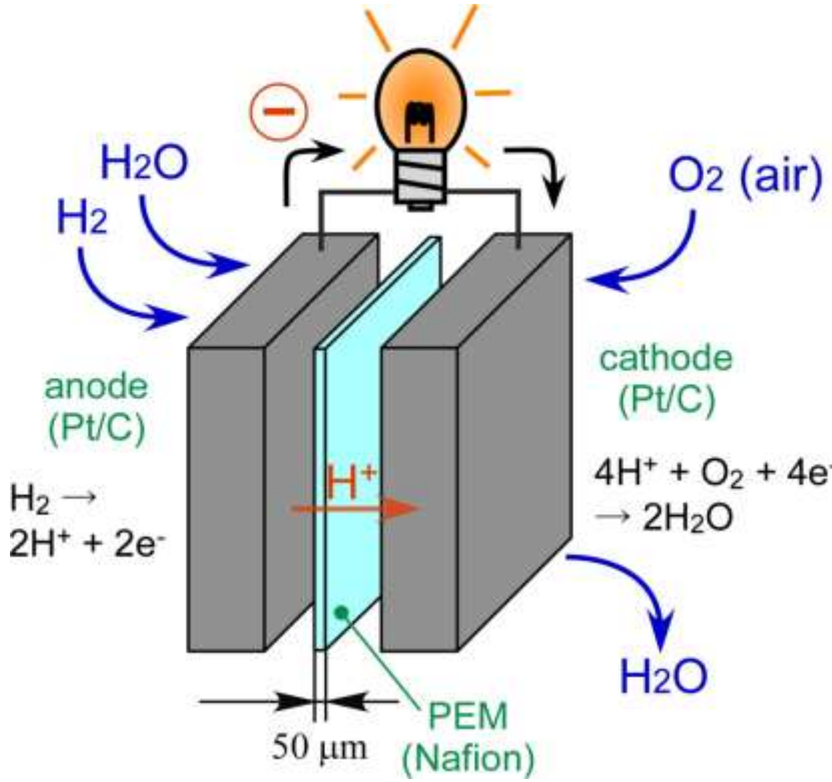

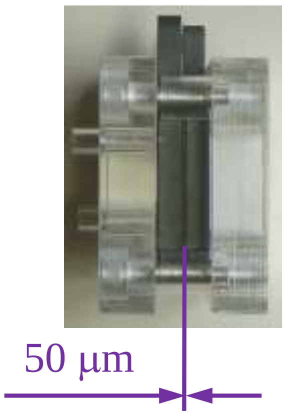

In situ monitoring of water in a proton exchange membrane (PEM) is important but difficult because the then membrane is sandwiched between two opaque electrodes. We have developed near-infrared (NIR) laser spectroscopy for the detection.

【Why NIR?】

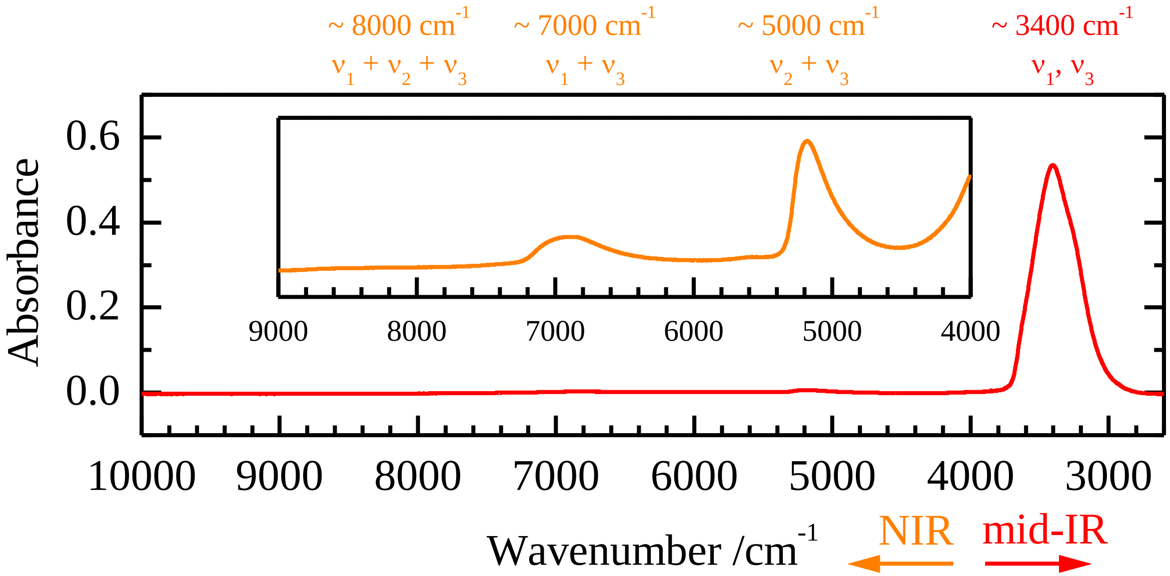
~ 8000 cm-1
ν1 + ν2 + ν3
~ 7000 cm-1
ν1 + ν3
~ 5000 cm-1
ν2 + ν3
~ 3400 cm-1
ν1, ν3
Absorbance
0.6
0.4
0.2
0.0
9000
8000
7000
6000
5000
4000
10000
9000
8000
7000
6000
5000
4000
3000
Wavenumber /cm-1
NIR
mid-IR

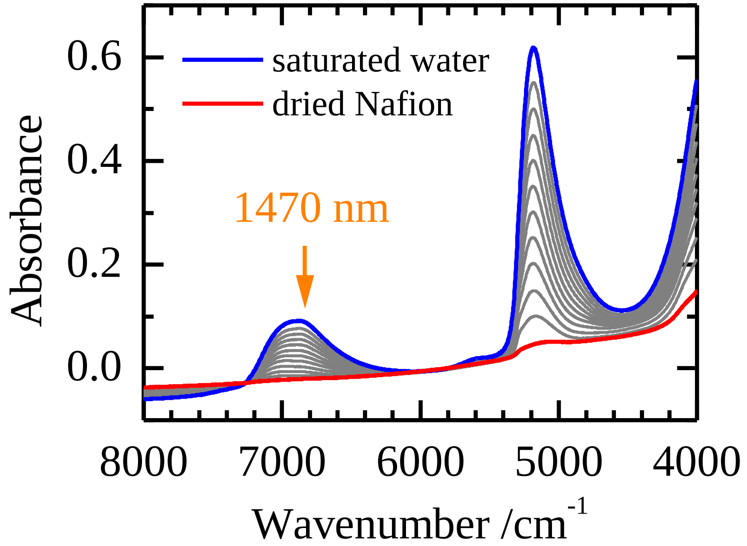
saturated water
dried Nafion
1470 nm
Absorbance
0.6
0.4
0.2
0.0
8000
7000
6000
5000
4000
Wavenumber /cm-1

【NIR LaserDetection of Water】

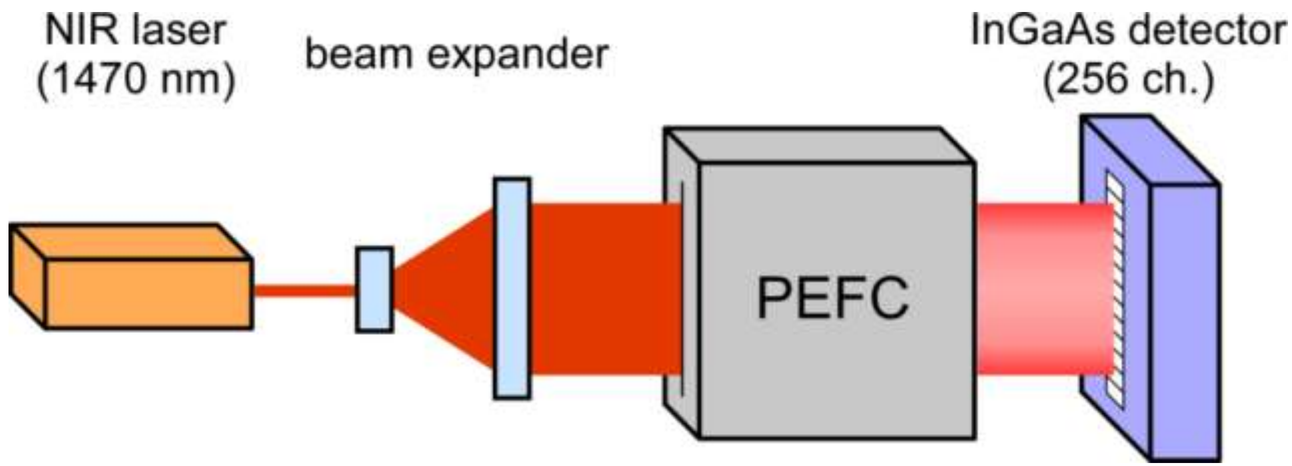

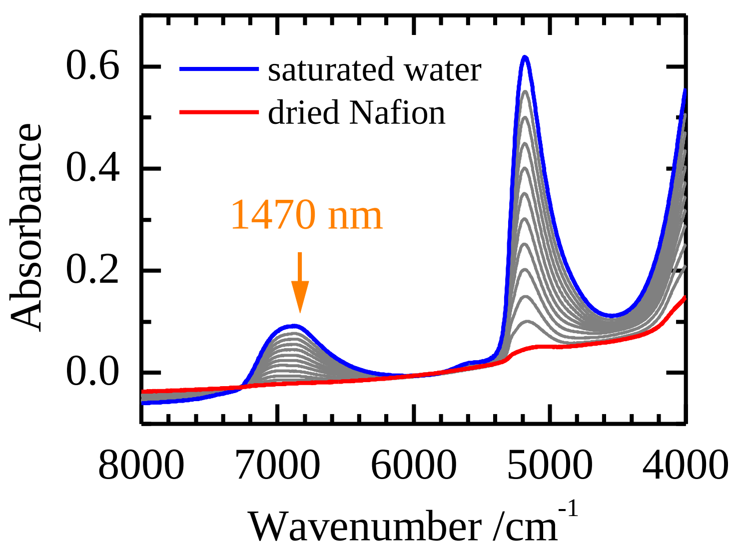

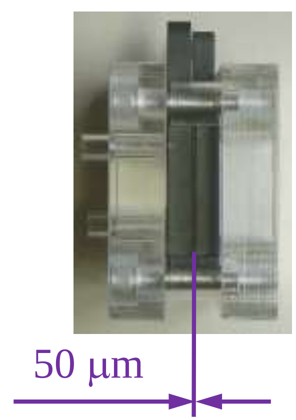

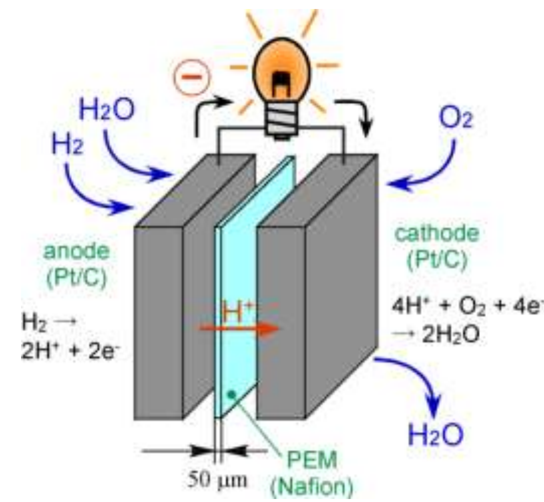

【2D Water Distribution】

One-way linear gas flow channel

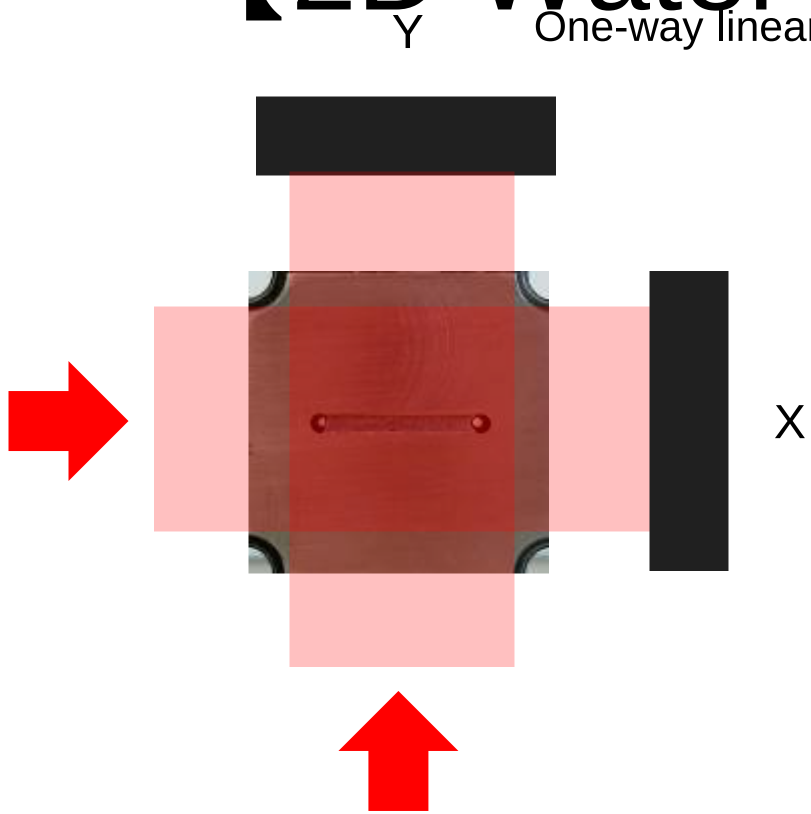

X-distribution

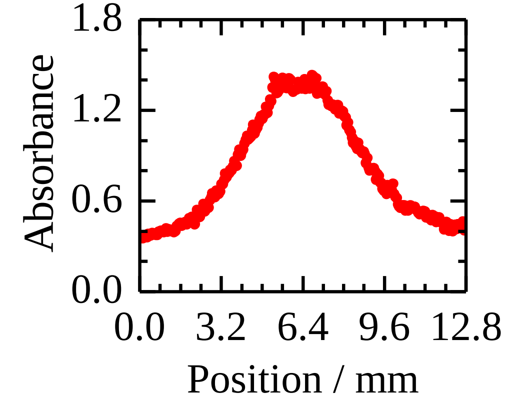

2D-distribution

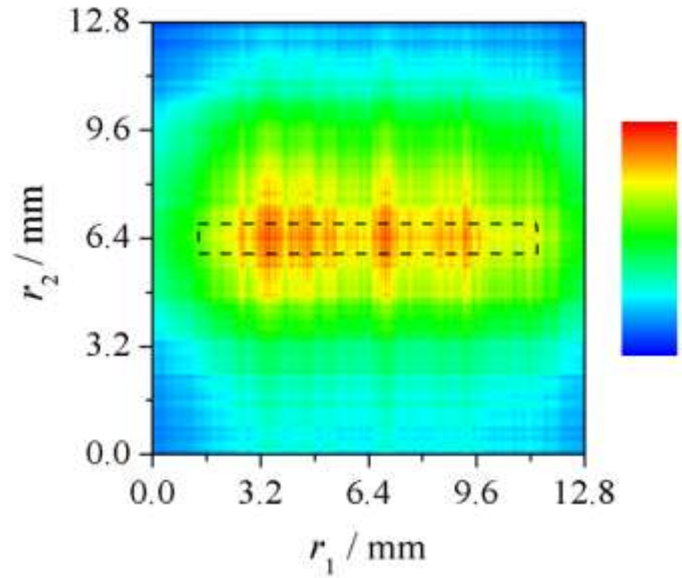

（X-distribution） × （Y-distribution） = [2D-distributiion]

【2D imaging by NIR laser】

1 frame / min.

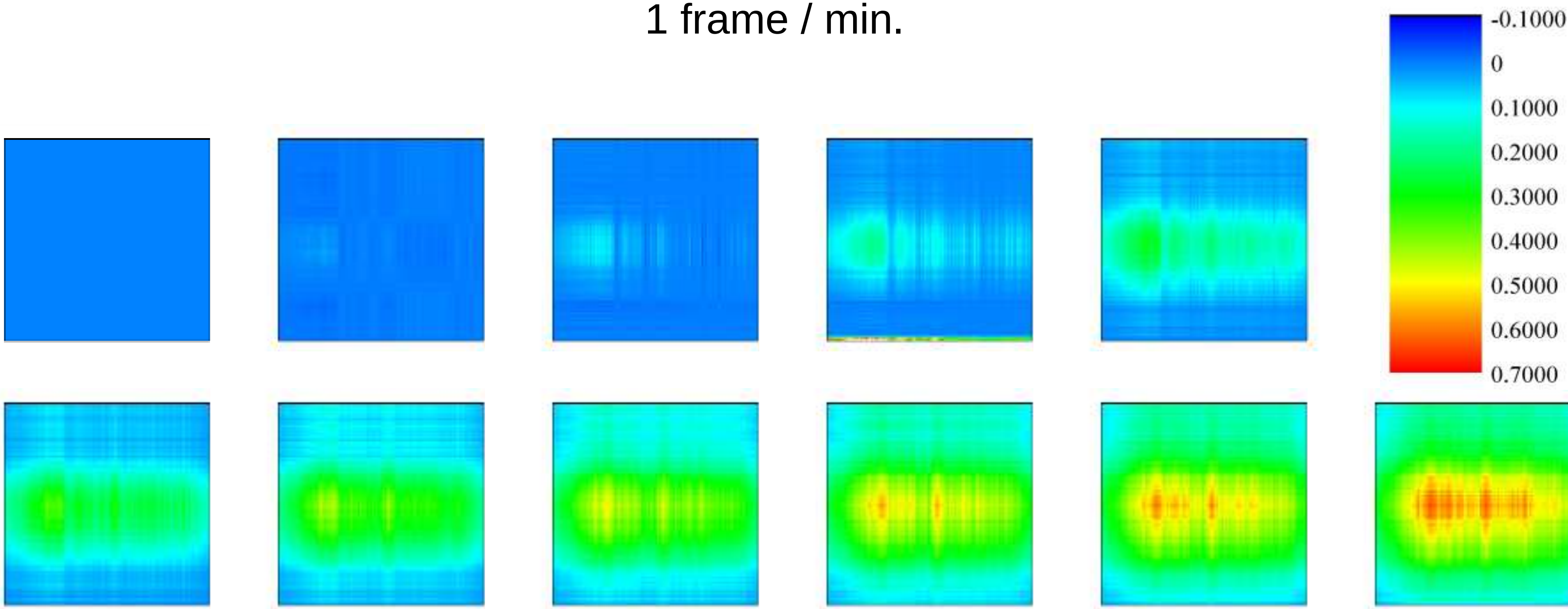

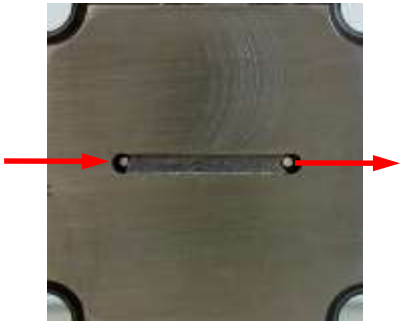

【CO poisoning onto a Pt catalyst】

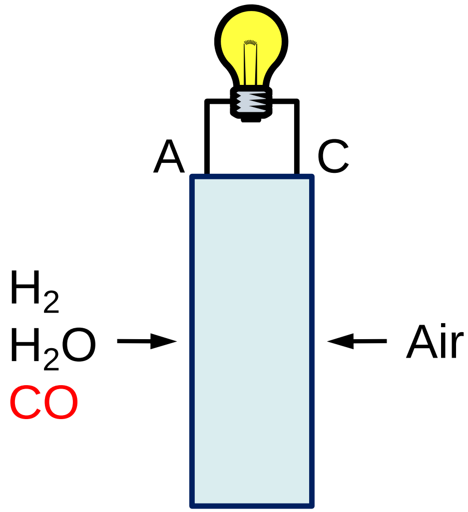

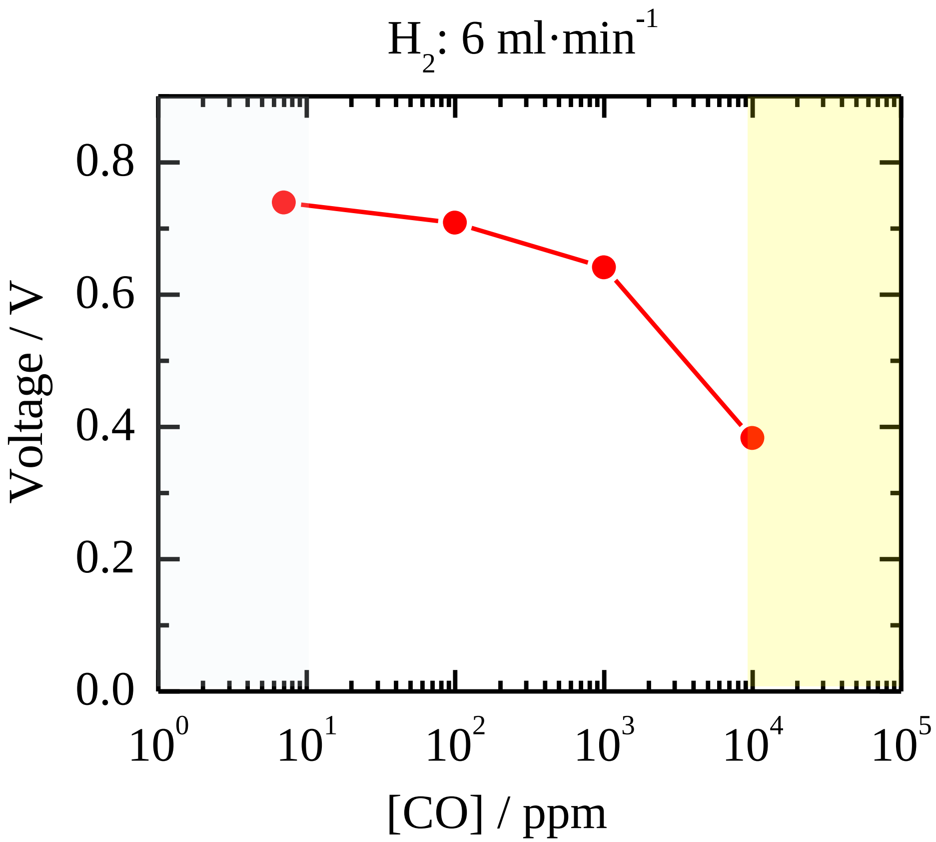

A hydrogen gas produced from hydrocarbons by steam reforming generally contains residual carbon monoxide (10^4 ~ 10^5 ppm). PEFC requests less than 10^1 ppm level of the residual CO.

【Catalysis at the Pt surface】

(a) Production of H^+
(b) Oxidation of H_2
(c) CO poisoning
(d) Oxidation of the adsorbed CO

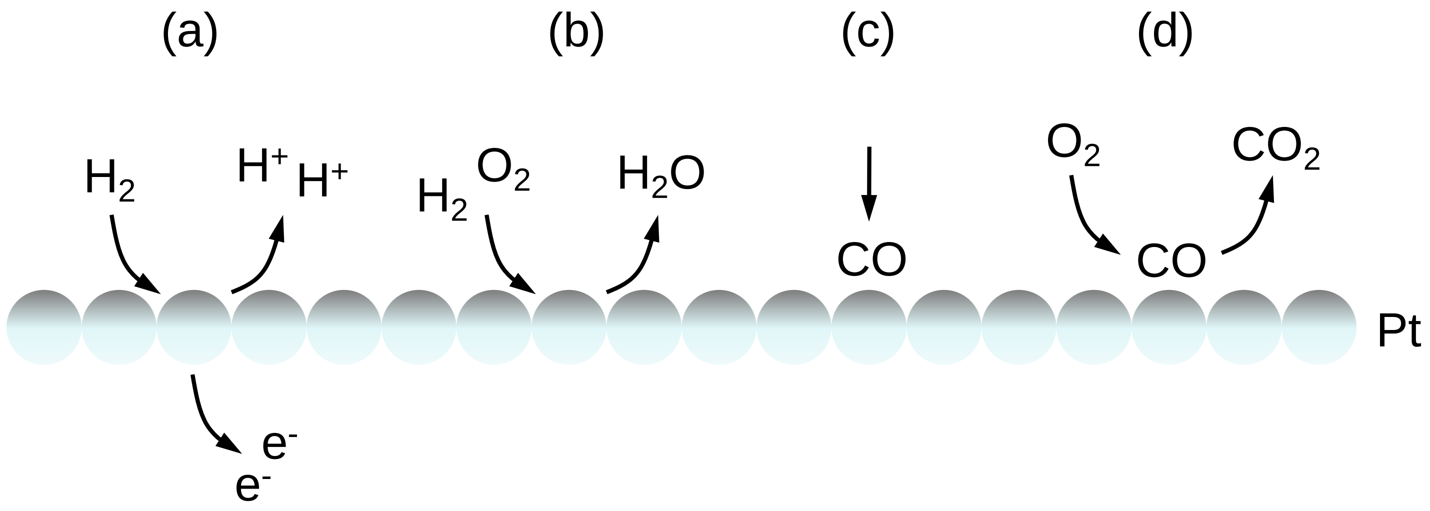

Result

H_2+CO ca.6mL/min

N_2+O_2 ca.3mL/min

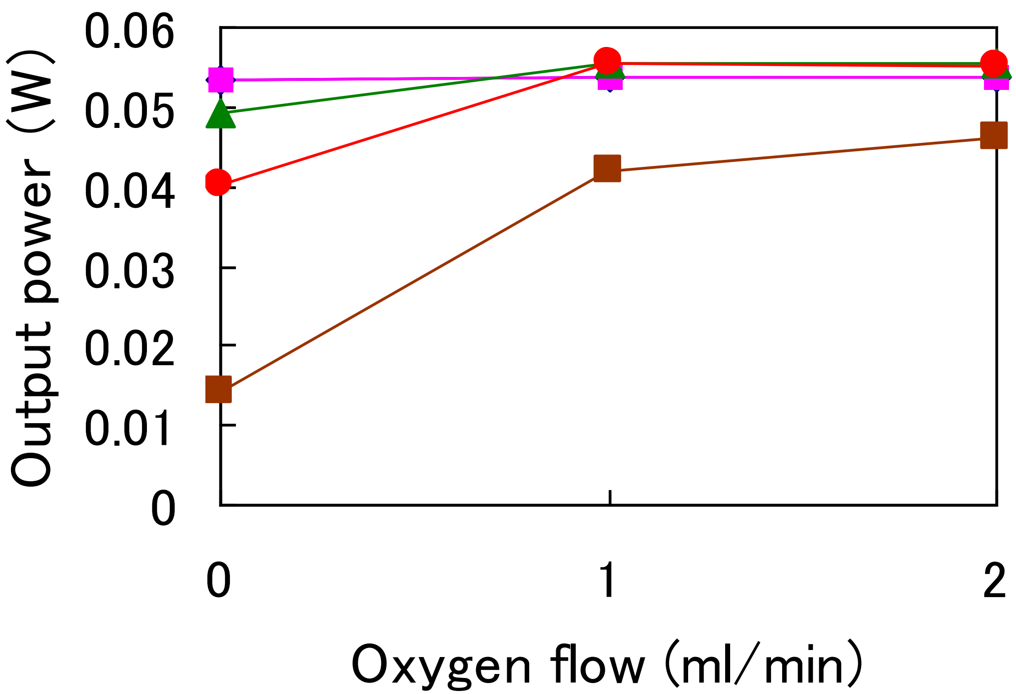

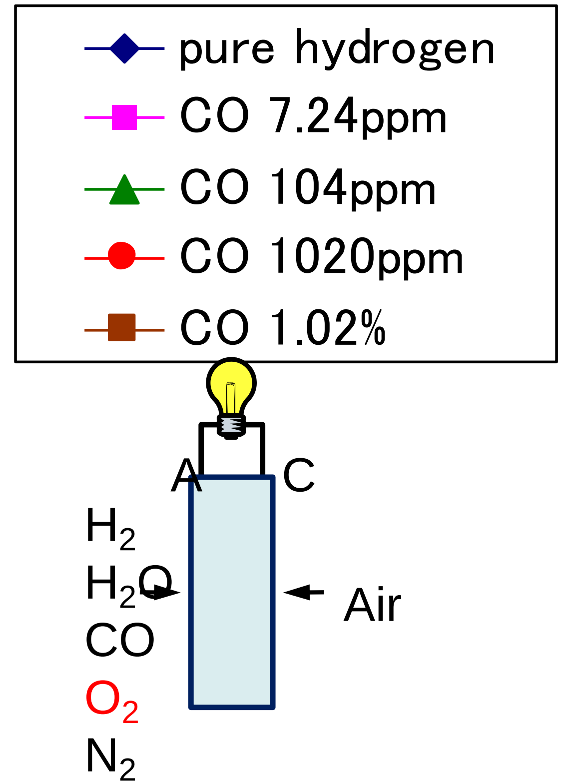

The deactivation by high concn. CO can successfully be suppressed.

EcoTopia Science Institute
NAGOYA UNIVERSITY

"Thin LED Panels for Soft and Uniform Illumination"

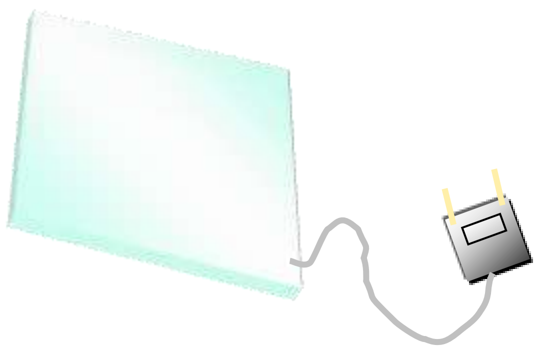

Conventional Fluorescent Lamps

開発の目的

Advantages of LEDs

Long life 70000hrs:7-10 times FL

No Hg waste (ca.3 tons/year in Japan)

Safety: Low voltage

Too bright point emission

Advantages of LED panels developed

Long life time : continuous operation for up to 70,000 hrs

Light : ca.1kg in letter size

Thin : 2–5 mm

Uniformity : uniform luminescence for diffusion panel

Power Control : Smooth adjustment of luminosity

Safety : Low unit driving voltage up to 15 V

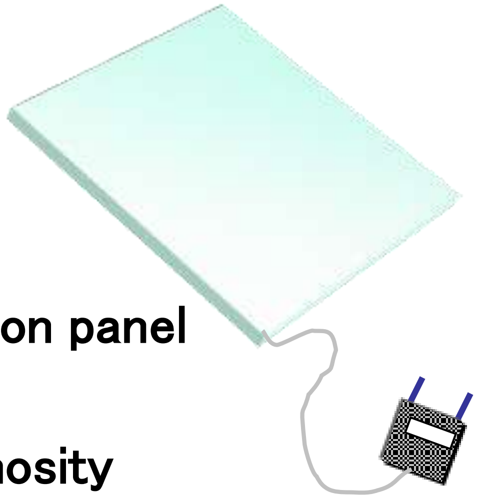

Evaluations

1. White LED panels: luminosity and power consumption
2. Human effect of pulse operation
3. Eye fatigue evaluation
4. Color temperature control

Thin LED panel

LED array

Double sides

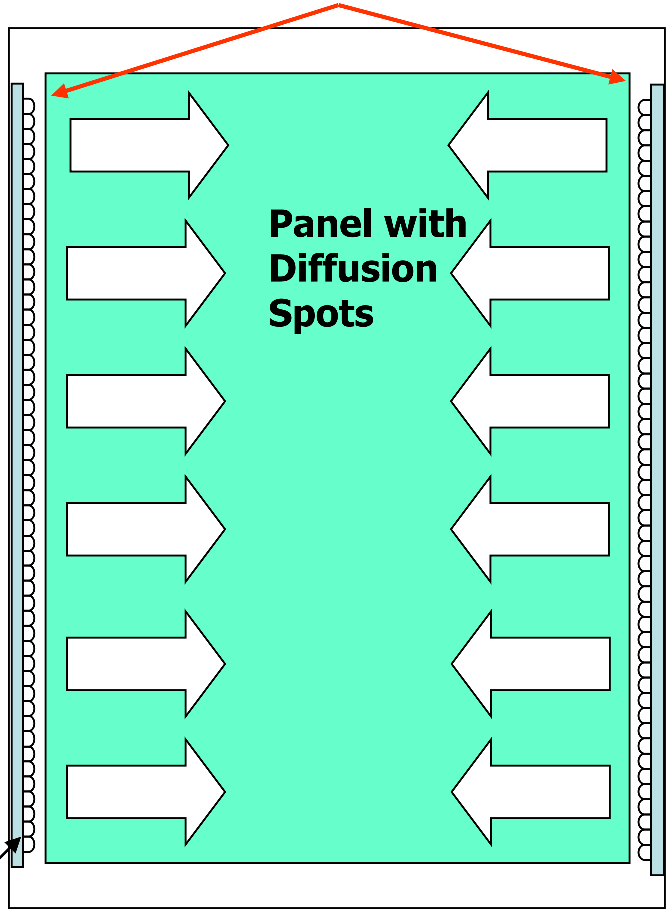

LED本体

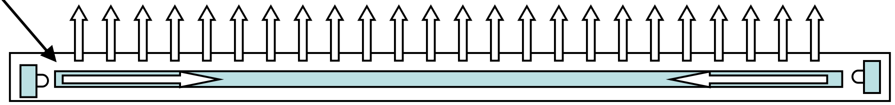

Test layout

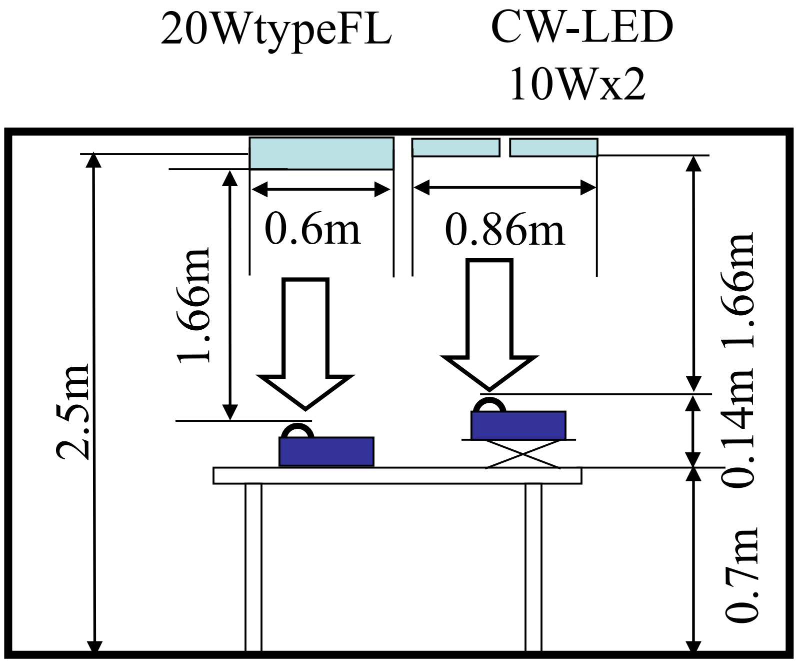

Power consumption

LEDx2	102.2Lx(100V/25W)
FL	99.1Lx（100V/25W）

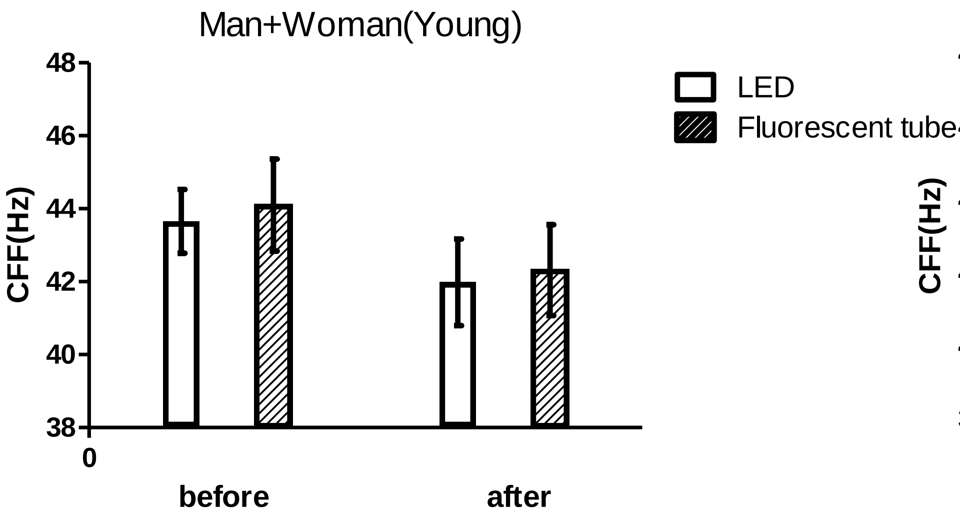

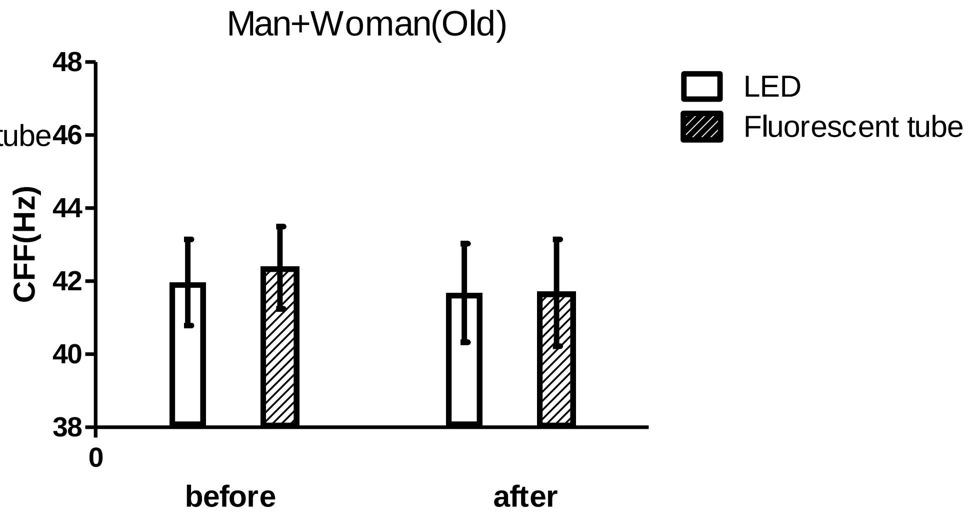

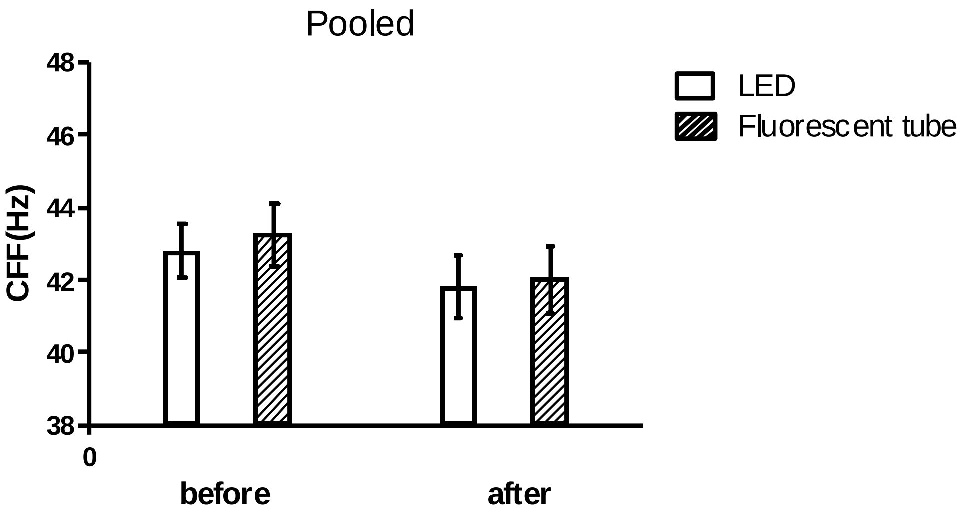

No difference: The LED panel can be used for an alternative as FLs.

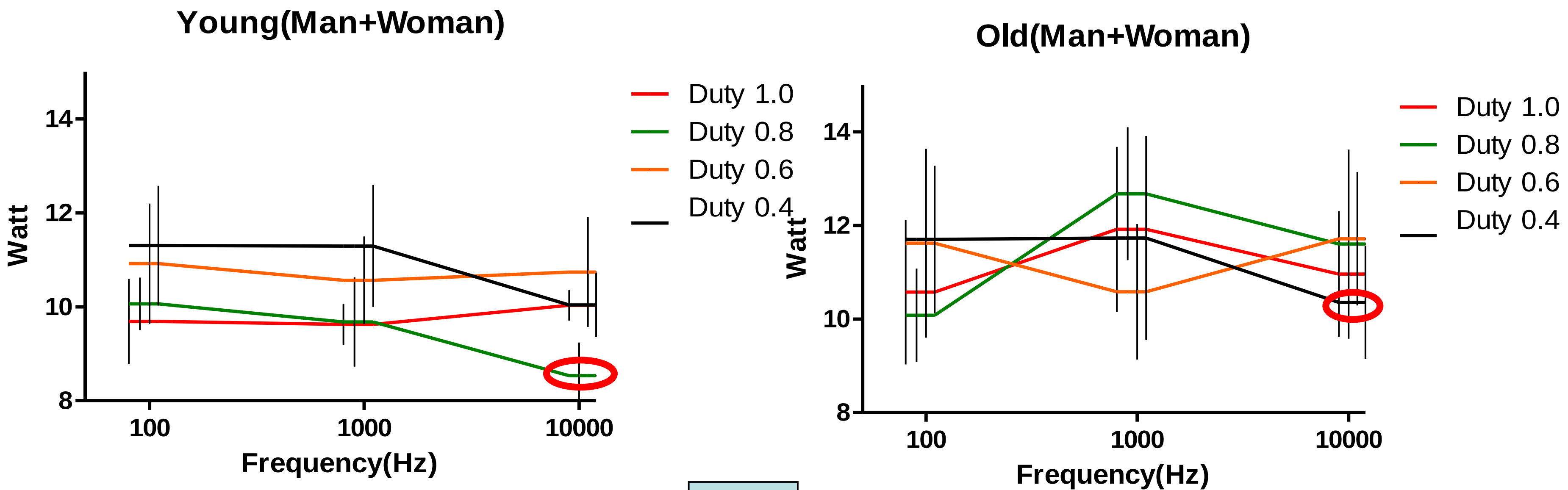

	Duty ratio	Power reduction
Young	0.8	15%
Aged	0.4	5.6%

Commercial application 1

Nagoya City Subway Station

Commercial application 2

Curved advertisement panel

TBS TV「夢の扉」より

A possible physiological problem

Melatonin :N-acetyl-5-methoxytryptamine

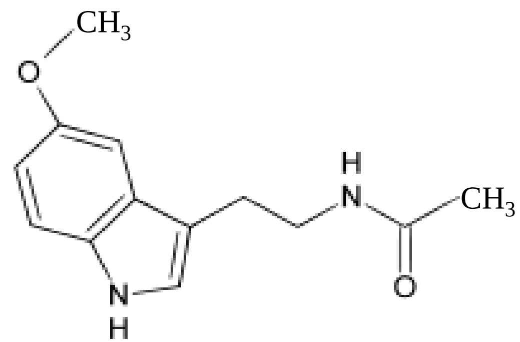

A hormone with
physiological rhythm adjustment and hypnotic effect
Commercially available as medicine for anti-jet lag but forbidden in Japan.

The residue blue radiation of **440-490 nm** used for the excitation of white LEDs has possibility to suppress the hormone secretion (at 464 nm) and to interrupt sleeping.

↓

Adjustment of color temperature to suppress the blue radiation using 3-color LEDs.

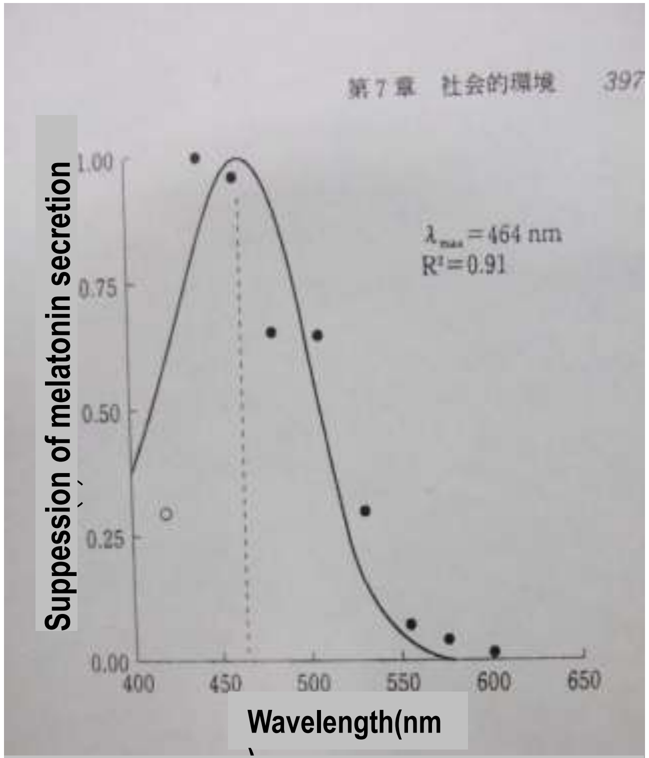

Fig. Effect of wavelength on suppression of melatonin secretion (cf. Brainard t. al., 2001)

Spectra

3 color LED panel at
a color temperature of 2591K
Close to that of W lamps.

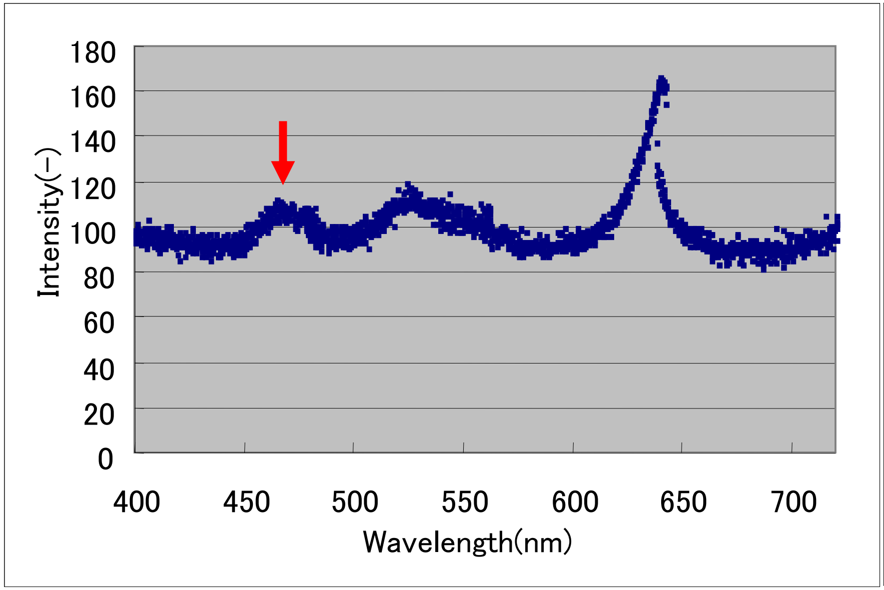

White LED panel at 6504 K

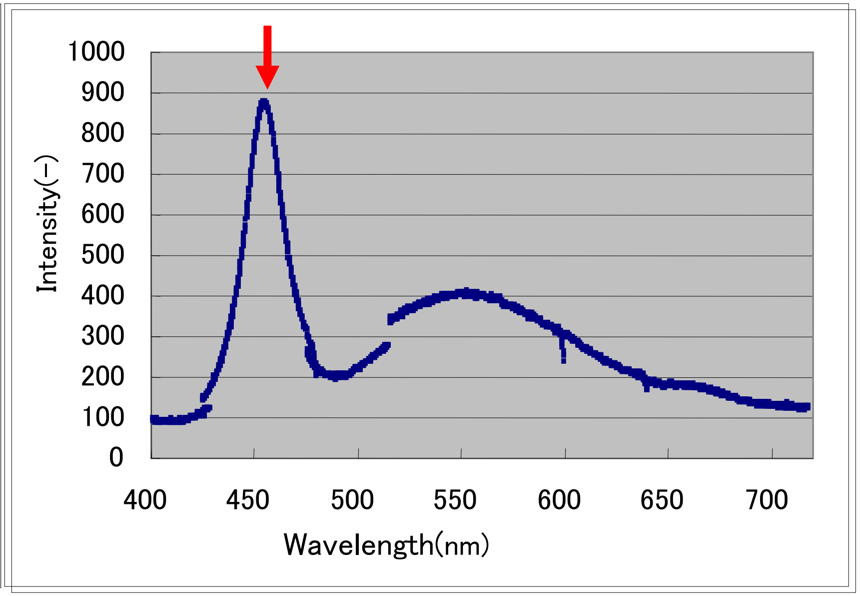

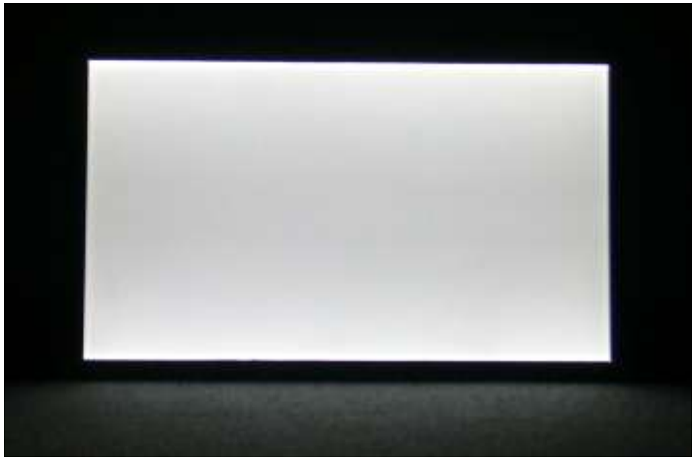

エネルギーシステム計測研究時代

- ＜助教授時代＞寺前先生の後任として新井紀夫先生と高温エネルギーシステム･計測研究
- 〇名古屋大学高温エネルギー変換研究センター所属 （平成6 - 12年）
- ＜教授時代＞
- 　分光可視化技術;火炎の可視化とともに、核融合プラズマの温度や密度、湿度の可視化などに成功した。名古屋大学の大野先生やメリーランド大学のGupta先生と共同研究。

  〇名古屋大学高効率変換研究センター所属（平成12 - 14年）
- 〇名古屋大学エコトピア科学研究機構＆研究所所属（平成14 - 25年）


2012 제1차 고령토 전문인력 양성 국제 심포지엄
World Green Energy & Resources Congress 2012

連携先の友人たち

第二の人生　実業と研究や後進の育成、社会科学と芸術の琢磨

〇ベンチャー会社と特殊LED製品開発および販売

〇アジアの大学においてボランティア講義およびエネルギーシステムを中心とした研究指導

〇趣味の研鑽：写真活動、楽器演奏、真空管アンプ、言語、宗教、民族文化、
　音楽・舞踊、歴史の再勉強　等々

四十二年の亘り、関係した皆様には、私の我儘を聴いていただき誠にありがとうございました。
また、ご迷惑をかけた方々にはこの場を借りてお詫びを申し上げます。
退職時の研究厄年以後、精一杯生きてゆきます。
また、どこかでお目にかかることができることを楽しみにしております。


芭瑠の里夕陽谷と伴に弐拾年余生夢観ん楽邦の華

- 奥さま、家族、亡き両親、ありがとう。
- 共著者、学生さん、共同研究の方々など、お世話になった方、数知れず、心からお礼を申し上げます。
- 奉職27年11ヶ月＋学生時代6年間、名古屋大学と皆様ありがとうございました。